NUCLEAR PORE PROTEINS IN REGULATION OF CHROMATIN STATE AND GENE EXPRESSION

Terra Kuhn

A DISSERTATION

in

Cell and Molecular Biology

Presented to the Faculties of the University of Pennsylvania

in

Partial Fulfillment of the Requirements for the

Degree of Doctor of Philosophy

2019

Supervisor of Dissertation

_____

Maya Capelson, Ph.D.

Assistant Professor of Cell and Developmental Biology

Graduate Group Chairperson

_____

Daniel S. Kessler, PhD

Associate Professor, Cell and Developmental Biology

Dissertation Committee

F. Bradley Johnson MD, PhD; Professor of Pathology and Laboratory Medicine
Doris Wagner, PhD; Robert I. Williams Term Professor of Biology
Kenneth S. Zaret, PhD; Joseph Leidy Professor of Cell and Molecular Biology
Thomas A. Jongens, PhD; Associate Professor of Genetics

NUCLEAR PORE PROTEINS IN REGULATION OF CHROMATIN STATE AND GENE EXPRESSION

Terra M. Kuhn

Acknowledgment

There are a lot of people to thank for helping me get to this point in life, and for helping me get through this phase of it. I firstly owe **my parents** so much for all of their support, encouragement and love, and always telling me, and believing, that I could do anything I set my mind to. I owe so much to my older sister **Ariane**, the most resilient, fun, caring role-model who helped make sure I got through my childhood unscathed, and in our adulthood has become one of my closest friends. Finally, my (first)-cousin (once-removed) **Kelly** has grown into one of my dearest family members and friends, and her support, love and midnight chats are some of the things I hold most precious.

There have been many educators and mentors in my life that were engaging, encouraging, and inspiring, and I owe so much of my love of learning and science to people such as **Christine In-Albon,** for always encouraging me to think outside the box, engage my brain, and be the best that I can be; **Michael Frank,** for showing me that biology is just THE MOST INTERESTING THING IN THE WORLD; **Megan Stirlir,** for always being so incredibly engaging and enthusiastic about science, and believing in me enough to apply for and score us an internship with NASA; and **Miloš Babić** for being an incredibly patient, thorough and trusting scientific mentor. All of these people cared so very much about those they were mentoring and teaching, and I will always strive to make a positive impact on others as these incredible people did for me.

The friends that I have made and maintained along this journey have been so critical to my happiness and well-being. I met **Kyle, Kory and Jessica** in 6th grade, and we were pretty much instantly life-long friends since my first terrifying day, halfway

through the school year, when they invited the new girl to each with them at lunch. The distances have done little to dull the joy, love, and support I receive from these wonderful people. If there is anyone in this world that understands me better than myself, its Jessica, and while we are now infrequently able to have sleepovers, get Coldstone, and go to the fair together, I still take her with me wherever I go.

When I interviewed at Penn I felt like I had found the most unbelievable concentration of “my people” that I had ever come across, packed into such a small space, and this was a huge influence for choosing this program. This first impression was not only true, but didn’t even prepare me for the number and quality of amazing friendships I would make here. I couldn’t have gotten through these 6 years without these amazing people. In alphabetical order, **Ayon** for all of the delicious food adventures across Philadelphia, and spectacular conversation about life, the universe, and everything; **Becky** for being an instant, steadfast, and incredibly real, relatable and wise friend; **Bobby** for teaching me EVERYTHING about beer, and for lots of good conversations while drinking it; **Danielle** for all of the life-analyses over coffee and wine, and for spontaneously traipsing to *ITALY* with me(!!!); **Devin** for years of unwavering support and kindness; **Haig** for never blinking an eye at staying in lab an extra hour to help impart his wisdom on everything from science to relationships to figuring yourself out; **Sam** for all of the games and cat appreciating; **Steve** and **Somdutta** for always being down to watch shows, troll center city, chat about life, or, you know, fly across the country for week-long hiking trips; **Vineet** for unknowingly putting himself in harm’s way through years of meeting me at the (unbeknownst to us) health-violating Mad Mex to commiserate, celebrate, and ponder; and **Colleen, Chris, Christin, David** and **Steve** for

being constant, fantastic game/brunch/happy hour connoisseurs that made my time here infinitely more fun, for making me feel unconditionally accepted, and for being “my people.”

I’ve also had the most incredible lab members that have made every day of these 6 years a constant struggle between being productive and enjoying the conversation of such hilarious, kind, and engaging human beings. I specifically need to thank my advisor **Maya** for being not only an incredibly smart, understanding, encouraging, trusting and supportive mentor, but just genuinely a kind and enjoyable person to spend all this time with, which certainly not everyone can say about their advisors. My dear **Pau** is one of the kindest human beings I have ever known, and every single day as his bay-mate has been hilarious, heartwarming, supportive, fun, engaging, helpful, and truly full of joy. He has picked me up off the floor more times than I can count, equally from tears of pain and laughter. I sincerely could not have done this without him. Finally, **Jen** and **Ashley** have both been the most amazing friends to get to spend these years with, and there is no one else I would rather have shared all of the daily ups and downs of science and life with.

I’d like to thank **Philadelphia Pan Stars Steel Band** for being my creative outlet and family away from home/science, and I’d like to thank my animals **Sonny, Sofi and Obi** for all of the pets, purrs and licks that got me through graduate school and thesis writing.

And finally I need to thank **Jeff Kapochus**. He has been the most incredibly supportive partner, taking the time to learn about my science, being more than

understanding of the time and energy it takes from me, and picking up the slack when I am stretched taut, never asking for anything in return or complaining (about science anyway). Having him to come home to and talk to and enjoy life with makes everything better, and I am incredibly grateful for his willingness to gallivant off to Europe with me for the next great adventure.

If you've actually read this novel of an acknowledgements section, here's a thanks to you too. And for reading this thesis itself. And now on to the science!

ABSTRACT

NUCLEAR PORE PROTEINS IN REGULATION OF CHROMATIN STATE AND GENE EXPRESSION

Terra M. Kuhn

Maya Capelson, PhD.

Nuclear pore complexes are best known for their regulation of nucleocytoplasmic transport as integral components of the eukaryotic nuclear envelope. Over the years, their importance in regulation of genome function has become apparent. Many of the 30 individual nuclear pore proteins, Nups, have been found to play distinct roles interacting with and regulating various genomic targets, especially in a cell-type specific manner. The mechanism behind this regulation is often unknown. We have developed a method by which to study the roles of Nups on chromatin using an ectopic-tethering system. *Drosophila melanogaster* provide a powerful tool with which to combine many genetic elements of interest together in individual organisms quickly and efficiently, and additionally has allowed for powerful high-resolution visualization of chromatin structure perturbations through the imaging of their larval salivary gland polytene chromosomes. Using this system we observed that tethering Nups to chromatin was sufficient to induce chromatin decondensation, visualized by robust and reproducible loss of DNA and histone fluorescene signal associated with Nup binding. Additionally we observed recruitment of chromatin-remodeling complex PBAP, and reliance on PBAP for the observed Nup-induced decondensation, suggesting an important functional relationship between these proteins. We then took our findings and hypotheses generated from this

ectopic-tethering imaging system to next conduct functional biochemical analysis of these proteins in *Drosophila* S2 cell culture. We found that nucleoporin Elys has a robust biochemical interaction with components of PBAP in an endogenous context, supporting the recruitment of these proteins we observed via immunofluorescence. Additionally, MNase experiments determined that Elys was critical for facilitating the formation and/or maintenance of open chromatin, both genome-wide and on a local nucleosomal level at Elys target genes. Together these results demonstrate the importance of nucleoporins in regulation of chromatin structure, and provide one mechanism to explain this phenomenon. These findings are of particular interest in the fields of chromatin biology and the study of nuclear pore protein function, demonstrating a possible explanation for not only associations of NPCs with decondensed chromatin at the nuclear periphery, but also regulation of Nup target gene expression, through regulation of chromatin accessibility.

Table of Contents

List of Tables

List of Illustrations

Chapter 1: Introduction

This chapter is adapted from:

Kuhn, T. and Capelson, M. Chapter 5, Nuclear Pores and Gene Expression in Drosophila. Nuclear Pore Complexes in Genome Organization, Function and Maintenance. Springer 2018.

and

Kuhn, T. and Capelson, M. Nuclear Pore Complexes in Regulation of Chromatin State and Gene Expression. Invited review article in Cells, *in preparation*

Nuclear Pore Complexes: Structure and Function

Nuclear Pore Complexes (NPCs) are massive >100 MDa protein complexes that span the eukaryotic nuclear envelope and are the channels through which nucleocytoplasmic transport is achieved. mRNA, proteins and molecules larger than 40kDa must pass through NPCs to gain access to the genome within the nucleus, or to exit the nucleus into the endoplasmic reticulum or cytoplasm (Knockenhauer and Schwartz, 2016). NPCs are comprised of ~30 distinct proteins called nucleoporins (Nups), each Nup copy-number present in roughly multiples of 8, forming the 8-fold rotational symmetry that is the basis for the overall structure of NPCs. There are 3 main classes of Nups, including; scaffold Nups which form incredibly stable structure of inner and outer rings comprising the core of the NPC, transmembrane Nups which anchor the scaffold structure into the fused double membrane of the nuclear envelope within which NPCs are imbedded, and peripheral Nups which include the accessory structures

protruding from the core scaffold into the nucleoplasmic and cytoplasmic spaces (D'Angelo and Hetzer, 2008).

The category of peripheral Nups also includes those filling the central channel of the pore, which interact with import and export factors that transit through NPCs. These are referred to as the FG Nups, as they each contain at least one domain filled with Phenylalanine(F) - Glycine(G) amino acid repeats, the regions of the Nups known to interact with the transport receptors. The structure of this FG-repeat-dense central channel is a matter of constant study and debate, as the natively unstructured, intrinsically disordered FG domains are both impossible to crystallize, and additionally have intriguing hydrogel-like properties both in vitro and ex vivo, which have been established to regulate pore permeability(D'Angelo and Hetzer, 2008).

Non-canonical functions of NPCs

Over the decades, NPCs and their constituent Nups have been found to play roles in regulation of many nuclear and cellular processes independent of nucleocytoplasmic transport. One pervasive theme is that Nups play important roles in multiple distinct processes in maintaining genomic integrity. For instance, several Nups have proven critical for multiple steps of proper chromosome segregation during mitosis, including regulating mitotic spindle assembly, the spindle assembly checkpoint, and serving as core components of kinetochores (Mossaid and Fahrenkrog, 2015; D'Angelo and Hetzer, 2008). Additionally, recent evidence has come to light linking Nup functions to suppression of retrotransposon activation, which, if left unchecked, can result in great

genomic disruption through aberrant integration into protein coding genes or their regulatory regions (Parikh et al., 2018; Ilyin et al., 2017). The greatest body of research with regard to Nups safeguarding the genome however lies in the field demonstrating the importance of the role of Nups in the linked processes of DNA damage repair and telomere maintenance. Many years of work in yeast has revealed that several types of DNA damage, including eroded telomeres, localize to, and require the function of, NPCs that serve as hubs for DNA Double Strand Break (DSB) repair machinery (Géli and Lisby, 2015; Nagai et al., 2011; Ptak and Wozniak, 2016).

NPCs serving as hubs to concentrate proteins for specific nuclear processes is also a common model to describe the role they play in transcriptional regulation. This is perhaps the most commonly studied “moonlighting” role of pores, and there is a large body of work in this field, much of which will be discussed below. It has now been 15 years that there has been clear evidence showing clear interaction of NPCs with the eukaryotic genome, most often at sites of active genes and regulatory elements (Casolari et al., 2004; Schmid et al., 2006). Evidence that Nups perform a functional role in that activation came with studies showing that active genes in yeast relocalize to NPCs upon activation, and required that interaction for transcription (Schmid et al., 2006; Taddei et al., 2006; Light et al., 2010). In metazoan cells, this regulation of gene expression may occur “off-pore,” as some Nups have been found to have low residence times at NPCs, and/or interact with chromatin utilizing intranuclear protein populations (Capelson et al., 2010; Kalverda et al., 2010; Rabut et al., 2004).

One general trend, as will be discussed in-depth in the “Regulation of Transcription by NPCs and Nups” section below, is that many genetic targets of Nups

tend to be developmental and cell-type-specific genes. Indeed, Nups and their mutations have been linked to many tissue-specific cellular functions and human diseases, including leukemia, cardiovascular development and neurodegenerative diseases (Raices and D'Angelo, 2012; Jühlen and Fahrenkrog, 2018; Capelson and Hetzer, 2009; Talamas and Capelson, 2015) (see also **Table 1.1** below for Nup mutations in Drosophila). For some of these associations, the mechanism of Nup involvement is known, be it through dysregulation in transport, aberrant protein aggregation, or, increasingly more common, regulation of transcription factor binding/activity. However many mechanisms of action are unknown, and based on the findings of this thesis, and the synthesis of disparate findings from the field throughout the last few years, I propose many as-of-yet unknown mechanisms may lie in Nup-based regulation of chromatin structure of genetic targets, which results in downstream transcriptional changes. For this reason, we will discuss these processes, and what is known about the involvement of Nups in these processes, in further detail.

Chromatin and Genome Organization

The amount of DNA that a single cell possesses would, if stretched out as a single molecule, be over 1 meter long, orders of magnitude longer than the diameter of a single nucleus. For this reason, and to also protect and regulate the accessibility of DNA to regulatory factors, DNA is wrapped up around histone protein octamers and compacted into a structure called chromatin. There are many different levels of chromatin organization in a nucleus, and differences in this organization changes upon different cellular states, different developmental stages, and between different tissue-

specific cell types. This is because the organization of chromatin, and thereby the accessibility of different genes that have cell-type-specific or context-dependent activity, define transcriptional programs and thereby cellular function.

Nucleosome Organization

Organization of chromatin structure starts on the level of the unit of the nucleosome, or roughly 147bp of DNA wrapped around a histone octamer core, canonically comprised of 2 each of histone proteins H3, H4, H2A and H2B. Nucleosomes are repeated at roughly regular intervals, on average 60bp from one another, in a “beads-on-a-string” structure about 10-nm wide (Maeshima et al., 2019). Positioning of nucleosomes throughout genes and regulatory elements regulates their accessibility to transcription factors and transcriptional machinery for regulation of gene expression, DNA repair machinery for maintenance of genome integrity, DNA replication machinery, and DNA digestive enzymes used to determine said structure. Nucleosome free regions, or sections of DNA depleted of nucleosomes, strongly correspond to actively utilized regulatory sites or promoters of active genes, and also with DNase hypersensitive sites. (Baldi, 2019). For these reasons, the proteins that regulate nucleosome occupancy and spacing, so-called chromatin remodelers, are key components in regulation of gene expression and genome integrity, as their activity controls downstream accessibility for any subsequent transcriptional or repair machinery. These will be explored more in the “Chromatin Remodeling Complexes” section below.

Histones have C-terminal “tail” regions with many amino acid residues that receive post-translational modifications (PTMs). Histone modifiers are responsible for depositing these PTMs. Histone tail modifications can sometimes directly regulate the level of interaction between nearby nucleosomal units, as in the case of histone acetylation, resulting in changes in chromatin compaction or condensation state, which subsequently changes DNA accessibility (Wolffe and Hayes, 1999; Tolsma and Hansen, 2019). More often however, histone PTMs seem to provide a signal to recruit other proteins that then more directly regulate chromatin compaction, or downstream transcription (Liyanage et al., 2012). While the exact function of many histone modifications remains elusive, general trends in whether specific marks are associated with active or repressed genes or their regulatory elements has been well explored, and can help us draw inferences about the relationships we find between them and nucleoporins, “Regulation of Chromatin Structure by NPCs and Nups” section below.

Chromatin Remodeling Complexes: SWI/SNF and Brahma

Based on the findings of the experimental work in this thesis, it is valuable to explore ATP-dependent chromatin remodeling in some detail. The “remodeling” of chromatin refers to movement of nucleosomes relative to DNA, whether that be by “sliding” the histone core down the strand of DNA and thereby changing the nucleotides protected by the nucleosome, by evicting histones entirely and leaving open, accessible, DNase hypersensitive sites behind, or by exchanging core histones for histone variants that may perform some context-dependent function at the location in question. All of these functions involve weakening or loosening the interactions of DNA with the histone proteins, and require energy in the form of ATP. ATP-dependent chromatin remodeling

complexes all have an ATPase protein capable of ATP hydrolysis, to provide the energy for these activities (Hargreaves and Crabtree, 2011).

The 3 main classes of chromatin-remodeling complexes in *Drosophila*, generally characterized by the ATPase utilized in each complex, are the SWI/SNF-type complexes utilizing ATPase Brahma (Brm), ISWI complexes, and CHD complexes (Bouazoune and Brehm, 2006). There are multiple different complexes within each category that utilize the same ATPases, and the individual subunits associated with each ATPase differentiate one complex from another, and are also responsible for target specificity. In *Drosophila,* the ATPase Brm is present in two main complexes, BAP and PBAP, differentiated mostly by the use of proteins Osa or Polybromo respectively. The binding profiles of BAP and PBAP have both complex-specific and overlapping genetic targets, and are generally both found at highly-acetylated chromatin (Mohrmann et al., 2004), which is typically associated with higher levels of chromatin decondensation and accessibility. This targeting to acetylated chromatin may in part be the function of bromodomain protein domains present in both Brm and Polybromo, however these domains are also capable of targeting other acetylated proteins, and could additionally facilitate protein-protein interactions to enable specificity in genomic targeting or downstream protein recruitment (Mohrmann and Verrijzer, 2005; Tamkun et al., 1992).

The function of SWI/SNF complexes have proven important for regulation of cellular specification and development throughout eukaryotic organisms (Hargreaves and Crabtree, 2011). In *Drosophila*, Brm complexes are found at almost all active loci, and are required for the localization of RNAPII at genetic targets genome wide (Armstrong et al., 2002). The original SWI/SNF complex in yeast was discovered based

on its requirement for the activation of genes associated with mating-type switching (SWI) and sucrose non-fermentatation (SNF)-based growth. The role in transcriptional activation undoubtedly lies in the ability of BAP complexes to remodeling nucleosomes and reveal “protected” genetic elements so they can become accessible for binding by transcription factors and transcriptional machinery, generally a necessary step in gene activation. This is likely accomplished through both the nucleosome sliding (Alfert et al., 2019) and nucleosome removal (Boeger et al., 2004; Brown et al., 2011) properties that SWI/SNF complexes have been found to possess. Interestingly, BAP complexes in metazoans have also been shown to be in competition with Polycomb repressive complexes, both in binding and activity at genetic targets (Tamkun et al., 1992). Through these functions by which SWI/SNF complexes are able to regulate chromatin structure and thereby downstream gene expression, it is not surprising that they have been found throughout evolution to be critical for proper cell, embryonic, and tissue development, and have been implicated in disease and cancer when disrupted (Alfert et al., 2019).

Higher-Order Chromatin and Nuclear Organization

The “higher-order” chromatin structures that nucleosomes form are still the topic of much research. A compacted rod-like form of chromatin with high intra-nucleosomal interactions, called the “30-nm fiber” based on its molecular diameter, has been observed repeatedly *in vitro*, but the existence of this structure *in vivo* remains mostly unobserved and now commonly believed to be an artifact of non-physiological salt and protein conditions *in vitro* (Maeshima et al., 2019). More recently, high resolution STORM microscopy and advanced algorithmic analysis has revealed structures *in vivo* referred to as nucleosomal clusters, or clutches, roughly ~700nm3, which can vary in

size between cell types, and may represent a more native chromatin state within the nucleus (Ricci et al., 2015). The next-largest chromatin structure refer to the well-studied higher-order chromatin domains referred to as Topologically Associating Domains (TADs), which comprise of, on average, ~180kb scale self-interacting chromatin globules, whose structures somewhat rely on architectural proteins, and have been visualized, to some extent, all the way down to bacterial genomes. The exact function of TADs however is unknown. General trends demonstrate that TADs often correspond to DNA replication domains, and that interacting genetic elements tend to be within the same TADs, but the consistency of TAD structure between distinct cell types, and lack of dramatic phenotypes upon perturbation, suggests we may not yet fully understand their true function (Dixon et al., 2016; Szabo et al., 2019).

Interactions between distant genetic regulatory elements, generally between gene promoters and enhancers, are known to be important for regulation of gene expression. Promoters are usually directly upstream of gene transcription start sites (TSSs), while enhancer elements can be kilobases to megabases upstream or downstream of gene promoters, and while the interaction between the two is generally considered to promote gene expression, the mechanism for this is still unclear, though it has been the topic of much study. Interactions between regulatory elements, often promoters, of multiple genes can be clustered together in 3-dimensional space, usually to facilitate co-transcription or co-repression of similarly regulated genes. Two prominent nuclear bodies that can form to promote these functions are transcription factories and polycomb repressive bodies, both visible by genome interaction methods as well as microscopic analyses (Erdel and Rippe, 2018).

These nuclear bodies are components of genome organization at the highest order scale within the nucleus, and generally the localization of genes within the nuclear space represents a critical method for regulation of both gene expression and genome integrity. It has been well established that individual chromosomes tend to occupy their own “territories” within nuclear space, with some intermixing that likely correlates with interactions between regulatory elements (Rosin et al., 2018). However where individual genes are localized within the nucleus can be integral to regulation of gene expression and genome stability. Perhaps the most prominent nuclear scaffold with which genes interact is the nuclear lamina, a network of intermediate filament-like proteins called lamins, along with an armada of other proteins. These comprise a proteinaceous layer just under the nuclear envelope with a canonically repressive role with regard to the transcriptional activity of the interacting genes (Zullo et al., 2012). Over the last 15 years or so it has become clear that the NPCs imbedded in the nuclear envelope are also playing a critical role in regulation of genome organization, which will be discussed in the next section and through the remainder of this thesis.

Regulation of Chromatin Structure by NPCs and Nups

Since early characterization of NPCs via electron microscopy (EM) in the late 1950s, “intranuclear channels” could be seen extending from pores into the nucleoplasm (Watson, 1959). These channels were clearly associated with pores, “cylindrical” in nature, and “sharply outlined” in contrast to the more dense adjacent material abutting the nuclear envelope; material which we now know to be lamina-associated condensed

heterochromatin. As understanding of DNA structure and function developed throughout the years, these initial EM observations of what appeared to be open chromatin at nuclear pores were validated biochemically through the finding that DNase sensitive chromatin specifically localized to these same pore-associated intranuclear channels (Hutchison and Weintraub, 1985). By this point in 1985, it had been known for a decade that active genes were particularly sensitive to DNase digestion (Weintraub and Groudine, 1976), and so it only followed that the famous gene-gating hypothesis coincided with such strong validation of open, active chromatin at pores. In this hypothesis, Gunter Blobel predicted decades worth of future research describing the nuclear pore as a scaffold to organize and facilitate transcription and processing of active genes, and facilitate efficient export of newly synthesized gene product (Blobel, 1985). Further supporting these findings, there have been many studies demonstrating a preference for viral genome integration at DNA associated with NPCs (Marini et al., 2015; Manhas et al., 2018; Lelek et al., 2015). Over time, there has indeed been mounting evidence demonstrating the functional role of NPCs specifically in facilitating the upstream step of regulating chromatin state, so important for downstream transcriptional processes. For this reason, and based on the findings of this thesis project, we will now take an expanded examination of research involving known Nup involvement in the regulation of chromatin state and structure.

Nups and histone modifications

Nup98/100 and H3K4me2/3

Transcriptional memory is the phenomenon of enhanced rounds of subsequent transcriptional activation after an initial stimulus-induced transcriptional event(D'Urso and Brickner, 2014, 2017). Some of the first evidence of the association between Nups and active chromatin marks came from studies of human Nup98 and its yeast homolog in regulation of transcriptional memory. In these experiments, enhanced reactivation of memory genes requires Nup98 and the deposition of H3K4me2 (Light et al., 2013), a mark associated predominantly with promoters of active genes (Bernstein et al., 2005; Koch et al., 2007). Interestingly, H3K4me2 deposition at these promoters is dependent on Nup98, and this is true in both yeast and human cells (Light et al., 2013). As the di-methyltransferase Set1 (also capable of tri-methylation) was shown in yeast to be required for this deposition, it is plausible to hypothesize that Nup98 may promote interaction of Set1 with these genes to promote deposition of this mark. This is supported by data in human hematopoietic progenitor cells, where Nup98 interacts with a component of the homologous histone methyltransferase Set1A/COMPASS complex and is required for the targeting of the complex to promoters (Franks et al., 2017). Furthermore, genome-wide binding of Nup98 in these cells is often adjacent to the Set1A/COMPASS complex histone mark, H3K4me3, another mark associated with active promoters, and depletion of Nup98 results in defects in deposition of H3K4me3 at co-targeted promoters (Franks et al., 2017). In *Drosophila*, Nup98 interacts with and regulates expression of target genes of Trx, the protein responsible for H3K4me2 deposition (Pau Pascual-Garcia, 2014), see **Fig 1.1D**. This is especially interesting,

because while yeast Set1 and human Set1A are direct homologs, Trx is more distantly related, and the direct homolog dSet1A in *Drosophila* is responsible for monomethylation at this lysine residue (Shilatifard, 2012). Together this suggests Nup98 is intimately related to regulation of specifically di- and tri-methylation on H3K4, even switching protein-partners at one point in evolution to do so, implying an essential functional role in the regulation of chromatin state in this way. An important discovery in this field was also the role of Nup98 in regulation of genome architecture by way of facilitating transcriptional-memory-associated enhancer (E) - promoter looping (P) (Pascual-Garcia et al., 2017), see **Fig1.1B**.

Nup153 and CBP

Nup153 has also been shown to associate with active chromatin and histone modifiers. Early ChIP-chip experiments in *Drosophila* showed binding of Nup153 predominantly at active loci, associated with active transcription and RNAPII, and that it is required for expression of its target genes (Vaquerizas et al., 2010). More recently, a pronounced link between Nup153 and CBP/P300 function has been observed in mammalian cells. CBP/P300 are in a well-studied histone acetyltransferase (HAT) complex known to acetylate both histones in chromatin and non-histone proteins. Its chromatin-related activity is robustly associated with chromatin decondensation and gene activation as a transcriptional co-activator (Jin et al., 2011), as histone acetylation has been well established to biophysically induce chromatin decompaction and DNA accessibility *in vitro* and *in vivo* (Tolsma and Hansen, 2019). In cardiac tissue, Nup153 was found to interact with P300 and P300/CBP associated factor (PCAF) and target a

similar set of genes, and that binding to targets is increased in muscular dystrophy mouse model (Nanni et al., 2016). Additionally, both target gene expression, and P300/PCAF global and gene-specific acetylation activity, were correlated with overall protein levels of Nup153, in either upregulated or knocked-down conditions (Nanni et al., 2016). Together these data suggest Nup153 either plays a role in recruiting PCAF/P300 to chromatin, or increasing its acetylation activity once there, to promote expression of cell-type-specific target genes. In support of this, a paper that extensively explored the role of Nup98 FG domains in human leukemia-associated transcriptional upregulation found that the FG domain of Nup98 physically associated with CBP *in vitro* and *in vivo*, and this interaction robustly facilitated Nup98-induced expression of a target reporter gene (Kasper et al., 1999). Importantly, they also found that the Nup153 FG domain increased reporter gene activation. It's plausible to think that the FG domain in Nup153 may also bind CBP in this assay, which would again suggest evolutionary conservation in the role of this nucleoporin in regulating gene expression through interactions with/recruitment of chromatin modifiers, specifically CBP.

High resolution imaging of chromatin at pores

In an attempt to characterize the chromatin landscape at the pore, one group has recently utilized high-resolution Structured Illumination Microscopy (SIM) and developed sophisticated data analysis software. Using HeLa cells, they were able to visualize first that the EM images showing open chromatin, or heterochromatin exclusion zones (HEZs), are reproduced by DAPI stain and high resolution fluorescence imaging (Fišerová et al., 2017). In support of this, they were able to see that heterochromatin-

associated histone modifications such as H3K27me2 and H3K9me2 were explicitly excluded from this same region. Interestingly, and perhaps unsurprisingly, this was not true for active chromatin marks H3K4me2 or H3K9ac. Interestingly, they found histone demethylase LSD1 present not only at the pore, but within the boundaries of the pore, as defined by TPR basket staining. LSD1 is known to demethylate both H3K4me2/1, commonly associated with active promoters, but also H3K9me2/1, commonly associated with condensed, repressed heterochromatin. As there is a deficit of this heterochromatin mark, and no deficit of this active chromatin mark, associated with the pore in this study, it is enticing to envision that the pore utilizes LSD1 in this context specifically to help maintain an open, active chromatin environment here, for transcriptional or other purposes.

Activation and Repression Dichotomy: Nup155/170p and compaction

One clear theme within the field of nuclear pore proteins, whether it's apparent in their roles in transport or their roles in regulating chromatin state and gene expression, is that the ~30 nucleoporins comprising the pore are truly individual proteins that can sometimes have very divergent functions. Although most of the pore and its constituent Nups seem to be involved in regulating activation, there are some examples where nucleoporins are involved in facilitating formation of repressed chromatin, and reducing gene expression levels. One potential explanation for this could be that the Nups bound to condensed chromatin may be binding genes across the boundary between euchromatin and the adjacent lamina-associated heterochromatin. Another could be that not all pores in a nucleus perform the same functions, and some pores may be involved

in more chromatin and gene repressive functions. While the reasoning behind this dichotomy is still a mystery, but it is still clear that in a few instances, NPCs/Nups appear to be involved in repression.

One of the first studies on this showed a relationship between Nup155 and HDAC4 in human cardiomyocytes (Kehat et al., 2011). HDAC4 is a histone deacetylase (HDAC), which is canonically and robustly implicated in inducing chromatin compaction and gene repression. Nup155 was found to physically interact with HDAC4 in these cells, and when their interaction was inhibited, the expression of many HDAC4 target cardiac genes sky-rocketed, suggesting Nup155 normally promotes HDAC4's silencing capabilities (Kehat et al., 2011). Nup155's role in promoting chromatin compaction and repression is conserved from yeast homolog Nup170p, where one study found Nup170p was required for localization of the silencing factor Sir4 to subtelomeric chromatin (Van de Vosse et al., 2013). While not a histone modifier itself, Sir4 is well-established as a critical protein required for chromatin compaction in yeast, recruiting HDACs to target genes which in turn induce formation of repressive chromatin (Xu et al., 2007). A few years later, it was shown that these interactions between Nup170p and Sir4 exist in a complex with a subset of Nups and telomere-localizing machinery in a complex distinct from fully intact NPCs in the nuclear envelope (Lapetina et al., 2017), lending credence to the hypothesis that there may be different NPC or NPC-like structures in the envelope with distinct functions, an intriguing concept worthy of more study. Compellingly, the importance of Nup170p role in facilitating chromatin compaction is bolstered by the finding that it also utilizes chromatin-remodeling proteins in addition to histone modifiers in promoting repression, as will be discussed in the next section.

Nups and polycomb repression

Interestingly, not only can different Nups have opposing roles in the regulation of chromatin state, but the same Nup can have opposing functions depending on cell type or developmental context. Nup153, which, as we previous discussed, regulates function of CBP/P300 complex to promote gene expression in cardiac tissue, also has a gene repressive role in mouse Embryonic Stem Cells (mESCs) (Jacinto et al., 2015). In this study they found that Nup153 loss in mESCs resulted in de-repression of many developmental genes, and thus promoted early differentiation. When they looked at the Nup153 binding profile via Dam-ID genome mapping, they observed co-binding with Polycomb Repressive Complex 1 (PRC1) components at developmental gene Transcription Start Sites (TSSs). Furthermore, not only did Nup153 biochemically interact with PRC1 components, but its loss also reduced binding of PRC1 component Ring1 to target differentiation genes (Jacinto et al., 2015). PRC1 is known for its role in depositing repressive mark H3K27me3 on histones. Importantly, Nup153, along with Nup107 and Nup62, were also found to regulate occupancy and activity of other polycomb complex components, and regulate gene imprinting repression in mouse embryonic endoderm cells (Sachani et al., 2018). Furthermore, Nup93 has been found to repress expression of the HoxA gene and promote polycomb-associated mark H3K27me3 in human cancer cells (Labade et al., 2016). The mechanism behind how Nup153 can recruit these repressive proteins to facilitate repression of some genes in some cell types, and simultaneously also recruits/activates CBP/P300 for activation of different genes in another cell type, is both an unknown and an intriguing question for future research to untangle. Regardless, the importance of Nups in recruiting histone-

modifying proteins to affect chromatin structure and downstream gene expression cannot be ignored, and is an exciting notion considering these proteins were once thought to merely provide a mechanism for nucleocytoplasmic transport.

Chromatin remodeling and compaction state

Nup170p and RSC

Here we will discuss several examples from throughout evolution in which Nups interact with, and have sometimes been shown to regulate recruitment or function of, chromatin remodeling proteins, providing further evidence that a key function of NPCs/Nups is to regulate chromatin compaction and accessibility for downstream transcription. As described in the previous section, mammalian Nup155/yNup170p interacts with repressive histone modifiers, or proteins that recruit them, to facilitate target gene repression. Interestingly, Nup170p is also involved in facilitating increased chromatin condensation and repression of targets, but instead employs chromatin remodeling proteins for this function. In one study demonstrated a relationship between Nup170p and RSC, a chromatin remodeler involved in telomere maintenance (Van de Vosse et al., 2013). A Nup170p genetic interactor screen came up with several protein complexes associated with formation of repressive chromatin, including a remodeler, 2 HDACs, and a histone ubiquitylase. However, physical interaction with these specific proteins could not be found, suggesting the genetic interaction was due to functioning in similar pathways. When analyzing differentially expressed genes in a Nup170p mutant line, 90% showed an increase in expression, demonstrating a

functional role of Nup170p in global gene silencing. In these upregulated genes, many ribosomal protein (RP) and subtelomeric genes were found, which led to discovery of a physical interaction between Nup170p and Sth1p of the RSC remodeling complex, associated with telomere maintenance and repression of subtelomeric genes. Nup170p is found bound to many of these subtelomeric genes by ChIP, and loss of Nup170p results in an increase in nucleosome occupancy surrounding subtelomeric gene TSSs, which phenocopied Sth1p depletion (Van de Vosse et al., 2013). Together these data strongly suggest Nup170p plays an important role in recruitment or activity of the RSC remodeling complex at these genetic targets, resulting in more condensed chromatin and downstream transcriptional repression.

Elys and chromatin remodelers

A lot of research has been generated demonstrating the importance of nucleoporin Elys and its homologs in regulating mitotic/meiotic chromosome segregation and seeding post-mitotic pore formation (Gómez-Saldivar et al., 2016), in addition to its canonical function as a component of NPCs. Consistent with this, Elys is the only nucleoporin with a putative Chromatin or DNA binding domain and additionally has demonstrated H2A-H2B dimer and nucleosome binding capacity in vitro (Rasala et al., 2008; Inoue and Zhang, 2014; Gómez-Saldivar et al., 2016; Zierhut et al., 2014). However when Elys was originally discovered, before it was even known to be a component of NPCs, it was as a Transcription Factor (TF) capable of inducing expression when targeted to a reporter gene (Kimura et al., 2002). The mechanism of this has not been elucidated, however there is some evidence to hypothesize it may be

through interaction with chromatin remodelers and therefore possible subsequent chromatin accessibility increase. There are a few examples of past findings of Elys interacting with chromatin remodeling proteins throughout evolution to support this notion. The *C. elegans* homolog of Elys, Mel-28, has been seen to interact with an accessory subunit of the SWI/SNF chromatin remodeling complex, specifically component swsn-2.2 (Ertl et al., 2016), homolog of human BAF-60, a remodeling complex also important for decondensing chromatin to allow for downstream transcriptional processes (Peterson and Herskowitz, 1992). A genetic interactor screen in the background of Mel-28 RNAi revealed an interaction with *pyp-1*, the homolog of *Drosophila* NURF-38, resulting in larval sterility (Fernandez et al., 2014). In human cells, a mass spectrometry screen unearthed an interaction between Elys and HMGN3 (Fasci et al., 2018), a member of a family of proteins known to interact with histone H1, promote chromatin decondensation, and upregulation of target genes (Rochman et al., 2009). NURF-38 is a core component of the Nucleosome Remodeling Factor (NURF) chromatin remodeling complex and promotes chromatin accessibility for downstream transcription (Gdula et al., 1998; Mizuguchi and Wu, 1999). Further exploration into this topic has been conducted during this thesis project, and will be explored in Chapter 2

Genome architecture and large-scale chromatin structure

Elys and global chromatin decompaction

So far we have discussed examples of how Nups interact with specific chromatin-modifying or remodeling enzymes, and examples of changes of specific

chromatin marks at select sets of target genes. In this section we take a step back and look at some examples of known functions of Nups in larger-scale, sometimes genome-wide regulation of chromatin and genome organization. The first example is related to the function of Elys in regulating global chromatin state. One study looking at DNA replication in *C. elegans* finds a defect in global genome decondensation in the background of mutant replication machinery, but this phenotype was rescued in an Elys mutant, suggesting functions in the same pathway (Sonneville et al., 2015). In a later studying expanding the analysis of the role of Elys in this context, the authors examine the genome decondensation that occurs upon fertilization in the *Xenopus* sperm nucleus. Here they found treatment with RNases depleted Elys off of chromatin, and this resulted again in defects in chromatin decondensation (Aze et al., 2017). Specifically they saw smaller nuclei with more intense nuclear H2B immunofluorescence stain and chromatin density by EM, and more compact chromatin by MNase digestion, which was proved to not be due to transport defects as treatment with WGA transport inhibitor did not present a defect. This data combined with the previously discussed relationships between Elys and various chromatin remodelers throughout evolution suggest a role for nucleoporin Elys in regulation of chromatin decompaction through interaction and regulation of chromatin remodeling proteins, which will be expanded on in Chapter 2.

Seh1 and chromatin accessibility

Along these lines, it is worth it to take a moment to look at a study about Seh1, a Sec13-like Nup and a component of the same NPC subcomplex as Elys, also known to play similar roles in NPC/Nuclear envelope formation and chromosome segregation

(Platani et al., 2018). Seh1 was found to bind genes with cell type specific expression in mammalian oligodendrocyte progenitor cells and regulate both the expression and chromatin accessibility of target genes involved in oligocyte differentiation, as measured by ATAC-seq (Liu et al., 2019). Additionally they found interactions between Seh1 and cell-type specific transcription factors in these cells, which we will discuss in the "Nups in Transcription" section below.

Nups, dosage compensation, and MOF

Over the years, several papers have been published involving the role of Nups in dosage compensation (DC). The inequality between X-chromosome number between male and female organisms requires a method by which to equalize gene expression from the X, which different species accomplish utilizing different mechanisms. This level of transcriptional regulation is no small feat, as it requires changing the transcriptional output of genes from an entire chromosome. In *Drosophila* the Dosage Compensation Complex (DCC) binds along the length of the X-chromosome, as is a common theme for DC machinery in all species, and is responsible for ~2-fold upregulation of X-linked genes in male flies. The DCC contains a HAT called MOF responsible for depositing the activating mark H4K16ac, which coats the male X-chromosome and is necessary for transcriptional upregulation (Lucchesi, 2018). In male *Drosophila* embryos, Nups Mtor and Nup153 were found to interact with MOF and other DCC components, and upon Nup depletion, the normally robust localization of MOF and other DCC machinery to the X-chromosome was completely abolished, along with the downstream transcriptional upregulation of X-linked genes (Mendjan et al., 2006). Interestingly, they also found an

interaction between the human orthologs of Mtor and MOF, even though the methods of DC are drastically different. In line with these findings, ChIP-chip binding patterns of Mtor and Nup153 are found throughout the *Drosophila* genome in large domains termed Nucleoporin Associated Regions (NARs), enriched especially at transcriptionally active regions (Vaquerizas et al., 2010). Fascinatingly, ~70% of these domains were localized to the male X-chromosome. Furthermore, this study found a robust co-localization of the genome-wide binding patterns of Nups, H4K16ac and MOF (Vaquerizas et al., 2010). In another intriguing conservation of function, interactions between the X-chromosome, dosage compensation, and pores have been found in *C. elegans* as well, even though DC is accomplished by condensation and down-regulation of the X, as in humans, rather than activation and transcriptional upregulation (Sharma et al., 2014). One comment of note is that the importance of Nups in *Drosophila* dosage compensation is in debate. A more recent study explicitly did not find a reliance of Nups in *Drosophila* larval tissue or S2 cell DC, and the authors propose a difference in knock-down methods as the culprit (Grimaud and Becker, 2009). However the independent findings of protein-protein interactions between Nups and DCC machinery in *Drosophila* and humans (Mendjan et al., 2006), the interaction of pores and the X-chromosome in *C. elegans* (Sharma et al., 2014), and the discovery of huge binding domains of Nups on the *Drosophila* male X-chromosome (Vaquerizas et al., 2010), are in support of the hypothesis that they have a conserved function in DC, and suggest that this topic warrants further study. For a visual summary of these phenomena, see **Figure 1.1C**.

Mtor in intranuclear bodies

A recent study provides another example of the function of nucleoporin Mtor in large-scale genome organization. Here they found that Mad1, a protein normally part of the mitotic spindle assembly checkpoint, was found in post-mitotic and interphase *Drosophila* spermatocyte nuclei in what the authors termed Mad1-containing IntraNuclear Territories (MINTs) (Raich et al., 2018). Of particular interest to those of us interested in NPCs, they also found other proteins in these chromatin-associated MINTs, including Mtor, which canonically has been shown to anchor Mad1 to the nuclear envelope for its spindle associated functions, in an evolutionarily conserved fashion (Lee et al., 2008; Lince-Faria et al., 2009). Furthermore, Mtor was required for the formation/maintenance of these intranuclear bodies, as depletion of Mtor caused a complete dissolution of proteins associated with MINTs from these structures. The function of MINTs is so far not known, but one hint may be in the role these authors found of Mad1. To test if Mad1's localization to these intranuclear bodies had anything to do with regulating chromatin function, the authors conducted a Position-Effect-Variegation (PEV) assay and an assay to test for genetic interaction with polycomb repressive complex, and found in both cases that Mad1 appears to promote open chromatin formation or maintenance (Raich et al., 2018). This finding suggests perhaps the function of the intranuclear MINT bodies may involve regulation of open chromatin, and since the existence of these bodies is Mtor dependent, implicate a possible role for Mtor in this process.

Mtor and open chromatin at the periphery

This relationship between Mtor and MINTs, and Mtor's role in DC, is not the extent of the data supporting that Mtor plays an evolutionarily conserved role in promoting an active chromatin environment. As mentioned at the beginning of this "Regulation of Chromatin by NPCs and Nups" section, the peripheral chromatin localized to NPCs is open and euchromatic in nature relative to the adjacent condensed lamina-associated heterochromatin. One group set out to understand what regulates these heterochromatin exclusion zones (HEZs), and found that the mammalian homolog of Mtor was required for their formation (Krull et al., 2010). In cells in which this Nup was depleted, HEZs were abolished and the heterochromatin at the periphery continued un-disrupted across NPCs. These were not in typical mammalian cells, as the pronounced HEZs here were produced by infection with a poliovirus. However HEZs have been detected for decades in many different, wild-type cells across species (Watson, 1959; Capelson and Hetzer, 2009), and here we have discussed mounting evidence that Mtor, and many Nups, do play pronounced roles in regulating chromatin structure.

Many of the interactions between Nups and chromatin factors have produced demonstrable functions in regulation of downstream gene expression. An interesting facet of the NPC field is that regulation of gene expression overall has become a well-established function of NPCs and individual Nups. We will discuss some prominent findings on this topic below, where, in the examples to follow, the roles so far of these Nups have not indicated any direct upstream regulation of chromatin state, but at a step closer to transcriptional activation. In some cases the mechanism is somewhat known, for example a common trend is that that Nups recruit specific transcription factors to

facilitate downstream gene expression. However I hope I have drawn some attention to the clear importance of Nups in regulation of chromatin itself, and that these findings may be kept in mind while examining future research as the field of Nups in regulation of gene expression continues to be explored, and my own work described in Chapter 2.

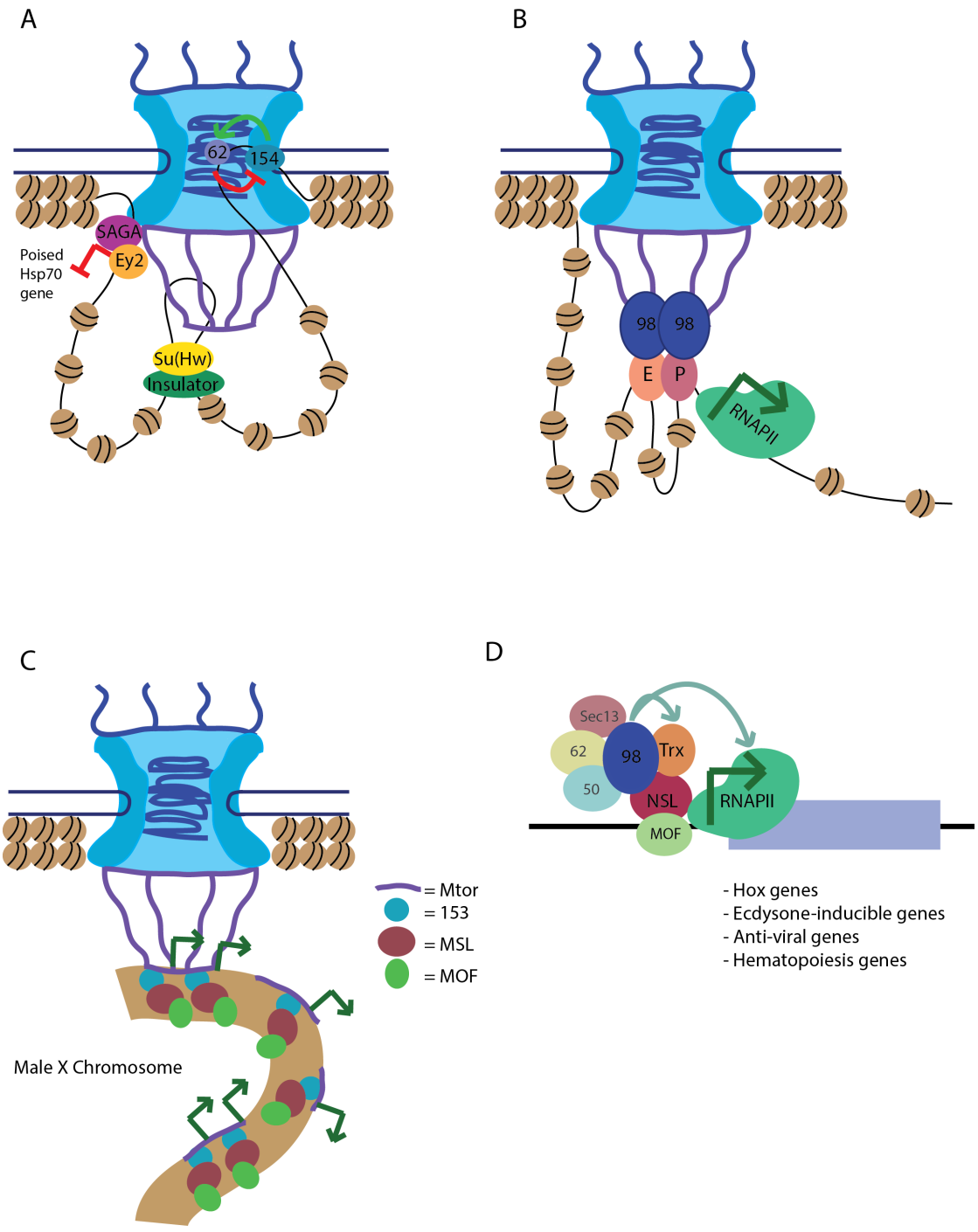

Figure 1.1 NPCs and Nup regulation of chromatin and transcription summary

Transcriptional Activation

As has been mentioned multiple times in previous sections, a critical upstream step of transcriptional activation is the decondensation or opening of chromatin to make genetic elements accessible to transcription factors and transcriptional machinery. In order to put that into context, and also understand better the currently known roles of Nups in transcription as discussed in detail below, it is important to introduce the basic factors involved in activating gene expression.

The term transcription factors (TFs) encompasses two main categories, termed general and specific TFs. Specific transcription factors are developmental, cell-type specific, or context dependent. Their expression, binding patterns and activity are varied, and they facilitate gene expression programs specific to the current needs of the cell. General transcription factors (GTFs) are proteins that are required by RNAPII at virtually all genes, requisite components for successful transcription. About 100 proteins, including multiple GTFs, comprise what is known as the Pre-Initiation Complex (PIC) present at promoters of genes, and represent the minimal complex required to localize and activate RNAPII for productive transcription of target genes. PIC components also include DNA helicases to unwind DNA, chromatin remodelers and the HAT SAGA complex to facilitate accessibility, and the Mediator complex, providing for communication of signal between specific and general transcription factors (Gottesfeld et al., 2018).

Also recruited to promoters is a host of kinases used to phosphorylate the C-Terminal Domain (CTD) Tail of RNAPII. Many additions of phosphorylation marks are

requisite for transcription, the two most famous being phosphorylation on Ser5, designating transcriptional initiation, and then subsequently on Ser2, observed on RNAPII found throughout the gene body, representing release from the promoter and productive elongation of RNA transcript (Phatnani and Greenleaf, 2006).

Regulation of Transcription by NPCs and Nups

Here I will survey research describing NPC and Nup regulation of gene expression in ways that are not known to be overtly related to regulation of upstream chromatin structure. Early work in this field, as covered previously, has established that Nups bind chromatin in multiple cell types, that many of the targets tend to be cell cycle and developmental genes, and that this binding can have an effect on gene expression (Capelson et al., 2010; Kalverda et al., 2010; Casolari et al., 2004; Taddei et al., 2006; Schmid et al., 2006). Over the years, more examples and mechanisms behind some of the specific functions Nups have with regard to regulation of transcription have been further elucidated, and so here I cover some of the most prominent discoveries in this field and trends among them.

Nup98 and Hox genes

The theme of Nups binding and regulating cell identity genes has proven robust between cell types and throughout evolution. This is very intriguing when taking into account that there are many tissue-specific defects and diseases amounting from Nup mutations and dysfunctions (Jühlen and Fahrenkrog, 2018; Talamas and Capelson,

2015). Perhaps the most famous of these involves Nup98 and the frequency with which it is a member of chromosomal translocations that results in mammalian leukemogenesis. One recent paper found a fusion of the N-terminus of Nup98 with the C-terminus of transcription factor (TF) HoxA9 to target many developmental Hox genes, known to regulate organismal body morphogenesis, present in facultative heterochromatin in multiple cell types (Oka et al., 2016). This association resulted in target upregulation, a common hallmark of Nup98 fusions. While specific targeting of Nup98 fusion proteins is often proposed to be regulated by Nup98's fusion partner, endogenous full-length Nup98 has been shown in *Drosophila* to bind and regulate expression of Hox genes (Pascual-Garcia et al., 2014). This targeting relies on MBD-R2, a component of the *Drosophila* NSL complex, in which MOF is also a member, responsible for depositing active histone mark H4K16ac. Nup98 is found to work in conjunction with canonical Hox regulator Trx, as reduction of Nup98 is sufficient to reduce expression of Trx targets. Overall these studies support the role of Nup98 in regulating expression of key developmental Hox genes in both endogenous and disease contexts. Though the mechanism of this regulation is still unknown, Nup98 in other contexts has been shown to associate with architectural proteins and regulate Enhancer-Promoter looping in the context of transcriptional memory (Pascual-Garcia et al., 2017), and perhaps could perform this function to regulate expression of many of its target genes.

Nup153, Nup93, and regulation of cell identity

Nup98 is not the only Nup known to bind enhancers. Nup153 and Nup93 have recently been found to bind super-enhancers (Ibarra et al., 2016), powerful clusters of enhancers especially known for regulation of cell-identity genes. Moreover, a third or more of superenhancers have one or both Nups bound in the multiple human cell types analyzed, and the binding of Nup153 or Nup93 was critical for appropriate gene expression. Of special interest, the direction of change in gene expression was not uniform, in that roughly half of each of their gene targets went up and the other half down upon reduction of either Nup. While a dichotomy between distinct Nups activating while others repress transcription is not novel, this is an interesting example of individual Nups having both positive and negative effects on gene expression in the same cell populations, and is consistent with findings of both Nup153 and Nup93 at, or involved in regulation of, repressed genes (Brown et al., 2008; Jacinto et al., 2015). While the possibility of secondary downstream affects in the RNA-seq data should always be taken into account, this could present an interesting case demonstrating the context-dependent nature of Nup functions at different genetic targets and would warrant further study to determine specific mechanisms utilized.

Nups and transcription factors

One mechanism behind regulation of specificity of function for individual Nups at different genetic targets may lie in differential protein binding partners, especially that of cell-type/context dependent transcription factors (TFs). Such binding partners have been identified for Nup153 in regulation of differentiation in neural progenitor cells (NeuPCs)

(Toda et al., 2017). Specifically, Nup153 has been found to interact with, and regulate genomic binding of, TF Sox2. While important for maintaining embryonic stem cell pluripotency, Sox2 has also been shown to cooperate with canonical NeuPC transcription factors to regulate both maintenance and differentiation of NeuPCs. Accordingly, many of the genes disrupted by Nup153 reduction were associated with neural development, and Nup153 loss promoted differentiation. In a manner consistent with previously discussed negative transcriptional regulation by Nup153 (Jacinto et al., 2015), there were an equal number of up- and down-regulated gene targets upon Nup153 reduction, suggesting again perhaps the ability to control transcription via multiple mechanisms. Importantly some of this regulation appears to be through targeting or maintenance of Sox2 on chromatin, as loss of Nup153 reduced Sox2 signal at over half of its genomic targets. Interestingly, the direction of transcriptional regulation by Nup153 correlated with its location on gene targets, in that 5' localization trended towards facilitating transcription, and 3' targets were more often associated with gene repression. This was in contrast with Sox2 localization, which was primarily at 5' TSSs regardless of its transcriptional effect on its targets (Toda et al., 2017).

Nups regulating binding or activity of cell-type specific transcription factors to control transcriptional programs is becoming a common trend in the field. This has also been seen for Nup210 in recruiting muscle TF Mef2C, and its genomic targets, to NPCs at the periphery of myofiber nuclei to promote expression of genes regulating muscle differentiation (Raices et al., 2017). Similarly, Nup Seh1 has recently been shown to recruit oligodendrocyte transcription factors Olig2 and Brd7 to NPCs to promote development from oligodendrocyte progenitor cells (Liu et al., 2019). To further support

this trend, a recent study in yeast has shown that simply tethering most transcription factors to yeast NPCs is sufficient to target their respective genes to the periphery (Brickner et al., 2019), which in many cases is associated with promoting target gene expression (D'Urso and Brickner, 2017). These findings provide further evidence to support the notion of NPCs and their constituent Nups as transcriptional hubs, utilizing interactions with context-dependent and cell-type-specific transcription factors to promote developmental transcriptional programs. It is of note that in the past Nups have been shown to interact and cooperate with general transcription factors/coactivators such as Mediator (Schneider et al., 2015) and the SAGA complex (Luthra et al., 2007) (see **Fig 1.1A**), whose roles are more canonically downstream from specific TFs and typically function as universal transcriptional machinery, with SAGA performing histone acetyl-transferase activity to promote chromatin decondensation and accessibility. Overall this data demonstrates the ability of Nups to regulate transcription of target genes via multiple mechanisms, one of which includes recruiting or stabilizing binding of cell-type specific transcription factors in order to regulate cell identity. The fact that Nups can be linked to various stages in general and specific transcriptional processes is a testament to the multi-functionality of the NPC and its constituent nucleoporins.

Nups and transposon silencing

Recently, multiple studies have demonstrated a role for NPCs and Nups in silencing of transposable elements (TEs). Specifically, Piwi, a critical component of the piRNA pathway responsible for silencing TEs, uses complementary piRNAs to seek and target TEs for degradation. Interestingly, genomic targets of Piwi were found to

substantially overlap with maps of NPC genomic targets (Ilyin et al., 2017). A further study demonstrated direct interaction between Nup358 and Piwi (Parikh et al., 2018). What is especially interesting is the additional requirement of Nup358 on piRNA biogenesis as well, which is a process not known to rely upon Piwi but other components of the transposon silencing pathway. Likely due to a combinatorial affect, Nup358 reduction resulted in a de-silencing of TEs, which had a predictable negative effect on genomic stability. As several Nups have been discovered in screens identifying factors involved in TEs silencing, it seems this may be a general function of NPCs/Nups that will likely warrant further study to fully understand (Handler et al., 2013; Muerdter et al., 2013). The suppression of transposable element expression by NPCs is especially interesting in the context of their other role in protecting genome stability through facilitating DNA damage repair and telomere maintenance (extensively reviewed in (Géli and Lisby, 2015; Nagai et al., 2011)).

Conclusion

That NPCs have developed multiple mechanisms throughout evolution by which to ensure genomic integrity, as well as regulate mitosis, nuclear organization, transcription and chromatin state and, of course, transport, truly speaks to the pleiotropic nature of the NPC and its constituent Nups. As we have discussed, these proteins have proven to be critical for many roles promoting proper nuclear organization and function, especially with regard to chromatin structure and gene expression. There are a multitude of associations and functions of nucleoporins in regulation of chromatin structure and target gene transcription. Some mechanisms are known, based on interaction with

histone modifying complexes (Nanni et al., 2016; Kasper et al., 1998; Kehat et al., 2011; Jacinto et al., 2015; Pascual-Garcia et al., 2014), specific transcription factors (Toda et al., 2017; Raices et al., 2017; Liu et al., 2019), or components of transposon silencing machinery (Parikh et al., 2018; Ilyin et al., 2017). However many associations between Nups and genomic changes are changes in gene expression or chromatin state of unknown mechanism (Krull et al., 2010; Aze et al., 2017; Kimura et al., 2002; Fišerová et al., 2017 etc). Through the work of this thesis described in the chapter below, we believe that many examples of Nup-based regulation of gene expression and chromatin with as-of-yet unknown mechanisms may rely on their interactions with chromatin remodeling complexes, and subsequent chromatin decondensation that facilitates downstream binding of transcription factors and transcriptional machinery. This work is consistent with aforementioned interactions between Nups and chromatin remodelers that were observed but not mechanistically pursued (Van de Vosse et al., 2013; Ertl et al., 2016; Fernandez et al., 2014; Fasci et al., 2018), and contributes to our understanding of the function of nucleoporins in regulation of the genome.

Table 1.1 Nup Mutations and their Phenotypes in *Drosophila melanogaster*

Nup	Nature of Aberration/ Perturbation	Phenotype	Paper(s)
Nup358/ RANBP2	RNAi in S2 cell culture	Inhibition of proliferation and mRNA export, relocalization of NXF1 to cytoplasm	Forler… Izaurralde 2004
	RNAi in S2 cell culture	Defective importinβ translocation into nucleus	Sabri… Samokovlis 2007
Nup214	RNAi in S2 cell culture	Inhibition of proliferation and mRNA export	Forler… Izaurralde 2004
	Mutant Nup214^{10444} excision allele, RNAi in S2 cell culture	Release of nuclear export factor CRM1 from the nuclear envelope, increase in general nuclear export efficiency, reduced Nup88 protein levels and localization to nuclear envelope, abolished nuclear import of NFκB factors	Xylourgidis… Samakovlis 2006
	RNAi in S2 cell culture	Reduced CRM1 at nuclear envelope, dependent on 214 FG repeats	Sabri… Samkovlis 2007
Nup88/ mbo	Null mutations mbo^{1} and mbo^{2}	-Trachea cell-type specific expression and defects -Defects in nuclear import of specific proteins, including yeast TF Gal4 and NFκB factors, with corresponding decrease in immune response gene expression, upon bacterial challenge	Uv… Samakovlis 2000
	Mutant fly lines (unlisted, mbo^{1} according to flybase)	Release pf Nup214 and CRM1 from the nuclear envelope, increase in general nuclear export efficiency	Roth… Samakovlis 2003
Nup98	RNAi in S2 cell culture	Reduced expression of canonically active nucleoplasmic developmental gene targets, reduction of nup50 interaction with target genes	Kalverda... Fornerod 2010
	RNAi in S2 cell culture and RNAi line 31198 (VDRC)	Reduced RNAPII recruitment to, transcription of, and chromatin decondensation at target genes in salivary glands, reduced transcription reactivation after heat shock	Capelson… Hetzer 2010
	RNAi in S2, DL2 cell culture and RNAi line 31198 (VDRC)	Increased cellular and organismal susceptibility to SINV, VSV, WNV and DCV viral infection and increased subsequent viral replication, and decreased *Drosophila* antiviral gene expression	Panda… Cherry 2014
	RNAi line from VDRC and null mutation *Nup98*$^{Df(3R)mbc-R1}$	Loss of progenitor cells in lymph gland primary lobe differentiating cells, likely through demonstrated reduction in Pvr expression	Mondal… Banerjee 2014
	RNAi in S2 cell	Reduction in expression of target genes,	Pascual-

	culture, RNAi lines 31198 and 109279 (VDRC)	including Hox genes Ubx and Antp in developing larval imaginal discs	Garcia… Capelson 2014
	RNAi in DL1 cell culture	Reduced expression of FoxK target genes	Panda… Cherry 2015
	RNAi in S2R+ cell culture	Increase in nuclear actin levels and actin mobility, indicative of decreased actin polymerization	Dopie… Vartiainen 2015
	Expression of leukemic Nup98-HoxA9 fusion protein in transgenic *Drosophila*	Overgrowth of lymph gland, aberrant hemocyte proliferation and differentiation, and non-cell autonomous expansion of the PSC hematopoietic niche	Baril… Therrien 2016
Rae1	RNAi in S2 cell culture	Reduced cyclin E levels and cellular proliferation, and increased accumulation in cell cycle phase G1	Sitterlin 2003 (lone author)
	Mutant lines $Rae1^{EX28}$ $Rae1^{EXB1\frac{1}{2}}$	Reduced stability of ubiquitin ligase Hiw protein, and subsequent aberrant synaptic terminal growth at neuromuscular junctions	Tian… Wu 2011
	Point mutant line $Rae1^{Z5584}$, VDRC RNAi line (unspecified)	Defects in spermatogenesis, nuclear integrity and chromosome condensation, metaphase plate and meiotic spindle morphology, and chromosome segregation defects, resulting in male sterility	Volpi… Prantera 2013
	Mutant line *Rae1*^{ex28} and RNAi lines v29303 (VDRC), 9862R-2 and 9862R-3 (NIG) and HMS00670 (TRiP)	Reduced cellular proliferation, resulting from decreased entry into cell cycle phase S and proteins levels of cyclins A and B, leading to reduced tissue/organ and organismal size	Jahanshahi…. Pfleger 2016
Nup160	Hybrid incompatibility	Lethality if simulans Nup160 hybrid in melanogaster background with *D. mel* X chromosome	Tang and Presgraves 2009, Barbash 2007, Sawamara…Matsuno 2014, Tang and Presgraves 2015
	Hybrid incompatibility	Recessive female sterility if $Nup160^{sim}$ in melanogaster background	Presgraves 2003, Tang and Presgraves 2009, Sawamura 2010
Nup107	RNAi in S2 cell	Impaired cytokinesis in meiosis, loss of	Hayashi 2016

	culture	contractile ring recruitment, and mislocalization of Lam (B) in meiosis	
	RNAi lines 22407 and 110759 (VDRC) and point mutation Nup107^{D364N} mimicking that in human disorder	Defective female oogenesis	Weinberg-Shukron 2015
	RNAi lines	Amelioration of eye degeneration phenotype associated with repeat expansion proteins in *Drosophila* ALS/FTD model	Boeynaems... Van Den Bosch 2016
Nup96	Hybrid incompatibility	Lethality if hybrid simians gene in melanogaster background, only in presence of D. mel X	Presgraves… Allen 2003,
Nup98-96	Hypomorphic mutation *nup98-96*^{2288} disrupting both proteins, and RNAi lines 31198 and 31199 (VDRC)	Defective transit amplification of germ line stem cells	Parrott 2011
Nup75	RNAi in S2 cell culture	Impaired nuclear import of activated MAD	Chen and Xu 2010
Seh1/ Nup44A	Null seh1$^{\Delta 15}$ *seh1*$^{\Delta 86}$ deletions	Defective female oogenesis leading to female sterility - improper oocyte fate, posterior centriole positioning, inappropriate Mtor distribution (Senger), reduced TORC1 activation and autophagy inhibition in female germ cells (Wei)	Senger 2011, Wei 2014
	RNAi lines	Exacerbation of eye degeneration phenotype associated with repeat expansion proteins in *Drosophila* ALS/FTD model	Boeynaems... Van Den Bosch 2016
Sec13	RNAi in S2 cell culture, RNAi line 50367 (VDRC)	Reduced RNAPII recruitment to, transcription of, and chromatin decondensation at target genes in salivary glands, reduced transcription reactivation after heat shock	Capelson… Hetzer 2010
	RNAi in S2 cell culture	Impaired nuclear import of activated MAD	Chen and Xu 2010
Nup37	Mutation	Increased immunity associated with decreased bacterial load and increased survivability upon infection	Von Ohlen 2012
Nup205	RNAi in S2 cell culture	Impaired nuclear import of activated MAD	Chen and Xu 2010
Nup154	Hypomorphic *tlp*^{1} *, tlp*^{2}, and	-Male and female sterility - defective cyst formation, regulation of spermatocyte	Gigliotti 1998, Kiger 1999,

	strong hypomorphic *nup154*^{1} and *nup154*^{6} mutations	proliferation and meiotic progression in testes; stunted egg chamber development and oocyte growth in ovaries -Mislocalized 414 FG Nups in egg chamber cells	Colozza 2011
	Strong hypomorphic mutations *nup154*^{1} *nup154*^{6}	Larval lethal, reduction in size of discs, brains, and testes	Kiger 1999
	Hypomorphic *tlp*^{2} mutation	Defect in chromatin structure in late stage egg chambers, corresponding in egg-chamber developmental arrest	Grimaldi 2007
	Hypomorphic and null mutations	Mislocalization of actin filaments in egg chambers, misregulation of apoptosis in egg chambers and spermatogonial germ cells	Riparbelli 2007, Colozza 2011
	RNAi in S2 cell culture and hypomorphic *tlp*^{1} mutation	Impaired nuclear translocation of MAD in culture and testes	Colozza 2011
	S2 and KC cell culture RNAi	Mislocalization of INM proteins LBR and otefin to cytoplasm	Busayavalasa… Sabri 2012
	RNAi lines	Amelioration of eye degeneration phenotype associated with repeat expansion proteins in *Drosophila* ALS/FTD model	Boeynaems... Van Den Bosch 2016
Nup93	RNAi in S2 cell culture	Impaired nuclear import of activated MAD	Chen and Xu 2010
	RNAi TRiP lines HMS00850 and HMS00898)	Increase in peripherally anchored chromatin in ovary	Breuer and Ohkura 2015
	RNAi in S2 cell culture	Release of Nup154 from nuclear envelope	Busayavalasa… Sabri 2012
	RNAi lines	Exacerbation of eye degeneration phenotype associated with repeat expansion proteins in *Drosophila* ALS/FTD model	Boeynaems... Van Den Bosch 2016
Nup62	RNAi TRiP lines HMS00850 and HMS00898	Increase in peripherally anchored chromatin in ovary cells	Breuer and Okhura 2015
	RNAi lines	Exacerbation of eye degeneration phenotype associated with repeat expansion proteins in *Drosophila* ALS/FTD model	Boeynaems... Van Den Bosch 2016
Nup54	RNAi in S2 cell culture	Reduction in cellular importinβ levels and nuclear import of NLS-GFP reporter	Sabri… Samokovlis 2007
Nup153	RNAi in S2 cell	Delocalization of MSL proteins from male X	Mendjan…

	culture	chromosome and corresponding decrease in expression of dosage compensated genes, mislocalization of Mtor away from nuclear envelope	Akhtar 2006
	RNAi in S2 cell culture	Defective Importinβ translocation into nucleus, reduction in NPC localization of Mtor, 214, Nup88, and mAb414 FG Nups	Sabri… Samokovlis 2007
	RNAi in S2 cell culture	-Global trend of down-regulation of genes within Nup-Associated Regions (NARs), which predominantly cover active genes -reduction in peripheral localization of otherwise peripheral NARs -reduction of MSL protein occupancy at X-chromosome and autosomal targets	Vaquerizas… Ahktar 2010
	RNAi VDRC line (unlisted)	Reduced nuclear import of clock protein PER, and subsequent disruption of circadian rhythms	Jang… Sehgal 2015
	RNAi lines	Enhanced toxicity phenotype associated with C9orf72 repeat expansion in *Drosophila* ALS model	Freibaum... Taylor 2015
Nup50	RNAi in S2 cell culture	Reduced expression of canonically active developmental gene targets, reduction of nup98 interaction with target genes	Kalverda… Fornerod 2010
	Mutant line $Nup50^{KG0955}$	Enhanced lifespan in flies overexpressing ALS-associated TDP-43 RNA-binding protein	Zhan… Tibbetts 2013
	RNAi lines	Amelioration of eye degeneration phenotype associated with repeat expansion proteins in *Drosophila* ALS/FTD model	Boeynaems... Van Den Bosch 2016
	RNAi lines	Enhanced toxicity phenotype associated with C9orf72 repeat expansion in *Drosophila* ALS model	Freibaum... Taylor 2015
Mtor/Tpr	RNAi in S2 cell culture	Reduction in number of cells undergoing mitosis	Hongying… Johansen 2004
	RNAi in S2 cell culture	Delocalization of MSL proteins from male X chromosome and corresponding decrease in expression of dosage compensated gene	Mendjan… Akhtar 2006
	RNAi in S2 cell culture	Accelerated mitosis resulting in metaphase plate structural changes, as well as improper spindle assembly checkpoint (SAC) response	Lince-Faria…. Maiato 2009
	Mtor RNAi lines v110218, BL32941, V24265 Mutant line $Mtor^{k03905}$	-Defects in GSC and CySC maintenance and GSC differentiation in testes -Reduced expression of E-cadherin and mislocalization of E-cadherin and Apc2 at hub-GSC interfaces -Defects in centrosome number and orientation, microtubule spindle formation, and chromosome segregation during mitosis	Liu… Hou 2015

Aladin	RNAi in S2 cell culture	Delay in formation of metaphase spindle	Carvalhal… Griffis 2015

Chapter 2: Chromatin Targeting of Nuclear Pore Proteins Induces Chromatin Decondensation

This chapter is adapted from:

Kuhn, T.M., P. Pascual-Garcia, A. Gozalo, S.C. Little, and M. Capelson. 2019. Chromatin targeting of nuclear pore proteins induces chromatin decondensation. J. Cell Biol. *218* (9).

Abstract

Nuclear pore complexes (NPCs) have emerged in recent years as chromatin-binding nuclear scaffolds, able to influence target gene expression. However, how Nucleoporins (Nups) exert this control remains poorly understood. Here we show that ectopically tethering *Drosophila* Nups, especially Sec13, to chromatin is sufficient to induce chromatin decondensation. This decondensation is mediated through chromatin-remodeling complex PBAP, as PBAP is both robustly recruited by Sec13 and required for Sec13-induced decondensation. This phenomenon is not correlated with localization of the target locus to the nuclear periphery, but is correlated with robust recruitment of Nup Elys. Furthermore, we identified a biochemical interaction between endogenous Sec13 and Elys with PBAP, and a role for endogenous Elys in global, as well as gene specific chromatin decompaction. Together, these findings reveal a functional role and mechanism for specific nuclear pore components in promoting an open chromatin state.

Introduction

Interactions between the genome and nuclear scaffolds are known to contribute to regulation of gene expression and cell fate control, but specific mechanisms by which scaffold components influence genome regulation remain poorly defined. One of the most prominent nuclear scaffolds is the Nuclear Pore Complex (NPC), which is known for its canonical function as a mediator of nucleocytoplasmic transport across the eukaryotic nuclear membranes. In recent years however, NPCs and their constituent ~30 Nucleoporins (Nups) have proven important for functions in genome regulation and maintenance (Raices and D'Angelo, 2017). Early electron micrograph (EM) images of mammalian nuclei have revealed decondensed chromatin preferentially associated with NPCs, interrupting the condensed heterochromatin associated with the repressive nuclear lamina. Such images have suggested a functional relationship between NPCs and open chromatin (Watson, 1959; Blobel, 1985; Capelson and Hetzer, 2009). The existence of interactions between NPCs/Nups and chromatin has now been well established in a variety of organisms via genome-wide chromatin binding assays and imaging methods (Sood and Brickner, 2014; Ibarra and Hetzer, 2015; Ptak and Wozniak, 2016). In agreement with the EM images, the majority of these interactions were found to occur at open chromatin regions, such as actively transcribing genes (Cabal et al., 2006; Capelson et al., 2010; Kalverda et al., 2010; Vaquerizas et al., 2010; Light et al., 2013; Liang et al., 2013; Casolari et al., 2004), DNase I hypersensitive sites (DHS) and regions marked with active histone modifications such as H3K27 acetylation (Ibarra et al., 2016; Pascual-Garcia et al., 2017).

Functionally, several Nups were found to be required for the transcriptional output and regulation of at least a subset of their target genes. In metazoans, Nup targets include genes important for tissue-specific development, regulation of the cell cycle, and anti-viral responses (Panda et al., 2014; Pascual-Garcia et al., 2014; Ibarra et al., 2016; Raices et al., 2017). One conserved regulatory mechanism that requires Nups is transcriptional memory, a process by which genes are marked as recently transcribed to allow more robust transcriptional responses to future activation (Light et al., 2013). Loss-of-function studies have demonstrated that specific Nups are required for multiple molecular steps involved in transcription and transcriptional memory, including binding of poised RNA Polymerase II (RNAPII), H3K4 methylation, nucleosome exchange, and formation of activation-induced genomic loops (Brickner et al., 2007; Tan-Wong et al., 2009; D'Urso et al., 2016; Pascual-Garcia et al., 2017). But, while Nups have been shown to be required for these molecular events, it remains unclear which specific steps of the transcriptional or epigenetic processes are executed by particular Nups.

In *Drosophila*, Nups such as Nup98, Sec13 and Nup62 have been detected at a large number of active genes via DamID, chromatin immunoprecipitation (ChIP) and imaging studies (Capelson et al., 2010; Kalverda et al., 2010). Depletion of Sec13 or Nup98 in fly culture cells or in salivary gland tissues has been shown to lead to more compact chromatin, decreased levels of active RNAPII, and reduced mRNA production at select target genes (Capelson et al., 2010; Kalverda et al., 2010; Panda et al., 2014; Pascual-Garcia et al., 2014). Nup98 has been extensively implicated in maintaining transcriptional memory of its target genes in yeast, fly and mammalian cells (D'Urso and Brickner, 2017), and we have recently reported that Nup98 is involved in stabilization of enhancer-promoter contacts of ecdysone-inducible genes (Pascual-Garcia et al., 2017).

But the molecular functions carried out by other transcription-associated Nups such as Sec13 and Nup62 at Nup-chromatin contacts remain unknown. Additionally, many of these Nup-chromatin contacts can occur off-pore in the nuclear interior (Capelson et al., 2010; Kalverda et al., 2010; Vaquerizas et al., 2010), as these Nups have been found to shuttle on and off NPCs and/or have distinct intranuclear pools (Rabut et al., 2004; Capelson et al., 2010). However, it remains unclear if gene regulatory functions of Nups are independent of nuclear localization.

To examine these functions and to identify which chromatin or transcription associated changes Nups are sufficient to induce, we utilized a gain-of-function approach. We generated a tethering system to create ectopic chromatin binding sites of Sec13 and Nup62 in the genome of transgenic *Drosophila* strains. Using this system, we observed that NPC component Sec13 consistently induces robust chromatin decondensation at multiple genomic locations. In dissecting the mechanism of this phenomenon, we implicated Nup Elys as the primary mediator of chromatin decompaction, and identified a robust interaction of Sec13 and Elys with the ATP-dependent chromatin remodeling complex Polybromo-containing Brahma-Associated Proteins (PBAP), as well as a role of Elys in endogenous chromatin decondensation. These findings suggest that promoting chromatin decondensation is a critical and previously underappreciated molecular function of specific Nups in the process of gene regulation.

Results

Ectopic targeting of Nups to chromatin induces chromatin decondensation at multiple genomic locations.

To define chromatin-related functions of Nups, and to better separate chromatin-associated roles of Nups from their transport-related functions, we utilized the *lacO*-LacI tethering system to create ectopic chromatin-binding sites of Sec13 and Nup62. We generated transgenic *Drosophila melanogaster* lines containing the DNA binding domain of LacI (Tumbar et al., 1999; Danzer and Wallrath, 2004) fused to either Nup62 or Sec13, under inducible control of the UAS element. We then genetically combined these LacI-Nup lines, or a pre-existing line containing a control LacI-GFP fusion (Deng et al., 2008) with a Gal4 driver expressed in 3rd instar larval salivary glands, and an integrated genomic *lacO* repeat array, to which the LacI-fusion proteins bind with high affinity **(Fig 2.1A).** We visualized this tethering using immunofluorescence (IF) of *Drosophila* larval salivary gland polytene chromosome squashes. These experiments allow high-resolution visualization of chromatin structure in the highly reproducible banding patterns of condensed and decondensed chromatin of the large polytene chromosomes, which have previously been shown to correspond to TAD and inter-TAD regions (Ulianov et al., 2016), demonstrating their relevance to generalizable chromatin structure across cell types. By performing IF on polytene chromosomes of larval salivary glands, we were able to visualize binding of the LacI fusion proteins to specific *lacO* sites to allow us to identify any chromatin changes brought about by LacI-Nup fusions. We first utilized a *lacO* integration site at cytological location 4D5, which is in close proximity to the easily recognizable end of the *Drosophila* X chromosome, to ensure accurate and robust

detection of targeting to the *lacO* site. At *lacO*-4D5, all our LacI-fusion proteins can be reliably visualized (**Fig 2.1B**). Additionally, we observed correct fusion protein size by western blotting of larval extracts (**Fig 2.2A**) and targeting of LacI-Nup proteins to the NPCs, as assayed by co-staining with mAb414 antibody in semi-intact salivary gland nuclei (**Fig 2.2B**), which is indicative of proper Nup fusion protein folding and function. Together these data suggest a robust assay for targeting Nups to genomic loci.

Since we aimed to assay for chromatin changes and recruitment of proteins associated with active transcription, we turned away from the *lacO*-4D5 integration site as it corresponded to an already highly decondensed and transcribing genomic locus (**Fig 2.1B, data not shown)**. Instead, we next utilized a *lacO* integration site at cytological location 60F, a sub-telomeric locus found in a highly condensed region of chromatin at the end of chromosome 2R. In order to interrogate changes in chromatin structure or protein recruitment in an unbiased and accurate way, we devised a highly sensitive and semi-automated method by which the fluorescent signals at the *lacO* site were analyzed (**Fig 2.1C**). The intensity of green fluorescence signal (LacI) was compared to the intensity of blue fluorescence signal (Hoechst DNA stain), or red fluorescence signal (proteins of interest), on a pixel-by-pixel basis for the area under the LacI-defined band. The Pearson Correlation Coefficient (PCC) representing the overall relationship of green to blue/red intensity was then calculated for each *lacO* site. By obtaining PCC measurements of *lacO* sites from many cells per gland from multiple animals, we can effectively observe and compare differences in chromatin density or recruitment of proteins of interest between LacI-GFP control, LacI-Nup62, and LacI-Sec13 bound to *lacO* loci on polytene chromosomes (**Fig 2.1C**).

Using this method, we observed a positive correlation between Hoechst signal and LacI-GFP, representing the bright DNA staining and highly condensed nature of chromatin at the subtelomeric *lacO*-60F site under control conditions (**Fig 2.1D**). However we can visualize a striking loss of DNA signal intensity associated with binding of LacI-Nup62 or LacI-Sec13, represented by a quantifiable and significant reduction in the PCCs between LacI fusion protein and Hoechst DNA stain (**Fig 2.1D**). This decrease in the correlation between bound LacI-Nups and DNA fluorescence intensity at *lacO*-60F suggests that chromatin becomes less compact upon LacI-Nup targeting, and implies that tethering nuclear pore proteins Nup62 or Sec13 to a genomic site is sufficient to induce chromatin decondensation.

To corroborate that the changes we observe in DNA signal intensity are associated with chromatin decondensation at this subtelomeric integration site, we stained for *Drosophila* telomere capping protein HOAP, which is known to bind heterochromatin at chromosome ends (Cenci et al., 2003). We found that targeting LacI-Nup62 or LacI-Sec13 to the *lacO*-60F locus results in a dramatically reduced area of HOAP signal at the 2R telomere compared to control (**Fig 2.2C**). These images also illustrate that, in some instances, decondensation by Sec13 can be so severe that the entire telomeric end of the chromosome appears to have been decondensed, revealed by the LacI-Sec13 signal appearing at the distal-most tip of the visible DNA signal compared to the more proximal location of the band of LacI-GFP (**Fig 2.2C**). These data support the notion that there is a loss of the condensed heterochromatic state at the *lacO*-60F site upon Nup62 or Sec13 tethering.

To determine if this phenotype is reproducible, we next tethered the LacI-fusion proteins to a *lacO* integration site at cytological location 96C, which is a non-telomeric condensed band on chromosome 3R. Here we again observed significant loss in DNA stain fluorescence signal density associated with binding of LacI-Nup62 or LacI-Sec13 compared to LacI-GFP control, and a corresponding significant reduction in PCC values, indicative of chromatin decondensation by Nups at *lacO*-96C **(Fig 2.1E**). Interestingly, Sec13 induces the apparent decondensation much more robustly than Nup62 at this *lacO*-96C locus. The difference in the magnitude of observed change in chromatin structure between Sec13 and Nup62 at *lacO*-96C provided an opportunity to further probe the mechanism of this Nup-induced phenomenon in later experiments, as it allowed for assessing a dose-dependent relationship.

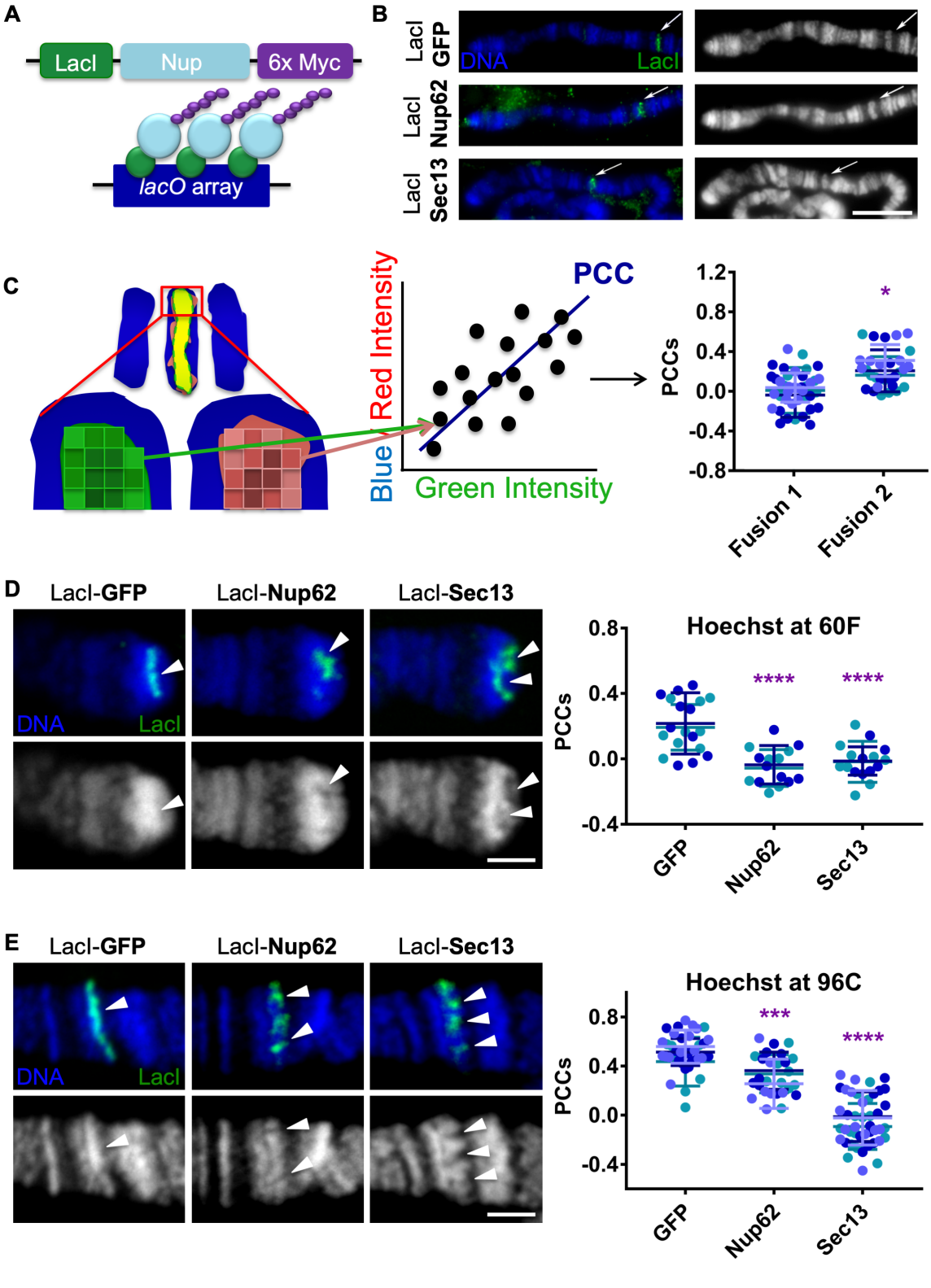
A
LacI
Nup
6x Myc
lacO array
B
LacI GFP
LacI Nup62
LacI Sec13
DNA
LacI
C
PCC
Red Intensity
Blue
Green Intensity
PCCs
1.2
0.8
0.4
0.0
-0.4
-0.8
*
Fusion 1
Fusion 2
D
LacI-GFP
LacI-Nup62
LacI-Sec13
DNA
LacI
Hoechst at 60F
PCCs
0.8
0.4
0.0
-0.4
****
****
GFP
Nup62
Sec13
E
LacI-GFP
LacI-Nup62
LacI-Sec13
DNA
LacI
Hoechst at 96C
PCCs
0.8
0.4
0.0
-0.4
***
****
GFP
Nup62
Sec13

Figure 2.1 Ectopic targeting of Nups to chromatin induces chromatin decondensation at multiple genomic locations.

(A) Schematic of *lacO*-LacI-Nup inducible chromatin tethering system.
(B) Widefield IF of squashed polytene chromosomes with Hoechst stain (labeled "DNA", shown as blue or white/grey here and hereafter) and α-LacI (green). Right column shows Hoechst only in grey scale, left shows overlay of both channels. Arrows point to *lacO* integration site at location 4D5 near the end of X chromosome. LacI-fusion protein expression driven with 2nd chromosome Nubbin-Gal4. Scale bar is 10μm.
(C) Schematic of Pearson Correlation Coefficient(PCC) method of analyzing fluorescence changes where intensities of blue Hoechst or red protein of interest and green (LacI) are measured pixel-by-pixel under green-defined LacI-band,PCC value between blue/red and green is determined for each image, and ~30 PCC values are measured per genotype.
(D) Confocal IF images of LacI-fusion proteins targeted to subtelomeric *lacO* integration site on squashed polytene chromosomes at location 60Fstained with Hoechst (blue or white) and α-LacI (green). Top row shows overlay of both channels, bottom row shows Hoechst only. "Holes" (areas of highly reduced staining density) in Hoechst staining can be reproducibly observed under LacI-Nup binding. Protein expression driven with Sgs3-Gal4. Arrows = observed decondensation or lack thereof under LacI. Scale bar is 2μm. Quantification displays PCCs between blue and green signal under LacI. Data from 2 biological replicates (colored), each from an independent experiment. GFP n = 19, Nup62 n = 15, Sec13 n = 17. **** = $p < 0.0001$. Error bars = standard deviation.
(E) Experimental conditions, staining and imaging identical to *(D)* above, with the replacement of cytological location 60F with location 96C and Nubbin-Gal4 driver. Holes in Hoechst can reproducibly be observed under LacI-Sec13 and occasionally under LacI-Nup-62. Data from 3 biological replicates (colored) from 2 independent experiments. GFP n = 39, Nup62 n = 27, Sec13 n = 44. **** = $p < 0.0001$ and *** = $p<0.001$. Error bars = standard deviation.

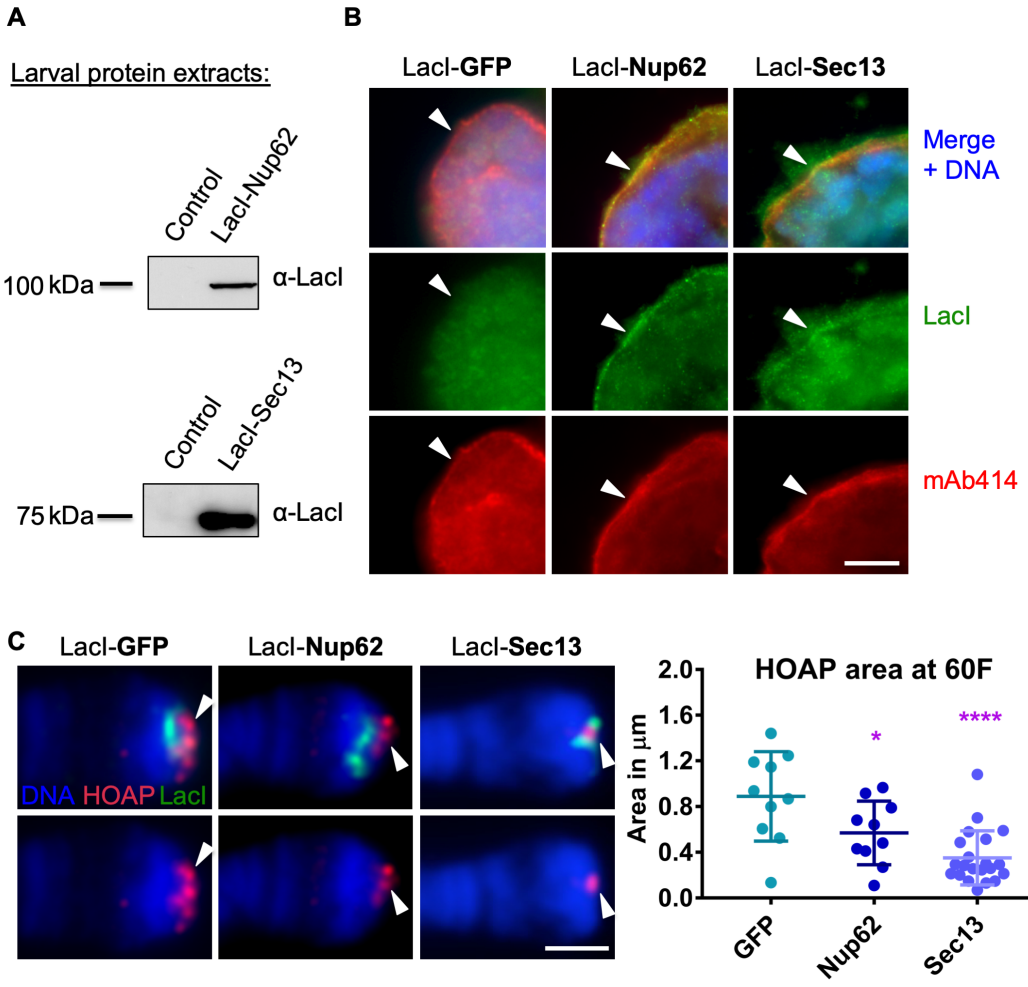

Figure 2.2 Generated LacI-Nup fusion proteins localize properly in vivo and affect heterochromatin at the subtelomeric locus.

(A) Western blots of whole larval extract of indicated control and transgenic animals (5 each) stained with α-LacI antibody.
(B) Immunofluorescence staining of semi-squashed salivary gland nuclei, staining LacI-fusion proteins with α-LacI and NPCs with mAb414, using widefield microscopy. Scale bar is 10µm.
(C) Immunofluorescence images of squashed polytene chromosomes displaying subtelomeric *lacO* integration site at cytological location 60F bound by indicated LacI-fusion proteins and stained with Hoechst, α-LacI, and antibody against telomere capping protein HOAP, using widefield microscopy. Arrows indicate locations of existing or reduced HOAP adjacent to/at LacI signal. Scale bar is 2µm. Plot shows quantification measuring area of HOAP signal. Data from 1-2 independent biological replicates from 1 experiment. GFP n = 10, Nup62 = 10, Sec13 n = 21. **** = $p < 0.0001$ and * = $p<0.05$. Error bars represent standard deviation.

Nup binding to chromatin is associated with a decrease in histone density and an increase in gene expression.

The loss of Hoechst intensity at the lacO sites upon Nup tethering suggested that chromatin is becoming less dense. This change in DNA stain intensity can come from the loss of nucleosomal density and/or be associated with specific histone modifications linked to active chromatin. To examine these possibilities and to further validate our conclusion that Nup tethering induces chromatin decondensation, we stained for the core histone H3 and observed a significant decrease upon Nup62 and, more robustly, Sec13 binding (**Fig 2.3A**). The observed decrease in histone density upon Nup tethering supports the notion that the loss of Hoechst staining, reported above (**Fig 2.1**), represents remodeling, or loss of nucleosomes. Furthermore, the difference in magnitude of H3 staining loss between Nup62 and Sec13 corresponds well with the difference in the observed Hoechst staining loss at *lacO*-96C between the Nups (**Fig 2.1E**). Next, we determined if accumulation of histone modifications associated with active transcription, such as H3K27 acetylation or H3K4 di-methylation, correlated with Sec13-induced chromatin decondensation. Interestingly, we did not observe an increase in the association of either active mark with LacI-Sec13 relative to LacI-GFP control, and instead detected a significant decrease in visible levels of both histone modifications upon Sec13 tethering (**Fig 2.3B and 2.4**), which is consistent with a reduction in general nucleosome occupancy at *lacO*-96C upon Sec13 binding (**Fig 2.3A**). While the nature of this assay does not exclude detection of alternative possible causes of the visual changes we observe, chromatin decondensation is consistent with these observations

and existing data describing Nup behavior, and therefore we set forward to further interrogate this as a decondensation phenomenon.

Chromatin decondensation is a critical step in facilitating transcription factor and RNAPII binding, as well as in subsequent steps of gene transcription. RNAi-mediated depletion of Sec13 in these cells has been previously shown to result in a loss of chromatin decondensation, along with concurrent reduction of RNAPII levels and of gene expression at endogenous Sec13 targets (Capelson et al., 2010). Thus we next wanted to determine whether Nup-induced decondensation at the ectopic site resulted in any transcription-associated changes as well.

To determine if RNAPII is recruited to the decondensed *lacO*-96C locus upon Nup tethering, we stained with the H5 antibody, which recognizes the Serine 2 phosphorylated (Ser2Ph) form and represents actively transcribing RNAPII (Phatnani and Greenleaf, 2006). Interestingly, we observed a modest but significant accumulation of the Ser2Ph form of RNAPII at *lacO*-96C when bound by Sec13 (**Fig 2.3C**). We then conducted RT-qPCR to measure expression levels of the *dan* gene, which is located approximately 1.3 kb downstream of the *lacO*-96C integration site (**Fig 2.3D** and personal communication L. Wallrath). We found a 2-fold increase in *dan* expression specifically when LacI-Sec13 was targeted to *lacO*-96C, relative to LacI-GFP control (**Fig 2.3D**). Together, these results suggest that the robust chromatin decondensation associated with binding of Sec13 at this locus allows for a small but significant amount of transcriptional machinery to bind and productively transcribe downstream genes.

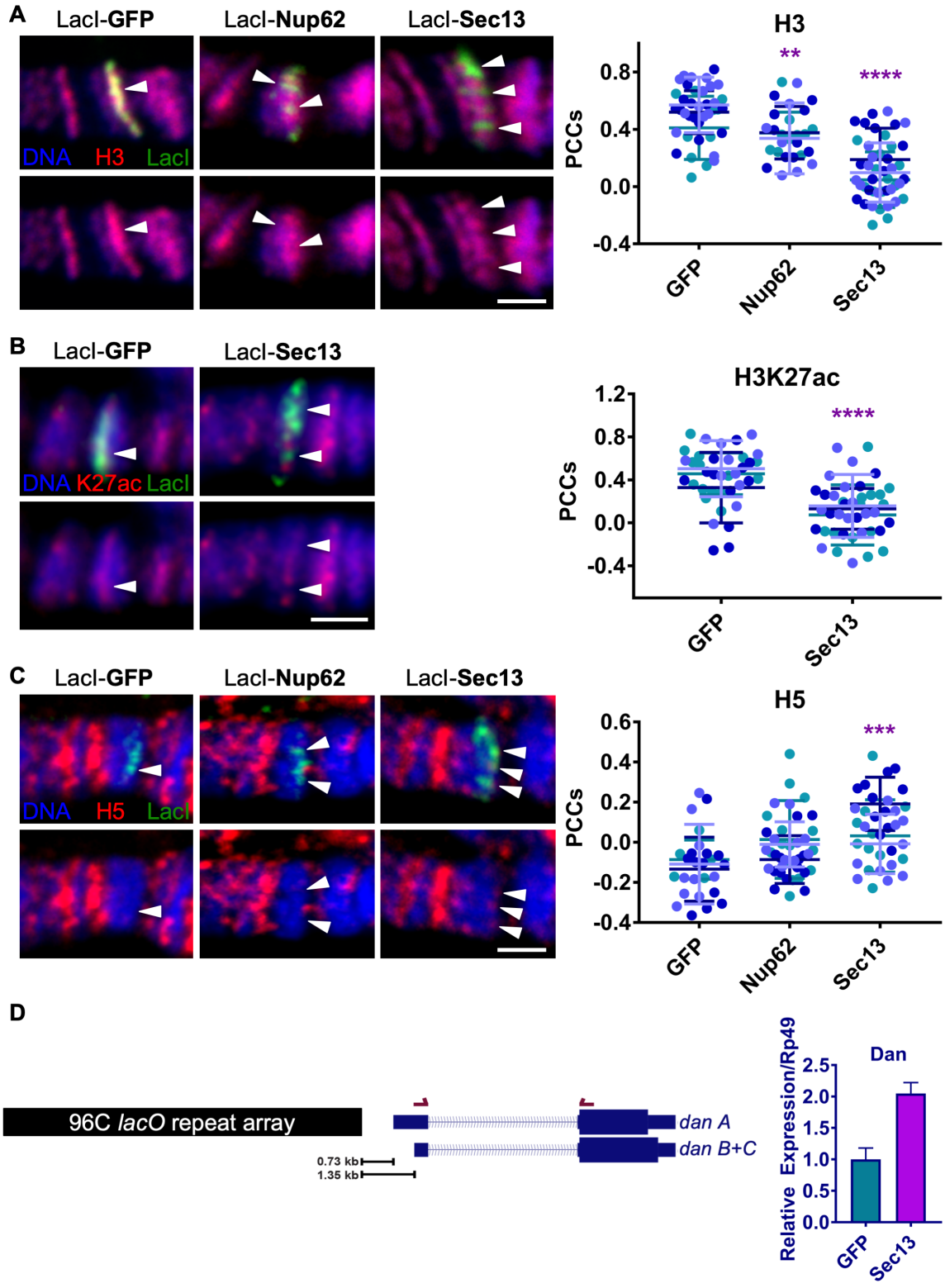
A
LacI-GFP
LacI-Nup62
LacI-Sec13
DNA H3 LacI
H3
**
****
PCCs
0.8
0.4
0.0
-0.4
GFP
Nup62
Sec13
B
LacI-GFP
LacI-Sec13
DNA K27ac LacI
H3K27ac
****
PCCs
1.2
0.8
0.4
0.0
-0.4
GFP
Sec13
C
LacI-GFP
LacI-Nup62
LacI-Sec13
DNA H5 LacI
H5
***
PCCs
0.6
0.4
0.2
0.0
-0.2
-0.4
GFP
Nup62
Sec13
D
96C lacO repeat array
dan A
dan B+C
0.73 kb
1.35 kb
Dan
Relative Expression/Rp49
2.5
2.0
1.5
1.0
0.5
0.0
GFP
Sec13

Figure 2.3 Nup binding to chromatin is associated with a decrease in histone density and an increase in gene expression

(A) Confocal IF images of LacI-fusion proteins targeted to *lacO* integration site on squashed polytene chromosomes at location 96C. Stained with Hoechst (blue) and antibodies against H3 (red) and LacI (green). LacI-fusion protein expression driven with Nubbin-Gal4. Top row shows overlay of all 3 colors, bottom row shows blue and red only (here and in B, C). Arrows indicate locations of existing or depleted H3 under LacI signal. Scale bar is 2μm. Quantification displays PCCs between red and green signal under LacI. Data from 3 biological replicates (colored) from 2 independent experiments. GFP n = 39, Nup62 n = 27, Sec13 n = 44. **** = $p < 0.0001$ and ** = $p<0.01$. Error bars = standard deviation.
(B) Experimental conditions and strains as *(A)* above, but with H3K27ac antibody (red) instead of H3 and GFP or myc antibodies (green) instead of LacI due to antibody animal source constraints, and with the use of widefield microscopy. Data from 3 biological replicates (colored) from 2 independent experiments. GFP n = 38, Sec13 n = 40. **** = $p < 0.0001$. Error bars = standard deviation.
(C) Experimental conditions and strains as *(A)* above, but with antibodies against LacI (green) and CTD tail Ser2 phosphorylated RNAPII (H5, red), and with the use of widefield microscopy. Arrows indicate LacI signal and recruitment or lack thereof of H5. Scale bar is 2μm. Quantification displays PCCs between red and green signal under LacI. Data from 3 biological replicates (colored) from 2 independent experiments. GFP n = 26, Nup62 n = 40, Sec13 n = 35. *** = $p<0.001$. Error bars = standard deviation.
(D) Schematic of the distance between integration of the lacO repeat plasmid and the downstream isoforms of *dan* gene along with location of primer set used for RT-qPCR. 3 technical replicates of each of 3 biological replicates (10 sets of glands per replicate) were used for quantification. Error bars = standard error.

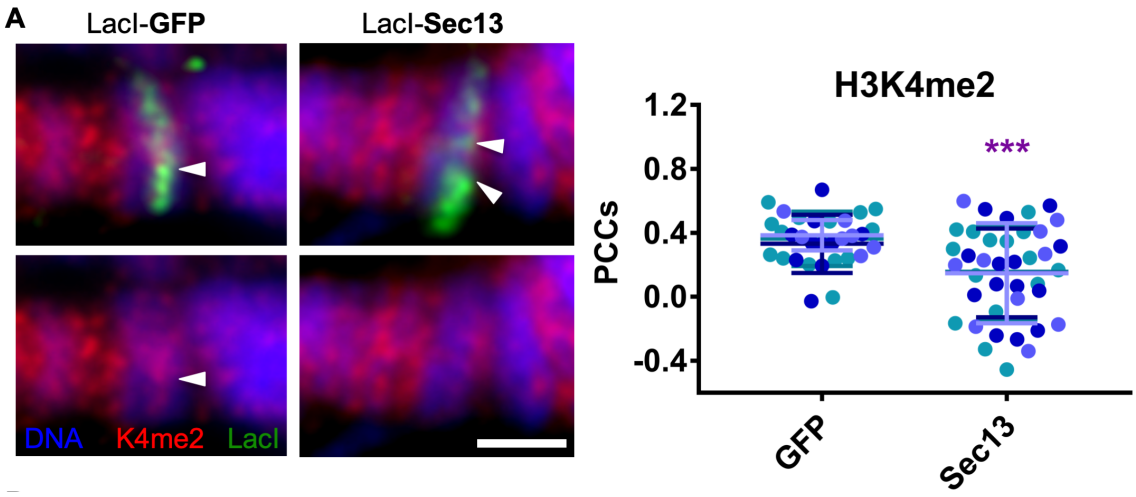

Figure 2.4 Chromatin targeting of Sec13 results in lower H3K4me2 density

(A) Widefield immunofluorescence images of LacI-fusion proteins targeted to *lacO* integration site on squashed polytene chromosomes at cytological location 96C on chromosome 3. Stained with Hoechst (blue) and antibodies against H3K4me2 (red) and GFP for control/myc (green). LacI-fusion protein expression driven with 2nd chromosome Nubbin-Gal4. Top row shows overlay of all 3 channels, bottom row shows overlay of blue and red only. Arrows indicate locations of existing or depleted H3K4me2 under LacI signal. Scale bar is 2μm. Quantification displays Pearson Correlation Coefficients (PCCs) between red and green signal under LacI. Data from 3 independent biological replicates (colored) from 2 independent experiments. GFP n = 34, Sec13 n = 39. *** = $p < 0.001$. Error bars represent standard deviation.

Nup-induced decondensation of chromatin is independent from localization to the nuclear periphery.

Metazoan Nups have been found to interact with chromatin both at and away from NPCs (Capelson et al., 2010; Kalverda et al., 2010; Vaquerizas et al., 2010), and many Nups demonstrate short residence times at NPCs, suggesting dynamic behaviors (Rabut et al., 2004). In light of this, we aimed to determine if ectopically chromatin-tethered Nups target the *lacO*-96C locus to NPCs at the nuclear periphery, and whether or not NPC association is correlated with chromatin decondensation.

To assess this, we conducted DNA FISH with fluorescently-tagged oligonucleotide probes complementary to the *lacO*-96C locus in intact nuclei of salivary glands in our system, followed by 3D analysis of the nuclear position of the *lacO* probe relative to the nuclear periphery (**Fig 2.5A-B**). Although the *lacO* locus in all genotypes showed peripheral localization bias, we observed no significant difference in the percentage of peripheral (<0.5μm from the nuclear border) *lacO* loci when bound by LacI-GFP, LacI-Nup62 or LacI-Sec13 (**Fig 2.5B**). Since Sec13 induces robust decondensation of chromatin at l*acO*-96C while the level of decondensation achieved by tethering Nup62 is significantly less (**Fig 2.1E**), the lack of difference in peripheral localization between either of these or the GFP control suggests that the ability of chromatin-bound Nups to induce decondensation is independent of nuclear positioning. Although polytene chromosomes are reported to be relatively immobile (Hochstrasser and Sedat, 1987), we conclude from our data that recruitment to the nuclear periphery does not appear to correlate with chromatin decondensation.

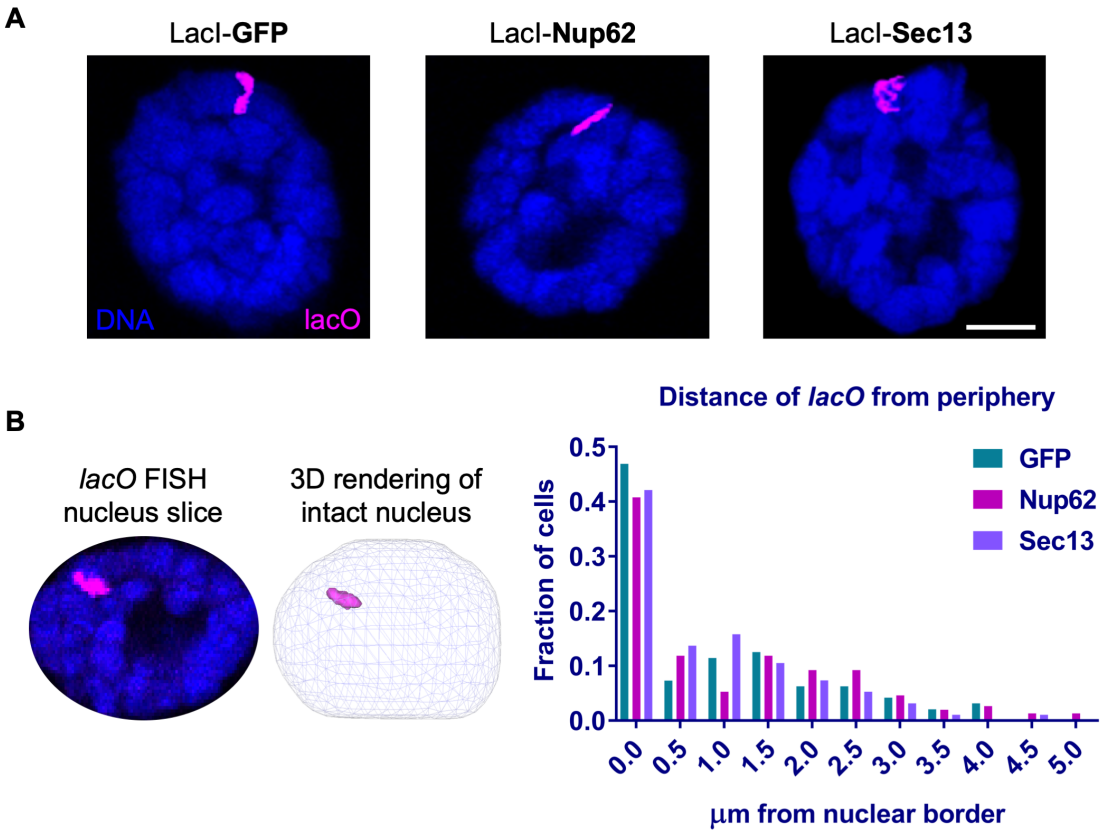

Figure 2.5 Nup-induced decondensation of chromatin is independent from localization to the nuclear periphery

(A) Representative images of DNA FISH (magenta) against the *lacO* array at 96C in intact salivary gland polytene nuclei, stained with Hoechst (blue), obtained using 3D confocal microscopy. Scale bar is 10µm.
(B) The TANGO plugin (Ollion et al., 2013) in FIJI image analysis software (Schindelin et al., 2012) was used to compile 3D renderings of confocal Z-stacks of nuclei, call nuclear and lacO objects, and calculate minimum 3D distances of edge of *lacO* locus "object" to edge of Hoechst DNA-defined nuclear periphery when bound by different LacI-fusion proteins. Distances of *lacO* to periphery were plotted to show the fraction of cells in the salivary glands of 3 biological replicates (>80 cells total) per genotype from two independent experiments with distance bins in increments of 0.5um.

Nup-induced chromatin decondensation correlates with recruitment of Nup Elys.

To further characterize Nup-induced chromatin decondensation, we went on to determine what other NPC components are recruited by chromatin-tethered Nup62 or Sec13 at *lacO*-96C. We observed that both Nup62 and Sec13 recruit stable core NPC component Nup93 to *lacO*-96C at comparable levels (**Fig 2.6A**), further suggesting similar levels of interaction with peripheral NPCs (**Fig2.5**). However, we did observe differential and highly robust recruitment of another Nup, Elys, by Sec13 at *lacO*-96C (**Fig 2.6B**). Elys is the only Nup with a clearly defined chromatin binding domain and activity (Zierhut et al., 2014), suggesting a potential role in chromatin regulation. Our highly-sensitive PCC quantification methodalso detected a mild recruitment of Elys by LacI-Nup62 at *lacO*-96C, however this is dramatically less than the amount recruited by LacI-Sec13 and is not discernable by eye. Furthermore, we did not observe either Nup62 or Sec13 recruiting core NPC component Nup107 (against which we have recently generated an antibody) (**Fig 2.7A-B**) or nuclear basket Nup Mtor to *lacO*-96C (**Fig 2.7CD**), supporting the specificity of the relationship between Elys and Sec13 at *lacO*-96C.

Given this correlation between recruitment of Elys and dramatic decondensation, we further probed whether the amount of Elys recruited to chromatin by Nups correlates with the degree of Nup-induced decondensation overall. To do so we assessed Elys recruitment to the subtelomeric *lacO*-60F locus, where Nup62 induces chromatin decondensation to a level more comparable to that of Sec13 (**Fig 2.1D**). Strikingly, both Nup62 and Sec13 recruit significantly high and, importantly, more comparable levels of Elys to this locus, where they both decondense robustly (**Fig 2.6C**). These results

demonstrate that the amount of decondensation in these assays correlates strongly with levels of Elys recruitment, and suggests a possible causal relationship between the two.

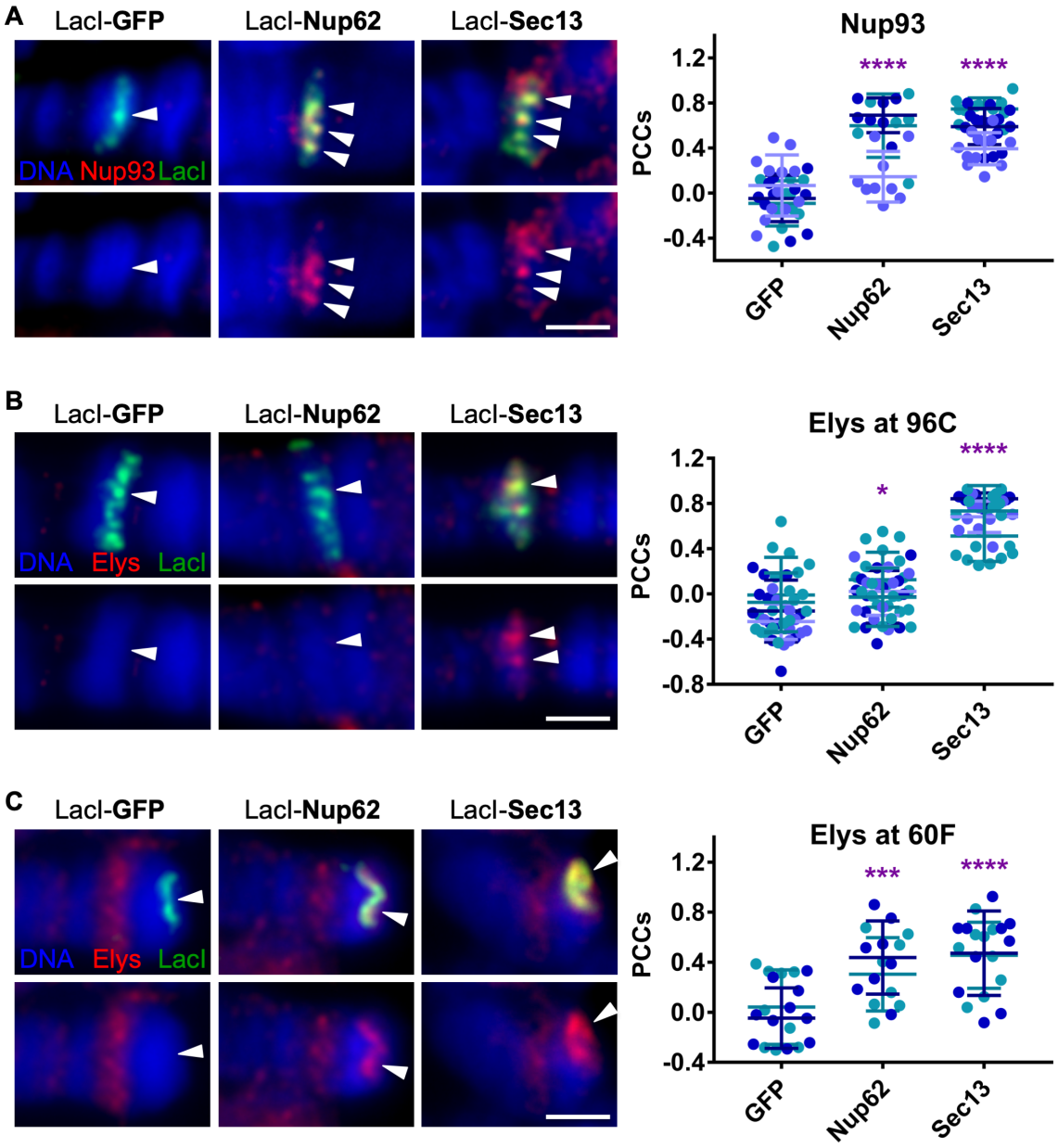

Figure 2.6 Nup-induced chromatin decondensation correlates with recruitment of Nup Elys

(A) Widefield IF images of LacI-fusion proteins targeted to *lacO* integration site on squashed polytene chromosomes at location 96C. Stained with Hoechst (blue) and antibodies against Nup93 (red) and LacI (green). Top row shows overlay of all 3 colors, bottom row shows blue and red only (here and in B, C). Arrows indicate locations of observed Nup93 recruitment or lack thereof under LacI signal. Scale bar is 2μm. Quantification displays PCCs between red and green signal under LacI. Data from 3 biological replicates (colored) from 2 independent experiments. GFP n = 32, Nup62 n = 22, Sec13 n = 37. **** = $p < 0.0001$ and * = $p<0.05$. Error bars = standard deviation.
(B) Experiment conditions, strains and imaging as in *(A)* above, but with antibodies against Elys (red) and myc (green). Arrows indicate locations of observed Elys recruitment or lack thereof under LacI signal. Quantification displays PCCs between red and green signal under LacI. Data from 3 biological replicates (colored) from 2 independent experiments. GFP n = 42, Nup62 n = 45, Sec13 n = 40. **** = $p < 0.0001$ and * = $p<0.05$. Error bars = standard deviation.
(C) Experimental conditions and imaging as in *(A)* above, but with antibodies against Elys (red) and myc (green), and at location 60F with Sgs3-Gal4 driver. Data from 2 biological replicates (colored) from 2 independent experiments. GFP n = 20, Nup62 n = 16, Sec13 n = 19. **** = $p < 0.0001$ and *** = $p<0.001$. Error bars = standard deviation.

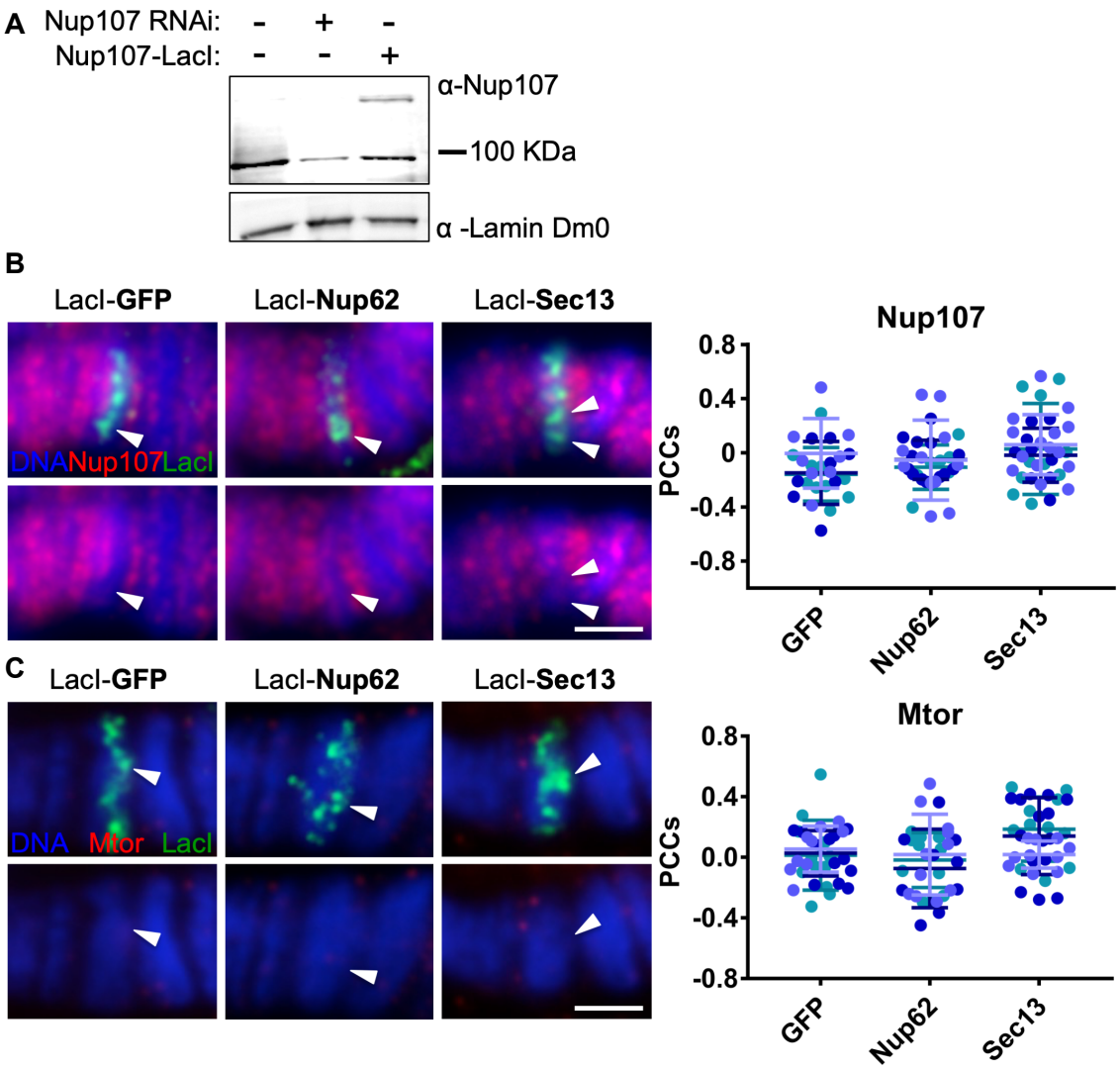

Figure 2.7 Chromatin targeting of Sec13 does not result in recruitment of Nup107 or Mtor

(A) Validation of the generated Nup107 antibody by western blot of extracts from S2 cells, either depleted for Nup107 by RNAi, or transfected with Nup107-LacI (carried in a cell expression vector), stained with Nup107 antibody, or Lamin DmO antibody as a loading control.
(B) Widefield immunofluorescence images of LacI-fusion proteins targeted to *lacO* integration site on squashed polytene chromosomes at cytological location 96C on chromosome 3. Stained with Hoechst (blue) and antibodies against Nup107 (red) and LacI (green). Scale bar is 2μm. Quantification displays Pearson Correlation Coefficients (PCCs) between red and green signal under LacI. Data from 3 independent biological replicates (colored) from 2 independent experiments. GFP n = 26, Nup62 = 31, Sec13 n = 34. Error bars represent standard deviation.

(C) Widefield immunofluorescence images of LacI-fusion proteins targeted to *lacO* integration site on squashed polytene chromosomes at cytological location 96C on chromosome 3. Stained with Hoechst (blue) and antibodies against Mtor (red) and LacI (green). Scale bar is 2μm. Quantification displays Pearson Correlation Coefficients (PCCs) between red and green signal under LacI. Arrows indicate LacI signal. Data from 3 independent biological replicates (colored) from 2 independent experiments. GFP n = 35, Nup62 = 32, Sec13 n = 36. Error bars represent standard deviation.

Chromatin-tethered Sec13 recruits the chromatin remodeling PBAP/Brahma complex and associated GAGA Factor.

In order to understand the molecular mechanism behind Sec13-induced decondensation, we next turned to chromatin remodeling complexes, as they are the known enzymatic drivers of chromatin decompaction (Tyagi et al., 2016). PBAP is a *Drosophila* ATP-dependent SWI/SNF chromatin remodeling complex comprised of 9 proteins, including Brahma (Brm), the ATPase, and Polybromo, the specific protein that distinguishes PBAP from the related Brm-associated proteins (BAP) complex (Mohrmann and Verrijzer, 2005). Strikingly, both of these proteins were significantly recruited by Sec13 to *lacO*-96C, most robustly Brm (**Fig 2.8A and Fig 2.9A**). As with Elys, a small increase in correlation between Brm and Nup62 is detected by our sensitive PCC quantification method, but again this is significantly less than that recruited by Sec13, and closer to the levels of control GFP fusion protein. This lower level of recruitment correlates with the lower level of Nup62-induced decondensation at this locus, suggesting a dose-dependent relationship between Brm and chromatin decondensation (**Fig 2.1E**). These results suggest that the Nup-induced chromatin decondensation at *lacO*-96C is facilitated by the chromatin remodeling complex PBAP.

Interestingly, one protein previously shown to interact with PBAP, GAF (Nakayama et al., 2012) was recently found to associate with Nups in *Drosophila* cells (Pascual-Garcia et al., 2017). GAF is known to both play an architectural genome-organizing role, and regulate formation of DNase Hypersensitive Sites (Ohtsuki and Levine, 1998; Fuda et al., 2015). Thus we assessed recruitment of GAF in our system and found GAF to be significantly recruited by Sec13 to *lacO*-96C, compared to control GFP or Nup62 (**Fig 2.8B**). To further verify specificity of proteins recruited by Sec13 to *lacO*-96C, we stained for architectural protein CTCF, which was also previously found to associate with Nups in certain conditions (Pascual-Garcia et al., 2017). Strikingly, the absence of CTCF at the *lacO*-96C under control conditions is maintained under conditions of Nup62 or Sec13 targeting (**Fig 2.8C**), supporting specificity of GAF and Brm recruitment by Sec13.

To investigate whether Sec13-induced chromatin decondensation indeed requires the PBAP complex, we introduced a Brm RNAi construct into our genetic tethering system. As validation, we observed that levels of Brm recruited to *lacO*-96C by tethered Sec13 were in fact reduced in the presence of Brm RNAi (**Fig 2.9B**). Analysis of Hoechst fluorescence levels at this locus yielded a visible and measureable increase in the correlation between LacI-fusion protein and Hoechst intensity levels in the presence of Brm RNAi, indicative of increased DNA density and reduced chromatin decondensation (**Fig 2.8D**). This result provides strong evidence that the observed robust recruitment of Brm, the ATPase component of the PBAP chromatin remodeling complex, is responsible for the Nup-induced chromatin decondensation.

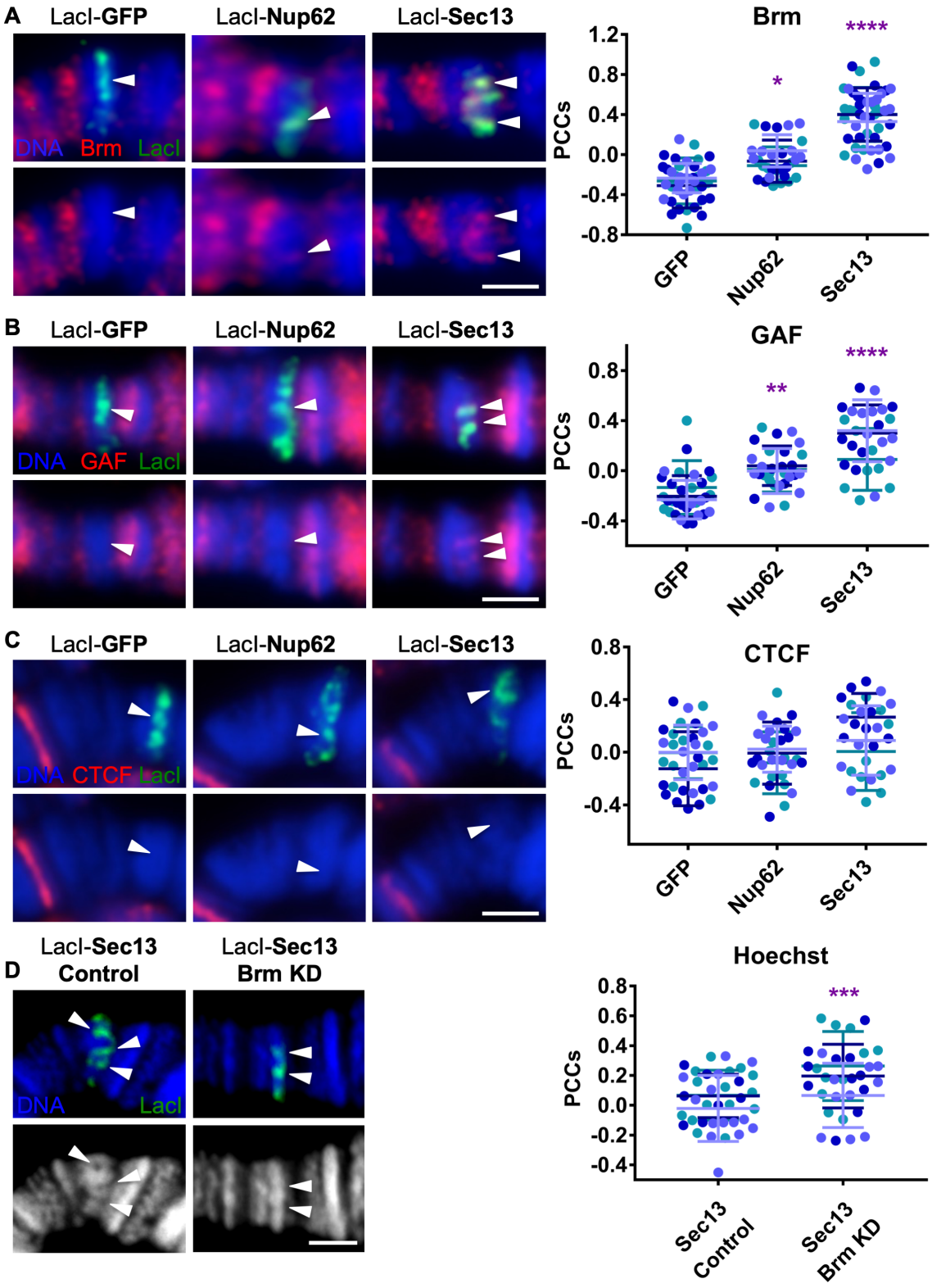
A
LacI-GFP
LacI-Nup62
LacI-Sec13
DNA Brm LacI
Brm
PCCs
1.2
0.8
0.4
0.0
-0.4
-0.8
*
****
GFP
Nup62
Sec13
B
LacI-GFP
LacI-Nup62
LacI-Sec13
DNA GAF LacI
GAF
PCCs
0.8
0.4
0.0
-0.4
**
****
GFP
Nup62
Sec13
C
LacI-GFP
LacI-Nup62
LacI-Sec13
DNA CTCF LacI
CTCF
PCCs
0.8
0.4
0.0
-0.4
GFP
Nup62
Sec13
D
LacI-Sec13
Control
LacI-Sec13
Brm KD
DNA LacI
Hoechst
PCCs
0.8
0.6
0.4
0.2
0.0
-0.2
-0.4
***
Sec13
Control
Sec13
Brm KD

Figure 2.8 Chromatin-tethered Sec13 recruits the chromatin remodeling PBAP/Brahma complex and associated GAGA Factor

(A) Widefield IF images of LacI-fusion proteins targeted to *lacO* integration site on squashed polytene chromosomes at cytological location 96C. Stained with Hoechst (blue) and antibodies against Brm (red) and GFP (green) for control or myc (green) for Nup fusion constructs due to antibody animal source constraints. Top row shows overlay of all 3 colors, bottom row shows blue and red only (here and in B, C). Arrows indicate locations of observed Brm recruitment or lack thereof under LacI signal. Scale bar is 2μm. Quantification displays PCCs between red and green signal under LacI. Data from 3 biological replicates (colored) from 2 independent experiments. GFP n = 41, Nup62 n = 30, Sec13 n = 45. **** = $p < 0.0001$ and *** = $p<0.001$. Error bars = standard deviation.
(B) Experimental conditions, strains and imaging as in *(A)* above, but with antibodies against GAF (red) and GFP (green) for control or myc (green) for Nup fusion constructs due to antibody animal source constraints. Arrows indicate locations of observed GAF recruitment or lack thereof under LacI signal. Data from 3 biological replicates (colored) from 2 independent experiments. GFP n = 32, Nup62 n = 29, Sec13 n = 28. **** = $p < 0.0001$ and *** = $p<0.001$. Error bars = standard deviation.
(C) Experimental conditions, strains and imaging as in *(A)* above, but with antibodies against CTCF (red) and GFP (green) for control or myc (green) for Nup fusion constructs due to antibody animal source constraints. Arrows indicate LacI signal. Scale bar is 2μm. Data from 3 biological replicates (colored) from 2 independent experiments. GFP n = 34, Nup62 n = 30, Sec13 n = 29. Error bars = standard deviation.
(D) Confocal IF images of LacI-Sec13 targeted to *lacO* integration site on squashed polytene chromosomes at location 96C on under control conditions (flies crossed to w1118 WT stock) or Brm KD conditions (flies crossed to Brm RNAi stock BL35211). Stained with Hoechst (blue or white) and α-LacI (green). LacI-Sec13 protein expression and Brm RNAi driven with Nubbin-Gal4. Top row shows overlay of the 2 channels, bottom row shows DNA stain only in white/grey scale. Arrows indicate locations of observed decondensation or lack thereof under LacI signal. Scale bar is 2μm. Quantification displays PCCs between red and blue signal under LacI. Data from 3 biological replicates (colored) from 2 independent experiments. GFP n = 27, Sec13 n = 33. Error bars = standard deviation.

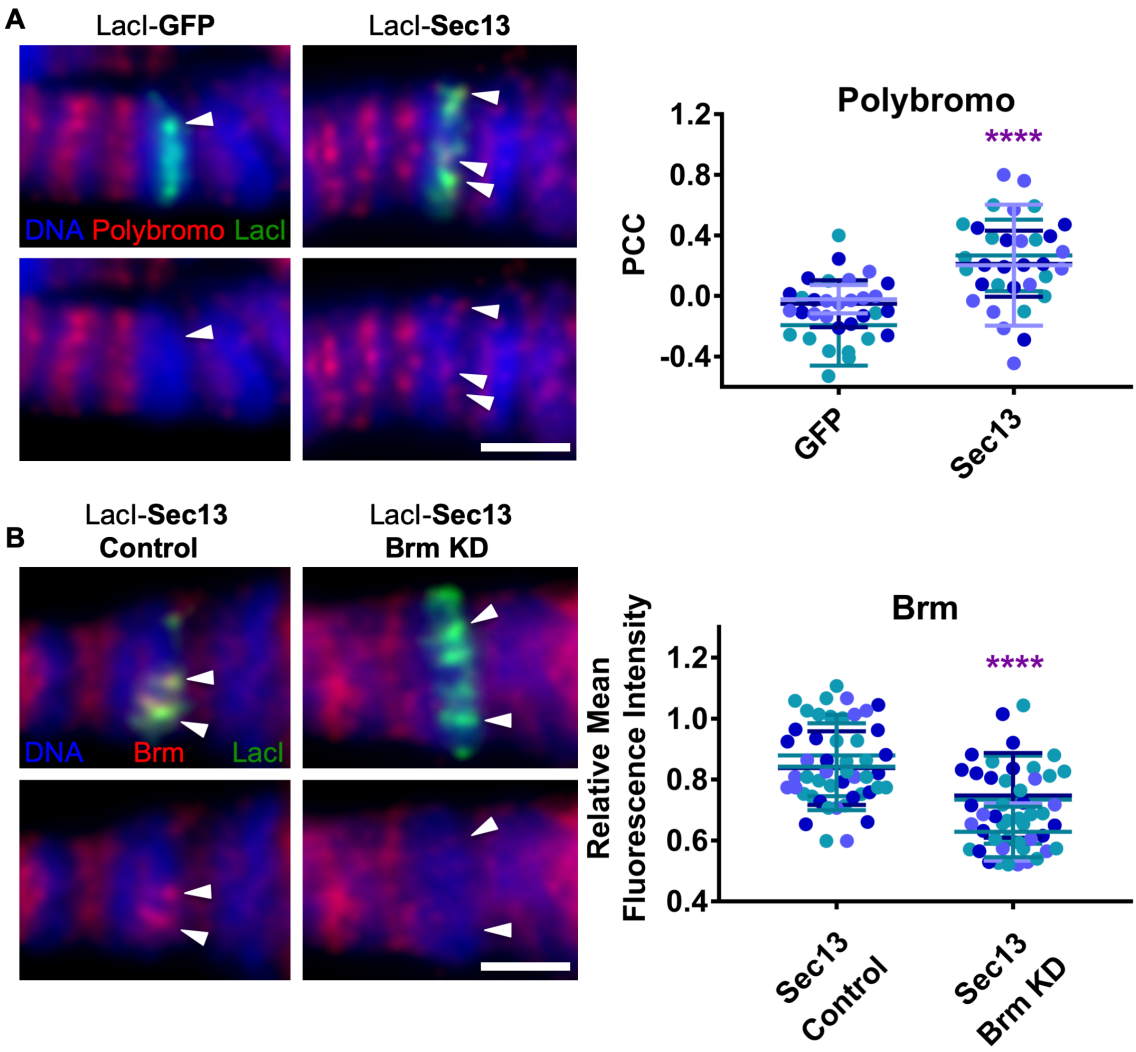

Figure 2.9 Sec13 recruits polybromo and RNAi validated Brm

(A) Widefield immunofluorescence images of LacI-fusion proteins targeted to *lacO* integration site on squashed polytene chromosomes at cytological location 96C on chromosome 3. Stained with Hoechst (blue) and antibodies against Polybromo (red) and GFP for control/myc (green). LacI-fusion protein expression driven with 2nd chromosome Nubbin-Gal4. Top row shows overlay of all 3 channels, bottom row shows overlay of blue and red only (here and in B). Arrows indicate locations of observed Polybromo recruitment or lack thereof under LacI signal. Scale bar is 2μm. Quantification displays Pearson Correlation Coefficients (PCCs) between red and green signal under LacI. Data from 3 independent biological replicates (colored) from 2 independent experiments. GFP n = 44, Sec13 n = 45. **** = $p < 0.0001$ Error bars represent standard deviation.

(B) Widefield immunofluorescence images of LacI-Sec13 targeted to *lacO* integration site on squashed polytene chromosomes at cytological location 96C on chromosome 3 under control conditions (flies crossed to w1118 WT stock) or Brm KD conditions (flies crossed to Brm RNAi stock BL35211). Stained with Hoechst (blue) and antibodies against Brm (red) and myc (green) for LacI-Sec13 myc-tagged fusion protein. Arrows indicate locations of observed Brm recruitment or lack thereof under LacI signal. Quantification displays mean Brm fluorescence signal intensity at *lacO* relative to nearby control band. Data from 3 independent biological replicates (colored) from 2 independent experiments. GFP n = 39, Sec13 n = 39. **** = $p < 0.0001$ Error bars represent standard deviation.

Endogenous Elys associates with Drosophila PBAP and regulates chromatin compaction.

To confirm that the relationship between Nups and chromatin remodeling proteins in our ectopic system are representative of their endogenous interactions, we conducted co-immunoprecipitation (co-IP) experiments in *Drosophila* S2 embryonic cultured cells. Immunoprecipitation of endogenous Sec13 and Elys, using previously characterized antibodies (Pascual-Garcia et al., 2017) resulted in a robust pull-down of PBAP components Brm and Bap60, especially in the case of Elys (**Fig 2.10A**). The reverse (co-IP) of PBAP components Brm, Bap60 and Polybromo demonstrated a reciprocal interaction with Sec13 and, again even more strongly, with Elys (**Fig 2.10A**). Interestingly, components of PBAP did not pull down Nup98, showing specificity of this interaction. These data indicate that endogenous Sec13 and Elys physically associate with PBAP chromatin remodeling proteins, and, based on the strength of these interactions, that Elys may be the primary interacting partner of chromatin remodelers. This conclusion is supported by our observation that there is a strong correlation between the level of Elys recruited by Nup62 (**Fig 2.6B-C)** and the degree to which Nup62 tethering decondenses chromatin at the two *lacO* loci, 96C and 60F (**Fig 2.1D-E**).

Additionally, this is supported by the similarity between levels of recruitment of Elys and of Brm by Nups at *lacO*-96C (**Figs 2.6B and 2.8A**). These results support a dose-dependent relationship, where levels of recruitment of Elys, and consequently, levels of Brm, regulate the degree of Nup-induced chromatin decondensation. Together, they point to Elys as the primary mediator of chromatin decondensation driven by Nups.

To further explore this, we wanted to determine whether Nups also contribute to chromatin decompaction in an endogenous context. Therefore we tested whether Sec13 and/or Elys are required for proper global nucleosome compaction, as assayed by genomic accessibility to Micrococcal nuclease (MNase) digestion, in *Drosophila* S2 cells. RNAi-mediated reduction of Elys versus control (**Fig 2.11A**) resulted in a reproducibly lower ratio of mononucleosomes to undigested genomic DNA upon MNase treatment **(Fig 2.10B-C**), indicative of more condensed chromatin upon Elys depletion. Interestingly, RNAi depletion of Sec13 did not manifest the same phenotype (**Fig 2.10B-C**), suggesting that Elys is the primary facilitator of chromatin decondensation. This is consistent with the stronger interaction of Elys with PBAP components compared to Sec13 in these cells, (**Fig 2.10**) and is also in agreement with our previously published ChIP-Seq profile showing binding of Elys to thousands of actively marked loci in fly tissues (Pascual-Garcia et al., 2017), further supporting the notion that Elys promotes chromatin accessibility throughout the genome.

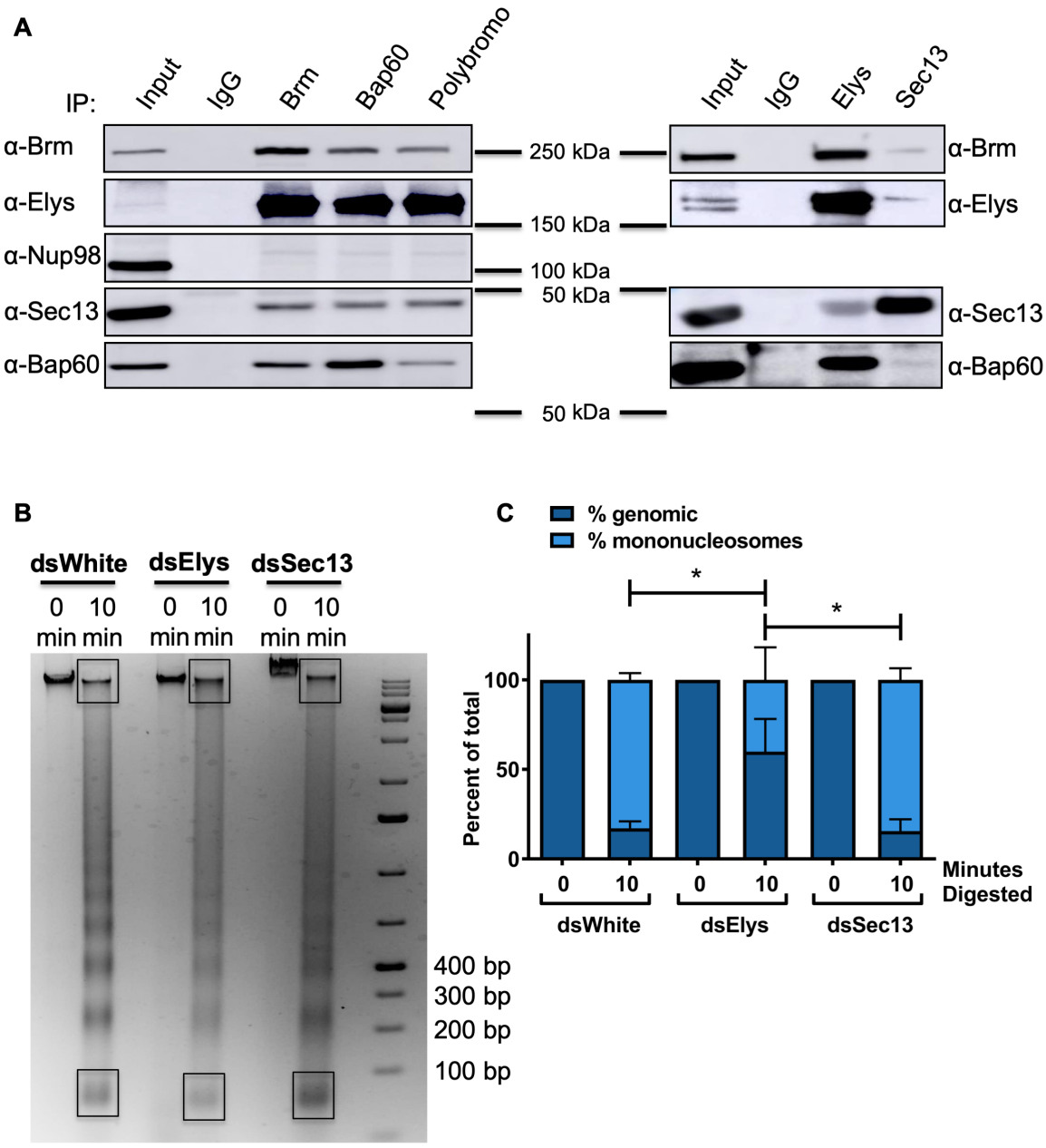

Figure 2.10 Endogenous Elys associates with Drosophila PBAP and regulates chromatin compaction

(A) Co-IP experiments in S2 cell lysates, , in which immunoprecipitates of the components of the PBAP complex were western blotted for Elys, Sec13, and Nup98, on the right.on the left. Co-IP experiments in S2 cell lysates in which immunoprecipitates of Elys or Sec13 were western blotted for components of the PBAP complex 10% of lysate relative to IP loaded for inputs, 40% per sample.

(B) Representative gel image of genomic DNA subjected to MNase digestion for indicated lengths of time from S2 cells treated with dsWhite (control), dsSec13, or dsElys RNAi (for 6 days). Black box indicates mononucleosome band, used in quantification of digestion (in C), relative to undigested genomic band at the top.
(C) Quantification of Mnase digestion of chromatin harvested from S2 cells treated with control, Elys or Sec13 dsRNA, displayed as a plot of relative amounts of the detected mononucleosome band and the undigested genomic band, at the indicated times of digestion. The mean and standard error bars are calculated from 4 independent biological replicates (2 replicates from 2 independent experiments), * = $p<0.05$.

Elys regulates levels of chromatin compaction and gene expression at endogenous gene targets.

To further characterize the regulation of chromatin compaction by Elys, we analyzed its proposed functions at endogenous target genes in S2 cells. Nups have been previously shown to bind and regulate expression of *Drosophila* genes *Hph* (Pascual-Garcia et al., 2014) and *B52* (Panda et al., 2014) in these cells, where both of these genes are expressed. Additionally, we have detected robust binding peaks of Elys at these genes in previous ChIP-seq experiments in fly tissues (Pascual-Garcia et al., 2017). We confirmed robust binding of Elys to *Hph* and *B52* promoter regions, relative to a negative control region (selected on the basis of lack of Elys ChIP-seq signal in fly tissues (Pascual-Garcia et al., 2017), by ChIP-qPCR (**Fig 2.11B-C**). We next set out to determine whether Elys exerts an effect on chromatin compaction of *Hph* and *B52*, with an MNase digestion followed by qPCR (MNase-qPCR) to determine occupancy levels of nucleosomes at specific loci. To verify our MNase-qPCR assay, we first tested it on a well-studied *Drosophila hsp70* gene that becomes highly activated and decondensed in response to heat shock (Petesch and Lis, 2008). As expected, upon heat shock of S2 cells, we detected a reduction in nucleosome occupancy throughout *hsp70* TSS and gene body (**Fig 2.11D**), as evidenced by a reduction of normalized qPCR signal in the

digested mononucleosomal fraction (as described in (Petesch and Lis, 2008)). The detected heat shock-induced difference in nucleosomal occupancy of *hsp70* supports the validity of this assay to measure levels of chromatin decondensation in a locus-specific manner.

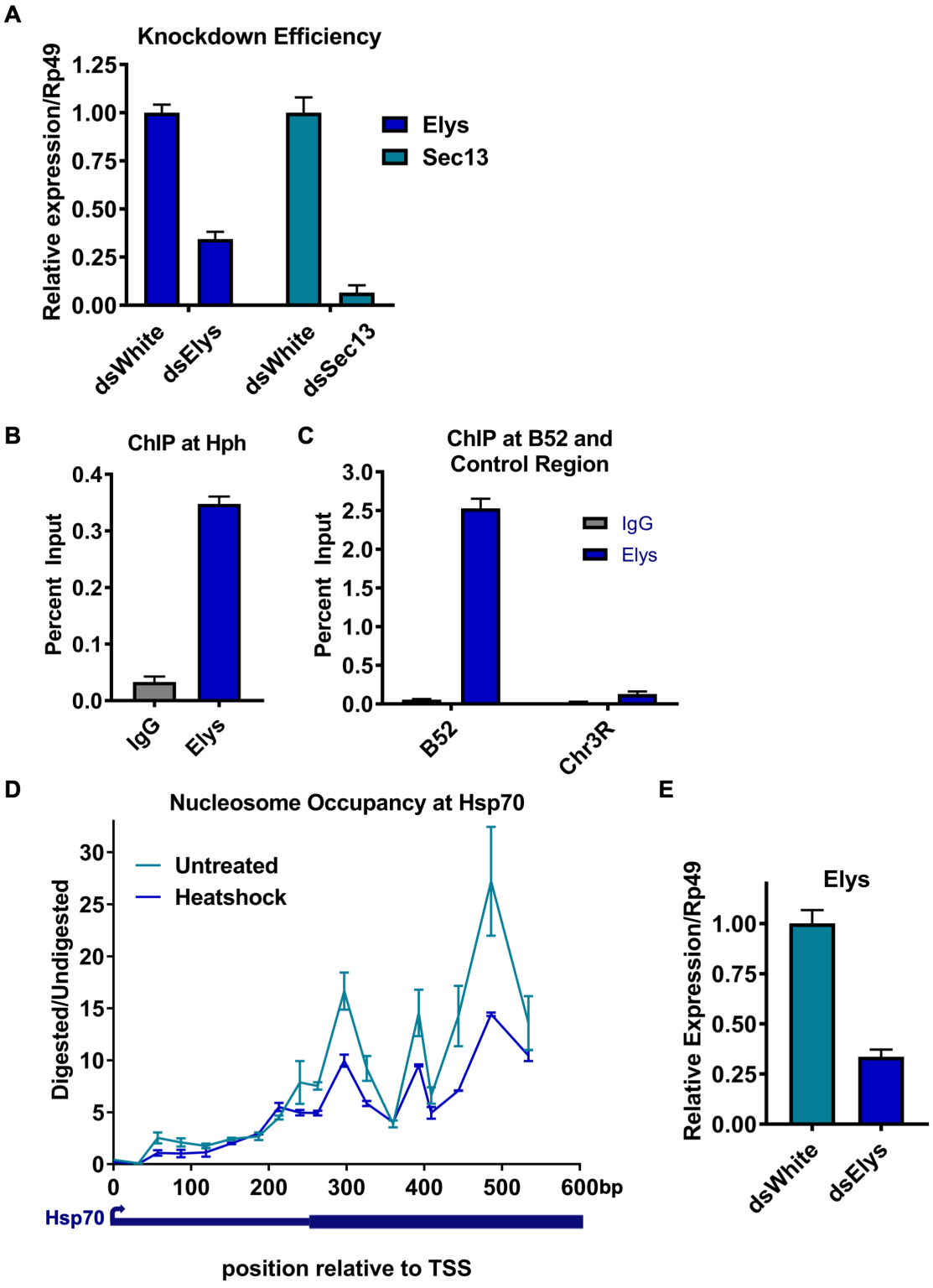
A
Knockdown Efficiency
Relative expression/Rp49
1.25
1.00
0.75
0.50
0.25
0.00
Elys
Sec13
dsWhite
dsElys
dsWhite
dsSec13
B
ChIP at Hph
Percent Input
0.4
0.3
0.2
0.1
0.0
IgG
Elys
C
ChIP at B52 and Control Region
Percent Input
3.0
2.5
2.0
1.5
1.0
0.5
0.0
IgG
Elys
B52
Chr3R
D
Nucleosome Occupancy at Hsp70
Digested/Undigested
30
25
20
15
10
5
0
Untreated
Heatshock
0
100
200
300
400
500
600bp
Hsp70
position relative to TSS
E
Elys
Relative Expression/Rp49
1.00
0.75
0.50
0.25
0.00
dsWhite
dsElys

Figure 2.11 Control experiments for testing the role of Elys in endogenous chromatin decondensation.

(A) qPCR validation of RNAi-mediated depletion of Elys and Sec13, relative to dsWhite control, in S2 cells, for experiments performed in Figure 6B-C. Error bars = SEM, from 4 biological replicates.
(B) Graph showing percent input recovery of chromatin in ChIP-qPCR using Elys or control IgG antibodies to detect level of binding of Elys at gene *Hph* TSS in *Drosophila* S2 cell culture. Error bars = SEM, from 2 biological replicates.
(C) Graph showing percent input recovery of chromatin in ChIP-qPCR using Elys or control IgG antibodies to detect level of binding of Elys at gene *B52* TSS in *Drosophila* S2 cell culture or negative control region on Chr3R. Error bars = SEM, from 2 biological replicates.
(D) Graph displaying nucleosome occupancy levels along a region spanning the first ~600bp of *Hsp70Ab* with the TSS marked as bp "0". Nucleosome occupancy measured by the ratio of digested to undigested chromatin (quantified by qPCR), retrieved following MNase digestion of genomic DNA from *Drosophila* S2 cultured cells under untreated or heat shock conditions. Schematic of corresponding regions of *Hsp70Ab* transcript below graph. Error bars = SEM, from 2 biological replicates.
(E) qPCR validation of RNAi-mediated depletion of Elys in S2 cells used for MNase-qPCR experiments, in Figure 7A-D. Error bars = SEM, from 3 biological replicates.

To test if Elys regulates nucleosome compaction levels at endogenous targets *Hph* and *B52*, we used the MNase-qPCR assay on S2 cells treated with control or Elys RNAi **(Fig 2.11E).** We found an increase in the occupancy of multiple nucleosomes throughout the TSS and gene body of *Hph* and *B52* upon dsElys RNAi treatment relative to dsWhite control (**Fig 2.12A,C, 2.11E**), suggesting an increase in chromatin compaction upon loss of Elys. To determine if reduction of Elys levels, and subsequent increase in chromatin compaction, also affected gene expression, we tested transcript levels by RT-qPCR, and found a significant reduction in the expression of both transcript isoforms of *Hph* (**Fig 2.12B**). This result supports the physiological relevance of Elys chromatin binding and regulation. Interestingly, expression of *B52* remained unaffected in Elys RNAi conditions (**Fig 2.12D**), despite increased nucleosomal occupancy we observed in the same conditions **(Fig 2.12C**). We postulate that *B52* may be regulated in

a different manner from *Hph*, such that the increase in chromatin condensation, caused by Elys depletion, is not sufficient to result in a significant down-regulation of expression of *B52*. However, the fact that Elys consistently affects chromatin compaction, regardless of its effect on expression, again suggests that chromatin decondensation is a primary chromatin-associated function of certain Nups such as Elys.

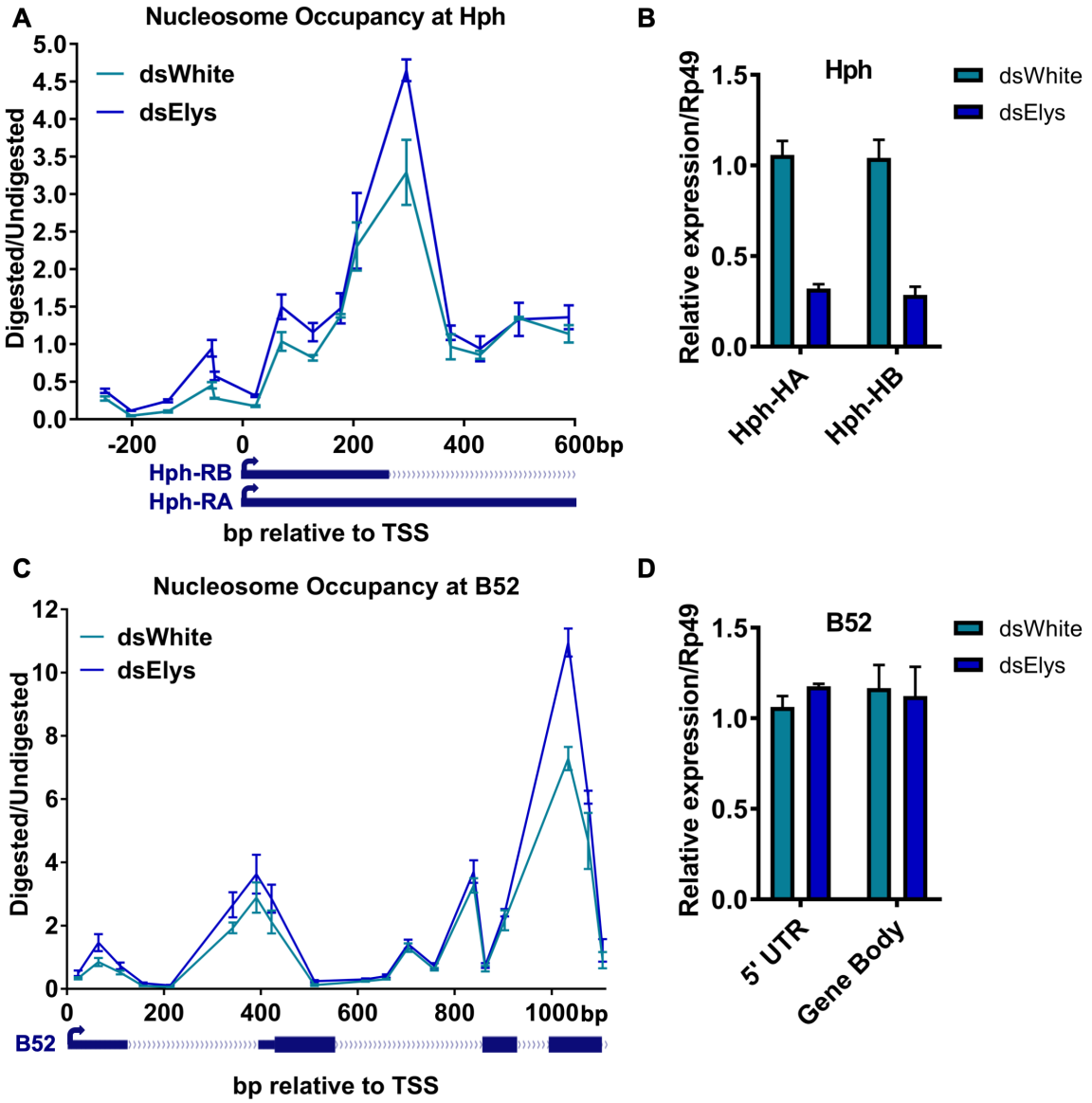

Figure 2.12 Elys regulates levels of chromatin compaction and gene expression at endogenous gene target

(A) Graph displaying nucleosome occupancy levels along a region spanning the first ~600bp downstream and ~200bp upstream from the TSS of *Hph* transcripts RA and RB (TSS marked as bp "0"). Nucleosome occupancy measured by the ratio of digested to undigested chromatin (quantified by qPCR), retrieved following MNase digestion of genomic DNA from *Drosophila* S2 cells treated with control dsWhite or dsElys RNAi. Schematic of corresponding regions of *Hph* RA and RB transcripts below graph. Error bars = SEM. Means and error bars obtained from 3 independent biological replicates here and in B-D.

(B) Expression data for HA and HB isoforms of *Drosophila* gene *Hph*, measured by RT-qPCR in *Drosophila* S2 cultured cells treated with control dsWhite or dsElys RNAi. Error bars = SD.
(C) Graph displaying nucleosome occupancy levels along a region spanning ~1000bp downstream of *B52* TSS (TSS marked as bp "0"). Nucleosome occupancy measured by the ratio of digested to undigested chromatin (quantified by qPCR), retrieved following MNase digestion of genomic DNA from *Drosophila* S2 cells treated with control dsWhite or dsElys RNAi. Schematic of corresponding regions of *B52* transcript below graph. Error bars = SEM.
(D) Expression data using primers against two regions of *Drosophila* gene *B52*, measured by RT-qPCR in *Drosophila* S2 cultured cells treated with control dsWhite or dsElys RNAi. The two target primer locations correspond to different locations within the *B52* gene region. Error bars = SD.

Discussion

The specific roles of different nuclear pore components in regulation of chromatin and gene expression remain poorly characterized. Our presented findings, combined with previous findings in the field demonstrating functional roles for Nups in regulating gene expression (Capelson et al., 2010; Kalverda et al., 2010; Light et al., 2010, 2013; Pascual-Garcia et al., 2014; Franks et al., 2017; Toda et al., 2017), lead to a compelling model whereby certain Nups primarily influence chromatin state, which in turn can affect downstream gene expression (**Fig 2.12E**). We propose that chromatin-bound Nups, such as Elys and Sec13, recruit factors associated with formation of open chromatin, specifically GAF and components of PBAP. This results in a permissive, open-chromatin state, which, in the right cellular contexts, may allow for binding of cell type/context-dependent transcription factors, RNAPII recruitment and activation, and subsequently an increase in downstream gene expression (**Fig 2.12E**). Together, our results and model suggest a specific chromatin-decondensing function of certain Nups, particularly Elys, as an early step in the process of gene activation.

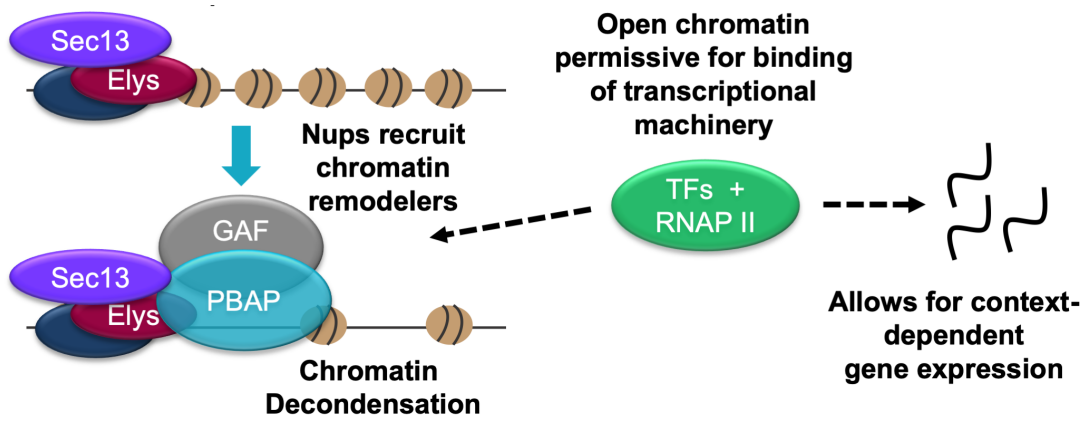

Figure 2.13 Model for chromatin state regulation by Nups.

Model whereby binding of Elys and Sec13 to chromatin recruit GAF and the chromatin remodeling complex PBAP, which promote chromatin decondensation/opening. Under proper developmental context, this may allow for transcription factors to access target genetic elements, promote RNAPII binding and activation, and contribute to subsequent downstream gene expression at Nup target genes.

Our article provides evidence that Nups facilitate chromatin decondensation. The resulting "holes" that appear in chromatin upon Nup tethering, visible by a decrease in DNA stain Hoechst **(Fig 2.1D-E),** and by loss of IF when using antibodies against both core histone H3 **(Fig 2.3A)** and histone modifications H3K27ac and H3K4me2 **(Figs 2.3B and 2.4)**, are consistent with the notion of chromatin decondensation. This is further supported by the observed recruitment and functional involvement of the chromatin remodeling PBAP complex (**Figs 2.8A,D and 2.9A**) and by additional biochemical data showing global **(Fig 2.10B-C)** and gene specific **(Fig 2.12A-D)** defects in nucleosome accessibility and occupancy, respectively, upon Elys depletion. Furthermore, the robust biochemical interaction between Nups and components of PBAP (**Fig 2.10A**), and the correlation between the amount of Brm recruitment by Nups and the level of observed decondensation at *lacO* 96C (**Figs 2.1E and 2.8A**) further

suggest to us that Nups have the capacity to promote target chromatin decondensation. One interesting outstanding question is whether these Nup-induced changes in chromatin structure can occur *de novo* (or rapidly after Nup binding), or require the process of chromatin assembly during replication to take effect. Our experiments have not differentiated between these possibilities. Further experiments, perhaps in blocking replication and assaying for similar Nup functions, could differentiate between these mechanisms further. Regardless, our findings strongly support the function of Nups in regulating compaction states of chromatin, while the particular cell cycle stage and the dynamic time frame, at which this process takes place, remain to be elucidated.

As previous studies have shown a relationship between Nups and gene expression changes, and transcription and chromatin decompaction are intimately intertwined, we were interested to know if our Nup-induced changes in chromatin were primary or secondary to transcriptional regulation. We observed increased transcription of the gene directly downstream from the *lacO* 96C integration, *dan*, upon tethering of Sec13, which also promoted decondensation here. However since Brm recruitment and chromatin decondensation appear to be much more robustly detected (**Fig 2.1E, Fig 2.8A**) than the presence of RNAPII **(Fig 2.3C)** upon Sec13 tethering**,** we believe that decondensation is likely the primary effect of Sec13 tethering, and increased gene expression a secondary consequence. This is supported by the fact that Nup62 is able to induce a small amount of detectable decondensation at 96C *lacO* (**Fig 2.1E**), associated with low level recruitment of Elys **(Fig 2.6B)** and Brm **(Fig 2.8A)**, but does not result in significant levels of RNAPII recruitment **(Fig 2.3C)**. Perhaps even more convincing evidence however is the increased nucleosome occupancy at both *Hph* and

B52 genes upon Elys KD **(Fig 7A and C)**, but only a transcriptional change detected in *Hph* expression **(Fig 7B and D),** which appears to decouple Nup-related changes in chromatin compaction and transcription. The differential effect of Elys depletion on Hph and B52 transcription again suggests that the primary role of Nups in this context is to facilitate the step of chromatin decondensation.

Although we found tethering of Sec13 to elicit chromatin decondensation in the ectopic context, our data suggests that Elys may be the Nup primarily responsible for facilitating decondensation. As discussed above, there is a striking correlation between levels of Elys recruitment and level of decondensation at multiple *lacO* loci (**Figs 2.6B-C and 2.1D-E**), and endogenous Elys appears to interact much more robustly with components of PBAP in S2 cells than Sec13 **(Fig 2.10A)**. Significantly, Elys depletion shows a defect in global genomic MNase digestion, whereas Sec13 depletion does not **(Fig 2.10B).** The latter experiment also suggests that the role of Elys in chromatin decondensation is independent of NPC integrity, as both Elys and Sec13 (which is a core component of the Nup107-Nup160 complex) are required for nuclear pore assembly (Walther et al., 2003; Rasala et al., 2008; Franz et al., 2007). Therefore a lack of phenotype of Sec13 RNAi in the MNase assay suggests that the observed reduction in nucleosomal accessibility in Elys RNAi conditions does not stem from a defect in NPC assembly. This conclusion is supported by the previously published observation that inhibiting transport capabilities of the NPC with WGA treatment does not lead to chromatin decondensation defects (Aze et al., 2017). We further hypothesize that since Elys exhibits a particularly robust genome-wide binding (Pascual-Garcia et al., 2017) while Sec13 appears to bind fewer loci (Capelson et al., 2010), Elys exhibits a stronger

and more detectable effect on global chromatin decompaction. It remains to be determined whether Sec13 and Elys share a subset of target genes, and whether chromatin-bound Sec13 co-functions with Elys in chromatin decompaction of such targets.

The data presented here provide functional and mechanistic evidence for the long-standing visual correlation between NPCs and open chromatin, and validates the hypothesized relationship between them. Interestingly, previous genetic and proteomic experiments have reported interactions between the *C. elegans* homolog of Elys, MEL-28, and chromatin remodeling complexes, including the SWI/SNF complex subunit SWSN-2.2 (Fernandez et al., 2014; Ertl et al., 2016), an evolutionarily conserved role for Elys in regulating chromatin state. Furthermore, genetic and physical interactions between yeast NPC components and the chromatin remodeling RSC complex have also been reported (Titus et al., 2010; Van de Vosse et al., 2013). Elys is known to bind condensed post-mitotic chromatin to nucleate NPC assembly during nuclear envelope reformation (Franz et al., 2007), and recent work has reported a defect in global post-mitotic chromatin decompaction associated with depletion of Elys from chromatin (Aze et al., 2017). Thus, an intriguing possibility is that in addition to NPC assembly, post-mitotic chromatin binding of Elys may also play a role in post-mitotic chromatin decompaction through mechanisms similar to those we have described here. A role for Nups in facilitating the formation or maintenance of open chromatin is also consistent with the evolutionarily conserved phenomenon of viral genome integration into open/active chromatin regions that are associated with NPCs (Manhas et al., 2018; Marini et al., 2015; Lelek et al., 2015). Finally, the interaction of Nups with developmentally critical

GAF and PBAP suggests that this relationship may be relevant to the establishment of tissue-specific open chromatin regions or the global genome decompaction during organismal development. It is possible that the potential role of Elys and possibly other Nups in post-mitotic chromatin decondensation has extended to regulation of chromatin structure in the context of interphase transcription, thus contributing to regulation of developmental transcriptional programs.

Chapter 3: Discussion and Future Directions

Summary and Perspectives

Over the last decade or so, it has become clear that Nuclear Pore Complexes and their constituent Nups play critical roles in regulating genome function in ways unrelated to nucleocytoplasmic transport. The 30 distinct nucleoporin proteins comprising this structure appear to have differential genome binding patterns and distinct functions at their respective gene targets (Light et al., 2013; Pascual-Garcia et al., 2014; Nanni et al., 2016; Kehat et al., 2011; Jacinto et al., 2015; Labade et al., 2016; Phatnani and Greenleaf, 2006; Vaquerizas et al., 2010). Sometimes an individual Nup can even have opposing functions from cell-type to cell-type or even locus to locus (Nanni et al., 2016; Vaquerizas et al., 2010; Jacinto et al., 2015). Considering that many of the genomic targets of Nups are critical for cellular, tissue, and organismal development, as has been discussed, understanding the intricacies of how different Nups function to regulate these transcriptional programs could be critical to understanding Nup roles in human development and disease. Here I have discussed our findings regarding the roles Nups Elys, Sec13, and Nup62 play in regulation of the genome through recruitment of chromatin remodelers, facilitating chromatin decondensation and accessibility for downstream transcription.

The Nucleoporin Elys was originally discovered and characterized as a transcription factor (Kimura et al., 2002) based on its ability to elicit significant target upregulation in a reporter gene assay, as well as observed tissue-specific expression patterns in mouse embryos. Eventually, its membership as a necessary component of

NPCs was discovered, along with its ability to bind condensed mitotic chromatin to seed formation of said pores during nuclear envelope reformation (Franz et al., 2007; Rasala et al., 2006). Elys has two DNA and chromatin binding domains which have proven important, both for this function, as well as an additional role as a component of mitotic and meiotic kinetochores, regulating chromosome segregation (Gómez-Saldivar et al., 2016). Based on the findings of this thesis, I believe these domains with the capacity to bind DNA and chromatin are likely important for yet another function of Elys: regulation of chromatin state.

We have found that nucleoporin Elys is robustly recruited to an ectopic locus by a chromatin-tethered Sec13, less robustly recruited by Nup62, and in this way have observed a strong correlation between Elys and observable chromatin decondensation at multiple target genomic loci. These immunofluorescence tethering experiments conducted with *Drosophila melanogaster* larval salivary gland polytene chromosomes have provided us with a unique opportunity to visualize the effect of Nups on chromatin state in a high resolution and also gain-of-function manner. Utilizing this method, we were also able to observe recruitment of components of the PBAP chromatin remodeling complex, which correlated strongly with Elys recruitment levels, and was shown to be required for the Sec13-induced decondensation we visualized.

The strong correlation between levels of Elys recruited to these loci, levels of the PBAP ATPase Brm recruited, and visible decondensation, suggested to us that Elys may play a role in recruitment of the chromatin-remodeling complex. Upon further probing these relationships in an endogenous context in *Drosophila* S2 cell culture, we found a strikingly robust biochemical relationship between Elys and components of

PBAP, especially relative to the less intense interactions with Sec13 and PBAP, through co-IP experiments. These detected protein-protein interactions occurred in an endogenous context in WT cells, completely independent of the ectopic tethering system we devised in the transgenic *Drosophila* lines. This provided strong support that the interactions we observed in that system were indeed indicative of true protein behaviors and a generalizable trend, at least within *Drosophila* cells. Upon observation of this robust interaction between Elys and chromatin remodelers, we combed through the literature to ultimately find obscure, but recurring, instances of Elys homologs in yeast and *C. elegans* interacting with chromatin remodelers in genetic or protein interaction screens (Ertl et al., 2016; Fernandez et al., 2014; Fasci et al., 2018). In two of these instances, the interaction of the Elys homolog with a chromatin remodeler was merely a single line in a large interaction table, once even only in the supplemental data. In the third however, the discovered interaction was explored in two experiments, demonstrating both co-localization of the two proteins on mitotic chromosomes, and the requirement for the remodeler in proper NPC assembly, assumedly through its interactions with Elys (Ertl et al., 2016). To date, this is, to our knowledge, the only existing data regarding Elys and its interactions with chromatin remodelers. These findings are not only incredibly supportive of the validity and evolutionarily conserved nature of our own observed interactions of Elys with remodelers, but also demonstrates the novelty of our findings on the function of Elys in this role.

Regarding this, we have, in my thesis work, shown that these interactions between Elys and chromatin remodelers appear to have functional consequences. In these same *Drosophila* S2 cells in which we observed robust biochemical interaction

between these proteins, we have additionally observed defects in global chromatin decondensation, based on large-scale MNase digestion patterns upon knock-down of Elys. Interestingly, we do not see this phenotype for Sec13 loss. These findings are consistent with the hypothesis that perhaps Elys plays a role at many of its genetic targets in localizing, stabilizing, or in some way facilitating the activity of chromatin remodelers such as PBAP in the action of inducing chromatin decondensation, our favored hypothesis being recruitment based on our findings in the ectopic tethering system.

Additionally, the finding that Sec13 loss does not produce defects in chromatin decondensation in this assay is in alignment with the reduced interaction we observed between Sec13 and PBAP in the co-IP experiments, compared to robust interactions with Elys. This suggests to us that perhaps in our ectopic tethering system, the main function of Sec13 was indeed just the recruitment of Elys based on their normal protein-protein interactions present as components of the same subcomplex within NPCs, and in fact Sec13 itself may not inherently play a role in chromatin decondensation. This is consistent with our findings, but is perhaps peculiar given the original findings that seeded this project: at endogenous Sec13 targets in polytene chromosomes, it is required for chromatin decondensation associated with target gene activation (Capelson et al., 2010). What is unknown is whether Elys is present at these genes in question at this stage in larval development, and if perhaps Elys may be involved in this phenomenon. Perhaps Sec13 is indeed a mediator or stabilizer between Elys and chromatin at some endogenous genetic targets, in order to facilitate some specificity in Elys targeting. This would likely be a minority of Elys genomic targets, as no defect was

detected upon Sec13 loss in the global chromatin compaction MNase assay. As Elys is the only Nup known to possess a chromatin or DNA binding domain however, it would seem rather more likely for Elys to be the link between other Nups and chromatin in their roles in regulating gene expression, as it is well-known to be in post-mitotic pore formation. It is possible that there is some combinatorial or synergistic effect of binding of multiple Nups to specific targets, but this is a question yet to be explored, and will be touched on in the “Future Directions” section below.

We next recapitulated our observations of Elys in promoting genome-wide chromatin decondensation also at the nucleosomal level at Elys target genes. All of this data combined suggests a role for Elys in regulating the localization and/or activity of chromatin remodeling proteins to promote the formation or maintenance of open chromatin at target loci. This is interestingly in line with what may have been an incidental finding from a study examining Elys’ role in NPC assembly, where nuclear envelope reformation was defective in conditions in which Elys was depleted from chromatin, and subsequent nuclear size and chromatin compaction did not return to pre-mitotic levels (Aze et al., 2017). They attribute the defect in nuclear size and chromatin compaction to a lack of nuclear import of factors that are required for “swelling” the nucleus and replicating the genome, but our findings would suggest perhaps Elys itself may also be playing a much more active role on chromatin to promote post-mitotic chromatin decompaction through its interactions with chromatin remodelers. What remains to be teased apart is the timing of these processes. Is Elys capable of promoting “*de novo*” chromatin decompaction on short time scales at genetic targets to promote quick decondensation for imminent transcriptional activity? Or does it require

progression through mitosis, mostly functioning in post-mitotic decondensation with perhaps some bookmarking of a few targets for future decondensation? These and other queries bring us to our next section where we will discuss some of these unresolved questions, and the exciting possibilities for future research.

Future Directions

As mentioned, one lingering question remains the timing of Elys in its ability to promote chromatin decondensation. Can Elys receive some cellular signal, bind a target, recruit chromatin remodelers, and facilitate decondensation, and therefore downstream transcription, on the time-scale of a transcription factor? Or does the role of Elys in regulating chromatin structure require and rely on its post-mitotic chromatin binding during the process of nuclear envelope reformation? This is a question we have thought a lot about, and would wish addressed. We unfortunately do not have the tools to do the elegant experiment of imaging live protein and chromatin dynamics in our ectopic tethering system to observe these processes in real time, as was suggested by an enthusiastic reviewer, which I genuinely regret. The next best experiment we believe that would begin to answer this question would involve conducting MNase-qPCR assays at the verified Elys genetic targets to determine if defects in nucleosome occupancy caused by Elys reduction persist in the presence of replication inhibitors. This would prevent DNA replication and stall progression through mitosis, and, given early enough timepoints, perhaps enlighten us as to the speed with which Elys can influence chromatin state. These experiments are difficult in *Drosophila* S2 cell culture however,

as these cells are notoriously resistant to mitotic synchronization, and would therefore likely be more successful in another cell type.

Another unknown about the phenomenon I have described here regards the other proteins likely required to facilitate the level of decondensation we have observed. As discussed in the introduction of this thesis, chromatin remodeling is just one mechanism of changing chromatin state, another major mechanism being the modification of histone tails by PTMs. Acetylation of histone tails has both *in vitro* and *in vivo* been reliably associated with decondensing chromatin by pushing nucleosomes farther apart from each other, not relative to the DNA strand, but relative to each other in 3-dimensional space. This is another important component of decondensation mechanisms that makes DNA more accessible to transcription factors and machinery. Chromatin remodeling complexes are capable of sliding nucleosomes and evicting histones, as we have observed in our MNase experiments, but large-scale decondensation we see on the level of half of a polytene chromosome band, (corresponding to the scale of a TAD (Ulianov et al., 2016)), in our system likely involves a mechanism in addition to remodeling. A literature search provided a known interaction between Brm and histone acetyltransferase CBP, and the reliance of CBP activity on functional Brm protein (Tie et al., 2012). This was especially interesting, because CBP has previously been found associated with Nup153 and Nup98 (Nanni et al., 2016; Kasper et al., 1999; Pascual-Garcia et al., 2017). Based on all of this information, I did assay for an increase in the CBP-associated mark H3K27ac at the *lacO*-96C site upon Sec13 tethering, and unfortunately saw none. While this could be simply because it would be difficult to detect an increase in presence of this mark here

due to the decreased overall nucleosome density, as we can see with staining against unmodified H3, I did also investigate whether CBP itself was recruited, and saw no such phenomenon (data not shown). This suggests to us that CBP and H3K27ac are likely not involved in this specific mechanism we have uncovered of Elys and PBAP-dependent decondensation. However an interrogation for other marks and histone-modifying proteins that may be involved in this process is worthy of future work in order to better understand the full magnitude and mechanism of Elys-induced chromatin decondensation.

Induction of transcription has, in the past, proven sufficient to induce chromatin decondensation at a gene target (Tumbar et al., 1999; Müller et al., 2001; Muller et al., 2004; Janicki et al., 2004). At the inception of this project, it was not known if the Sec13-dependent decondensation observed previously in polytenes was a cause or consequence of the RNAPII recruitment and transcription of those genes, also dependent on Sec13 (Capelson et al., 2010). We hypothesized that the decondensation was primary, based on careful timing experiments showing Sec13 localizing to these loci seemingly prior to RNAPII, however this was not conclusive. In my work, we have furthered the case that decondensation is a primary consequence of Nup binding in this context, and not secondary to transcription. This is primarily based on two pieces of data, 1) the magnitude of the recruitment of Brm to the decondensed loci dwarfs the minute amount of active RNAPII recruited, or transcriptional change, suggesting an upstream mechanism, and 2) upon Elys loss in S2 cells, we have observed in one target gene, B52, a change in nucleosome density without a change in transcriptional output, again suggesting decondensation as primary to transcriptional changes. However none

of these is conclusive evidence. To definitively verify that Nup-induced decondensation is independent of transcription, the next experiment would simply be to conduct the MNase-qPCR assay at Elys target genes and inhibit transcriptional elongation of RNAPII with a kinase inhibitor, such as 5,6-dichloro-1-β-D-ribofuranosylbenzimidazole (DRB). If this successfully eliminates expression of targets genes but does not affect Nup-induced nucleosome occupancy changes, then that would robustly support the hypothesis that Nup-induced decondensation is transcription-independent. Conducting this same inhibition in the salivary glands and examining decondensation at the ectopic loci would also be a valuable experiment with which we could address this question.

It has become clear that the numerous individual Nups have differential functions regarding regulation of the genome. Some Nups bind active cell cycle and developmental genes, and some bind repressed genes, many of which are also cell-type specific. In addition to the questions I have raised regarding the downstream functions of Nup interactions with chromatin, there are many outstanding questions regarding the initial patterns and mechanics of Nup binding. What targets different Nups to specific gene targets? Elys is the only Nup known to have a chromatin/DNA binding domain, is it required as a mediator for all other Nups to interact with the genome, and if not, what adaptor proteins are they using to interact with chromatin? How much of Elys function at its endogenous genes relies on any other Nups? Does a given Nup bind different sets of genes in different cell types? What determines if a given Nup will have a repressive function at one gene and an activating function at another?

These questions represent likely multiple theses worth of work, but they are questions that I believe are incredibly useful to understanding the role that Nups are playing in regulating gene expression programs. A side project I wished to embark on during my

tenure in the lab, but did not end up procuring the time for, would be the jumping off point to begin to answer questions such as these. It would be incredibly useful to develop a database of binding patterns for multiple Nups in distinct cell types. Understanding simply the differences in binding patterns from Nup to Nup and cell type to cell type could be incredibly informative as to their functions, and give us information with which to ask more nuanced questions. These experiments are technically especially challenging with *Drosophila* cells, as the antibody number and quality are limited for *Drosophila* Nups, so such an endeavor would likely be more fruitful in mouse or human cells. As many Nups have been implicated in regulation of development, gathering binding data of Nups in mouse Embryonic Stem Cells (mESCs) and also a differentiated cell type such as Mouse Embryonic Fibroblasts (MEFs), would perhaps be an interesting starting point. I would hypothesize that Nups likely narrow down their binding profiles throughout differentiation to tune in on regulation of specific transcriptional programs over time. Once this kind of database was procured, comparisons of Nup binding profiles against the vast databases of other chromatin binding proteins that have been generated for such commonly used cell types could also give us hints as to what other proteins specific Nups tend to co-localize with in these different contexts. This would thereby provide for potential candidates to test for mediating Nup-genome interactions, and for co-operative functions with Nups in regulating target gene expression. Data that could be gleaned from such experiments could provide for a wealth of information about the intricacies of how nucleoporins are functioning to regulate chromatin and gene expression programs in cellular and organismal development.

Concluding Remarks

The pleiotropic nature of nuclear pore proteins continue to impress and awe me. This giant multimeric complex is being utilized by the cell and nucleus for so many functions other than nucleocytoplasmic transport, and the number of proteins involved, and the context-dependent, sometimes antagonistic functions of individual Nups, demonstrate that there is so much more to be discovered about the true depth of their reach. I have through my work provided a novel understanding to the field of how the nucleoporin Elys performs an integral function working with chromatin remodeling proteins to facilitate gene expression through regulation of chromatin structure. Based on the number of Nup mutations that have negative consequences in human development and disease, and the critical role Elys likely plays in facilitating the functions of many Nups on chromatin, it is my hope that this research will end up providing useful contributions to the field, and perhaps one day even to human health in some meaningful way.

Chapter 4: Materials and Methods

This chapter is adapted from:

Kuhn, T.M., P. Pascual-Garcia, A. Gozalo, S.C. Little, and M. Capelson. 2019. Chromatin targeting of nuclear pore proteins induces chromatin decondensation. J. Cell Biol. *218* (9).

Cloning, Transgenic Line Generation and Protein Verification

Gateway cloning was used to add the LacI sequence (NCBI E.coli GeneID 945007), missing the last 8 amino acids that represent the tetramerization domain, on the N terminus of full length Nup62 or Sec13 within a pTWM Gateway vector containing a C-terminal myc tag and N-terminal UAS regulatory sequence. These were sent to BestGene Inc for embryo injection for random p-element mediated genomic integration. Lines were verified by homogenizing 5 larvae per genotype in Laemmli buffer, loading supernatent into SDS-PAGE acrylamide gel and western blotting resulting membrane with α-LacI antibody (Fig S1).

Drosophila Stocks and Genetics

Drosophila were raised at 22 degrees on standard molasses fly food. Stocks with genomically integrated *lacO* arrays are as follows: *lacO*-96C (line P11.3 from (Li et al.,

2003), *lacO*-60F (Bloomington #25371, generated by Sedat lab) and *lacO*-4D5 (from (Danzer and Wallrath, 2004)). Crosses for larval salivary gland IF were made using females from generated stocks containing *lacO*-4D5 and driver Nub-Gal4 (Bloomington # 42699), *lacO*-60F and driver Sgs3-Gal4 (Bloomington #6870), or *lacO*-96C and driver Nub-Gal4, crossed to homozygous males from UAS-LacI-Nup fusions lines or UAS-LacI-GFP (Danzer and Wallrath, 2004). Brm RNAi KD line is Bloomington #35211. Larvae were raised in undercrowded conditions and dissected at later wandering 3rd instar stage, where larvae are minimally moving but anterior spiracles have not yet protruded.

Polytene Chromosome Squashing, Immunostaining, and Fluorescence Imaging

Salivary glands were dissected from wandering 3rd instar *Drosophila melanogaster* larvae in 0.1% PBSTween (PBST), fixed in 2%PFA / 45% acetic acid 1' @RT, squashed in a drop of 45% acetic acid between Sigmacoted (SL2 Sigma) coverslip and poly-L-lysinated slide (Polysciences 22247) with rubber hammer, snap-frozen in liquid nitrogen, coverslips were flipped off, and slides were stored for <1 hr in 0.1% PBST in coplin jar before blocking in 3% BSA PBST for 30' @RT and incubated O/N @4C in 30ul in blocking solution containing primary antibodies under coverslip in humid chamber. The following day they were washed 3x10' PBST, stained with secondary antibodies in blocking solution 1 hr @RT in dark, and then washed 3x10' again before treatment with Hoechst stain 10 ug/mL in PBS for 2 minutes followed by 5' PBS wash before mounting in Prolong Gold Antifade ThermoFisher P36930, sealing with nail polish, and storage in 4C. Slides were imaged within 1 week of fixation. Widefield fluorescence imaging was

conducted at room temperature on a Leica DM6000 Microscope with PL APO 100X/1.40-0.70 Oil objective using Type F Immersion Oil Leica 11513859, DFC365 FX Camera and Leica LAS-X 3.3 Software. Confocal imaging was conducted at room temperature on a Leica TCS SP8 Confocal using PL APO 63x/1.40 Oil objective, 4x Zoom, Type F Immersion Oil Leica 11513859, and Leica Software LAS-X 3.3. Fluorochromes used are listed in antibodies section. A minimum of 3 animals and, on average, 10-15 *lacO* sites per animal were imaged and analyzed for all experiments, with the exception of squashes with *lacO*-60F due to limitations in ability to reliably localize sufficient LacI protein levels bound to *lacO*, possibly due to the repetitive nature of this locus in the sub-telomeric chromatin being frequently under-replicated.

Antibodies for Immunofluorescence

Primary antibodies and dilutions used: GFP #1020 from Aves Labs Inc at 1:500, LacI #600-401-B04S from Rockland Inc at 1:100, Myc 9E10/sc-40X from Santa Cruz Biotechnology at 1:100, mAb414 (NPC marker) #902901 from Biolegend at 1:20, H3 #39763 from Active Motif at 1:100, HOAP from Yikang Rong Lab at 1:100, H3K27ac #39135 from Active Motif at 1:100, H3K4me2 #39141 from Active Motif at 1:100, H5 (Ser2ph RNAPII) #920204 from Biolegend at 1:20, Mtor #12F10 from DSHB at 1:30, Brm, Bap60 and polybromo from Susumu Hirose Lab at 1:100, GAF from Julia Zeitlinger Lab 1:50, CTCF from Victor Corces Lab 1:100, Nup107 #29864 from Capelson Lab at 1:100, Nup93 #2648 at 1:100 and Elys at 1:50 both from Capelson Lab (Pascual-Garcia et al., 2017), Hoechst DNA stain Thermofisher H3570 1:1000. Fluorescently conjugated

secondary antibodies: ThermoFisher Alexafluor conjugates of goat anti-mouse, anti-rabbit, and anti-guinea pig to 488 and 568.

H3 alternative fixation conditions for polytene squashes

Polytene chromosome squashes for use with the H3 antibody required an alternative fixation protocol to prevent extraction of histones from chromatin, which replaced standard fixation of glands with a 30 second fix in 2% PFA, followed by 2’ in 2% PFA / 45% acetic acid, and a final placement into a drop of 45% acetic acid during squashing all @RT. After flash freezing in liquid nitrogen, slides were kept at -20C in 70% Ethanol at least 30 minutes before 2 quick rinses in PBST and standard subsequent blocking and staining protocol.

Polytene chromosome nuclei semi-squashes

Semi-squashes used to better preserve nuclear shape to verify rim staining of LacI-Nup fusions (**Fig S1**) use an identical protocol as full squashes with instead, a 2' fixation in 8% acetic acid / 2% PFA and a 2% PFA droplet used on the coverslip, at which point coverslip is not hammered but gently moved ~1mm in each direction 2x before freezing. Antibodies and dilutions are listed in Supplemental Table S1.

Pearson Correlation Coefficient (PCC) Analysis

Intensity correlation analysis was performed to determine the extent to which a given LacI fusion protein (the "tester") resulted in enrichment or depletion of components of chromatin modifying complexes or other factors (the "targets"). Each image consisted of three channels representing Hoechst and the immunofluorescence signals of the tester and target. To select pixels for inclusion in the correlation calculation, image segmentation was performed on the Hoechst and tester images using custom MATLAB software. First, manual input was used to select a candidate threshold from the Hoechst DNA image, followed by balanced histogram thresholding of the tester. Further manual input was used to refine the tester- and Hoechst-based masks to ensure that 1) the majority of pixels included in the correlation calculation contained non-background levels of tester signal, and that 2) these signals were localized to the chromosome. Values reported are Pearson's linear correlation coefficients (PCCs) calculated using target-tester value pairs for all pixels found in the joint Hoechst-tester mask. In cases of measuring chromatin decondensation, Hoechst channel was used as the target as well. Statistical significance was determined by one-way ANOVA test with Tukey's multiple comparisons post-test where 3 genotypes are compared, and unpaired t-test where only 2 genotypes are compared.

HOAP area quantification

Using ImageJ, red HOAP capping signals at the telomere of chromosome 2R, designated by the presence of LacI-fusion protein signal at adjacent *lacO*-60F, were

manually traced and the areas measured and compared for each condition. Statistical significance was determined by one-way ANOVA test with Tukey's multiple comparisons post-test

3D FISH in Intact Salivary Glands

Inverted larval heads (removing fat, gut and heart but preserving brain, discs and glands), were dissected in cold PBS, collected on ice, and fixed using 200ul 4%PFA/0.5%IGEPAL/PBS + 600ul Heptane, hand-shaken vigorously, and incubated 10' on nutator. Fixation solution was changed out for PBST, washed 3x5', rinsed 3x in 2XSSCT, transferred to 20% formamide in 2XSSCT 10' @RT, transferred to 50% formamide 10'@ RT, then 50% formamide for 3-5hrs @37C on rocker in hybridization oven. Heads were then incubated in 100ul hybridization buffer (2XSSCT/10%dextran sulfate/50%formamide) + 200ng lacO probe (sequence listed in **Table 4.1**) for 30' @80C before O/N incubation in hybridization oven rocking @37C. After probe incubation heads were washed 2x in 50% formamide 30' @37C, washed in 20% formamide 10' @RT, rinsed 4x in 2XSSCT, stained with 10 ug/mL Hoechst in 2xSSCT 5', washed 5' in 2XSSCT, and 10' in 2XSSC, after which glands were dissected from heads in 2XSSC and gently mounted in non-hardening VectaShield antifade (Vector-Labs H-1000) and stored upside down in slide box with raised slots to prevent nuclei flattening until imaging using 3D confocal microscopy.

Brm Reduction Quantification

Using ImageJ, green LacI-Sec13 protein fusion bands at each *lacO*-96C site were manually traced and the corresponding mean intensity value of the red Brm fluorescence signal under those bands was measured. The mean fluorescence intensity of nearby Brm control band located in the interband of nearby 96D observed to remain unchanged between preps at this stage in development was also measured. A ratio between each *lacO*/control band was generated and plotted for control and Brm KD conditions. Statistical significance was determined by unpaired t-test.

Co-immunoprecipitation and Western Blotting

S2 cells were harvested and washed twice in PBS. 3x10^7 cells were resuspended in 250ul of High-Salt buffer (10mM Tris-HCL, pH 7.4, 400mM NaCl, 1% Triton X-100, 2mM EGTA, 1mM MgCl2, 1mM DTT and C0mplete EDTA-free Tablet (1 per 10 mL)) (Sigma Aldrich 11873580001) and Pierce Nuclease (1:500) for 45 min at 4C. The sample was then sonicated 3x10 seconds on setting 2 of Fischer Sonic Dismembrator Model 100, resting 10 seconds on ice between sonications. The sample was spun down at 10,000 rcf for 10 minutes and 500 ul of No-Salt buffer (10mM Tris-HCL, pH 7.4, 2mM EDTA, 1mM DTT) was added. 6 ul of antibody was added to the lysate mixture and incubated O/N on a rotator at 4C. 30 ul of Dynabeads (Life Technologies) were washed in blocking buffer (0.3% BSA in PBS) and blocked for 30 minutes. Beads were washed in no salt buffer once, added to the antibody/lysate mixture, and incubated on a rotator 3hrs @4C. After incubating, beads were washed 5 times in wash buffer (1:3 High-Salt : No-Salt),

eluted in 1x Laemmli buffer, run on SDS-PAGE gel, transferred to membrane, and blotted against indicated antibodies.

Cell Culture and RNA Interference

Drosophila S2 cells were grown in Schneider's medium (Life Technologies) supplemented with 10% heat inactivated fetal bovine serum (GIBCO) and antibiotics. Double-stranded RNAs (dsRNA) against White, Elys and Sec13 genes were generated from PCR templates of fly genomic DNA using specific T7 primers listed in **Table 4.4.** dsRNAs were synthesized using Megascript T7 kit (Ambion) following manufacturer instructions. S2 cells were seeded at 15 x 10^6 cells per plate in a 10 cm dish plate, treated with 10ug of specific dsRNA per 10^6 cells every 48h, and harvested after 6 days of treatment.

RNA extraction and RT-qPCR expression analysis

Total RNA was isolated using Trizol (Ambion) from salivary glands vortexed at 4C for 2hr, or S2 cell pellets vortexed for 30', extracted with ethanol precipitation and subsequently purified with PureLink RNA Kit columns (Invitrogen). 1 µg of the extracted RNA was used for first-strand cDNA synthesis using one-step RT-PCR kit (Qiagen). To measure mRNA levels, quantitative real-time PCRs (qPCRs) were carried out on resulting cDNA using gene-specific primers, listed in **Table 4.2**.

Global Micrococcal Nuclease (MNase) Digestion Assay

MNase accessibility assays were performed on equal amounts of collected dsRNA-treated S2 cells (described above). Cells were incubated for 10' on ice with buffer A (15mM Tris pH 7.4, 60mM KCl, 15mM NaCl, 5mM MgCl2, 300mM Sucrose and 0.1% IGEPAL) and treated to 10 strokes using a Dounce homogenizer. Lysate was centrifuged and washed once with buffer A without detergent. Nuclei were then resuspended in MNase buffer (15mM Tris pH 7.4, 60mM KCl, 15mM NaCl, 3mM CaCl2 and 200mM Sucrose) and digested at 37C with 1U of MNase (Takara #2910A). Reaction was stopped adding 0.15 volumes of Stop solution (4% SDS and 100mM EDTA). RNA and proteins were digested with 70ug of RNAse A for 1h at 37C followed by 70ug of freshly made proteinase K for 2h at 55C. Digested DNA was purified with phenol chloroform extraction followed by ethanol precipitation. Finally, DNA was resuspended in TE (10 mM Tris pH 8 and 1 mM EDTA) and analyzed on a 1.7% agarose gel stained with ethidium bromide.

Heat shock of S2 cells

For heat shock treatment we followed (Petesch and Lis, 2008). The media volume of S2 cells growing at 25C in 10 cm^2 dish plate was adjusted to 7.5 mL. To heat shock the cells we added 7.5 mL of media that was pre-warmed at 48C and incubated the cells for 3 min at 37C. Heat shock treatment was stopped by supplementing the media with 5 mL of 4C media, and cells were then immediately fixed for downstream MNase-qPCR procedure.

MNAse-qPCR

MNase-qPCR experiments were performed as described previously in (Infante et al., 2012) with some modifications. S2 cells were fixed with 1% formaldehyde for 10 min with gentle rotation. Fixation was quenched adding Glycine to a final concentration of 125 mM, and then cells were washed twice with cold PBS. Cells were then resuspended in 3mL of Buffer A (10mM of Tris pH 8.0, 3mM CaCl2, 2mM MgAcetate, 300mM of Sucrose and 0.5 mM of DTT) + 1% of TX-100 and lyses was promoted with 5 passes through a 25G needle. Lysates were washed twice with Buffer A and once with Buffer D [50mM of Tris pH 8.0, 5mM MgAcetate, 5 mM of DTT and 25% of Glycerol]. The nuclei were then resuspended in 200 uL of MNase buffer (15mM of Tris pH 7.4, 60mM KCl, 15mM NaCl, 2mM CaCl2, 0.5 mM of DTT and 25% of Glycerol) and incubated for 10 min at 37C prior the add of 120U of MNase (Takara #2910A). Digestion was conducted at 37C for 30 min. For each of the conditions, we run in parallel an undigested sample with no MNase enzyme that was used for normalization purposes during qPCR analysis. MNase digestion was stopped by adding SDS and EDTA to a final concentration of 0.5% and 12.5 mM respectively. Reverse crosslinking was achieved incubating samples at 65C overnight, and RNA and proteins were then digested with 70 ug of RNase A and proteinase K. Finally, DNA was recovered with phenol-chloroform extraction followed by ethanol precipitation. To enrich for mono-nucleosomes, digested samples were run in an agarose gel, and mono-nucleosomes were gel-purified following standard procedures. Undigested and mono-nucleosome enriched DNA was then quantified using Qubit fluorometer following the commercial protocol.

Subsequent qPCR analysis is also detailed in (Infante et al., 2012). Primers used are listed in **Table 4.5**. We determine the relative amount of each primer set in the undigested genomic DNA and the gel-purified mono-nucleosome DNA. The relative protection value is then calculated for each amplicon which corresponds to the fold-enrichment of the target sequence in the mono-nucleosomal DNA sample over the undigested DNA sample. Finally, we normalize the relative protection values for each amplicon to differences in DNA concentration among different samples.

ChIP-qPCR

Cells were crosslinked with 1% methanol-free formaldehyde and quenched with 0.125 mM Glycine. Cells were then harvested and washed with PBS + 0.2mM PMSF. Cells were then treated with ChIP Buffer I (50 mM HEPES pH 7.6, 140 mM NaCl, 1 mM EDTA, 0.5 mM EGTA, 10% glicerol, 0.5% IGEPAL, 0.25% Triton X-100, and C0mplete protease inhibitors (11836170001), incubated on a rotator at 4C, and spun down at 4C. Pellets were were resuspended in ChIP Buffer II (20 mM Tris pH 8.0, 200 mM NaCl, 1mM EDTA, pH 8.0, 0.5 mM EGTA, pH 8.0, and C0mplete protease inhibitors), incubated on a rotator at 4C, and spun down at 4C. Pellets were resuspended in ChIP Buffer III (20 mM Tris, 100 mM NaCl, 1 mM EDTA, 0.5 mM EGTA, 0.5% Sarkosyl, 0.1% Na-Deoxycholate (NaDOC) and C0mplete protease inhibitors) and sonicated in a S220 Covaris (peak power 140, Duty Ratio 5, Cycles 200) 15'. Samples were transferred into 1.5 mL Lo-bind tubes, Triton X-100 to 1% at final volume was added and samples were spun down at max speed 10' at 4C. Supernatants were then quantified using a Bradford

assay. IPs were set up with 200ug of protein, (12ul of Elys antibody, 2ul of IgG antibody) and Dilution Buffer (20 mM Tris, 100 mM NaCl, 1 mM EDTA, 0.5 mM EGTA) in a 1:2 ratio of lysate:dilution buffer. IPs were incubated on a rotator O/N at 4C and 10% Input and verification samples were stored at -80C. 40ul of Dynabeads per IP were washed and then blocked in 0.3% BSA in PBS on a rotator O/N at 4C. Beads were then washed twice in dilution buffer and added to the IPs and incubated on a rotator at 4C. After incubation, beads were washed in Low Salt Buffer (20 mM Tris-HCl pH 8, 150 mM NaCl, 2 mM EDTA, 0.1% SDS, 1% TritonX-100), High Salt Buffer (20 mM Tris-HCl, pH 8, 500 mM NaCl, 2 mM EDTA, 0.1% SDS, 1% TritonX-100), LiCl Buffer (10 mM Tris-HCl pH 8, 250 mM LiCl, 1% IGEPAL, 1% NaDOC, 1 mM EDTA) once followed by TE50 (10 mM Tris-HCl pH 8.0, 50 mM NaCl, 1 mM EDTA) twice. Beads were resuspended in Elution Buffer (100 mM NaHCO3, 1% SDS) and eluted at 65C at 600 rpm for 30'. Samples (IPs and Inputs) were de-crosslinked at 65°C. After de-crosslinking, equal volume TE (10 mM Tris-HCl pH 8.0, 1 mM EDTA) was added to samples and 0.2 mg/ml final concentration RNAse A was added and incubated at 37C followed by addition of 0.2 mg/ml final concentration Proteinase K and incubation at 55C. 1X sample volume of Phenol/Chloroform/isoamyl alcohol was added, samples were incubated at RT and then spun down at max speed. 1X sample volume of chloroform/isoamyl alcohol was added to the aqueous layer and samples were incubated at RT and then spun down at max speed. 0.1X sample volume of sodium acetate (pH 5.2, final concentration of 0.3 M), 1.5µl glycogen (stock 20 mg/ ml, Roche) and 2.5 X sample volume of cold 100% ethanol was added the aqueous layer and samples were mixed and incubated at -20C. Samples were then spun down at max speed, the DNA pellet was washed with 70% cold ethanol, spun down at max speed and then air-dried until all ethanol was removed. DNA pellets

were then re-suspended in TE buffer and used for downstream qPCR analysis, using primers listed in **Table 4.3.**

Tables of Sequences

Table 4.1: LacO DNA FISH probe

Probe	Sequence	Notes
lacO DNA FISH probe	+GT+GA+GC+GG+AT+AA+CA+ATT	where + preceeds locked nucleic acids (LNAs) for more rigidity and specificity of probe. Made by Exiqon, with N-terminal conjugation to TYE665 fluor

Table 4.2: RT-qPCR Primers

Gene target	Forward Primer	Reverse Primer
Dan	CTAAAAGACGCCAAGCTGTTCG	CATGCGGATGTTCATGTGGG
Sec13	from Capelson et al 2010	from Capelson et al 2010
Elys	TTGCTCCCCCAGTTCCAAAG	GATTCCAATGGATGCCACGTC
Hph-RA	AGCAAGCTGACTAATCAAGGCA	GCGCTCACGCTTGTCCAAAA
Hph-RB	ACAAACATCTGCCAGTGAAACAA	CATAGCGGCGCTCAACCG
B52 5' UTR	ACACGCGACATCCTCATCAA	TCTTCGAATTCCACAAAGCCG
B52 Gene Body	GCGATCCAACAAATCGCGTG	GCTTTTGAACGACCACCGTT

Table 4.3: ChIP qPCR Primers

Gene target	Forward Primer	Reverse Primer
Hph	TGCAATTGGTTTGGCTTGGC	GCGAAAAACCGAACTGAACG
B52	ATTGCCCGCCCAAAATATCG	AGTGACAGACGAAAGCGATG
Chr3R Neg Control	AGCAGCCACAACACAACAAC	GCACGTGCCTCATATAATCG

Table 4.4: T7 RNAi Primers

RNAi Target	Source
dsWhite	Pascual-Garcia et al. 2017
dsElys	Pascual-Garcia et al. 2017
dsSec13	Capelson et al. 2010

Table 4.5: MNase qPCR Primers

Primer Direction	Primer Sequence	Position relative to TSS	Genomic coordinates relative to dm3 Drosophila genome
Hph			
F	CCGGGATAGACGTACAGTTCA	-249	1090415
R	ATGAGTGCTCGAATTCTGGTG	-115	1090549
F	AAATGCCTCAAGTATTGCTCGT	-202	1090462
R	CAGAGCGTTTTAAGAGCAGGTG	-56	1090608
F	CACCAGAATTCGAGCACTCAT	-135	1090529
R	CTGAGCAGGTCGCTCTCG	-6	1090658
F	TCTCTCCTTCGTAACCAACGGTA	-51	1090613
R	TGAAGCAGCTGAACCGAAC	48	1090712
F	GAGTGCGGTTCGGTTCAG	23	1090687
R	TCACTGGCAGATGTTTGTTTTG	144	1090808
F	CCGAAGCTGAGTAATACACAAACG	70	1090734
R	GGCCGGCTGCCTATATATTTC	180	1090844
F	ACAAACATCTGCCAGTGAAACA	127	1090791
R	AATGTGTTGGTGGGGAGGT	227	1090891
F	GGCCCCAACAAATGCAAA	177	1090841
R	GGGAAAGAGTGCGAGTTATACG	285	1090949
F	CGTACCTCCCCACCAACA	206	1090870
R	CGAAGGGGAGCCTCGAAT	309	1090973
F	GAACCCGTCATCTCCCAAG	376	1091040
R	TGTTGTGCAGAGAAAGGGTGA	484	1091148

F	GGATCCTGAAACAATTCAAATGC	429	1091093
R	ACTCTTGAGACAGCTTTAAGACTGAAG	546	1091210
F	TGTGGAGATACAAAGATAGGACTTCA	499	1091163
R	TGGAGGTTATCATTTTGCCTTG	610	1091274
F	CAAGGCAAAATGATAACCTCCA	589	1091253
R	CCGCTTGTCCAAAAGTTCC	696	1091360
B52			
F	GTCGAGTCGCTTGCGTTT	23	9487056
R	CCGTTCAGTGAAGGATATTTGTG	122	9487155
F	GAGAGAGTACGGCAGCGACTT	65	9487098
R	AACCGCTGCAAAAACGAGT	199	9487232
F	CTTCACTGAACGGTACGTGCT	110	9487143
R	TCGCAATGTACCGGGTGT	221	9487254
F	CGCGTATTTCGCGTTGTT	157	9487190
R	ACGCGCCGTGTATGTTTC	275	9487308
F	ACATTGCGAGCGTGTGTGT	213	9487246
R	CGTTGCAGTTTGCAGCTTCT	347	9487380
F	GCAACGGTTCCCTTGCTG	342	9487375
R	ACACTCGAGATCCCACCATGA	441	9487474
F	CACCTGCTCCAGATACGTAAGG	391	9487424
R	CCTTTGAAAAAGCGCTCCA	499	9487532
F	CATGGTGGGATCTCGAGTG	422	9487455
R	TGATGAGGATGTCGCGTGT	528	9487561
F	CACGCGACATCCTCATCA	511	9487544
R	AATGCAGAAATGTCTTCAAATCAA	629	9487662
F	GACATTTCTGCATTTCTCTGTTTG	616	9487649
R	TTTAAGCGTCACTGTATTTGACAGA	744	9487777
F	TTCAAGCCGACCCTTGAAT	659	9487692
R	TGGAAATACGCTGGGTGAA	776	9487809
F	TTTGTTCCATCATTTGTCTGTCA	704	9487737
R	TTGAAGCTACCCTGCCTGTG	806	9487839
F	TTCACCCAGCGTATTTCCA	758	9487791
R	CATCGTCGGCATCACGATA	880	9487913
F	TGAATTTTCAGGAATTCGAAGACTA	839	9487872
R	GCTTATATCTAACAACTCACCGTTCG	940	9487973
F	ATCGTGATGCCGACGATG	863	9487896
R	TTCAACAACCACACTGCAAAA	998	9488031
F	AGAGCTGCTTGGCGAACG	903	9487936

R	CCTGGCGGGTTCAACAAC	1007	9488040
F	CCGCTACGACGATCGATATG	1034	9488067
R	CGCTACTTTGGTCCGGTTT	1138	9488171
F	GCGGTCGTTACAACGAAAAG	1075	9488108
R	GGGCAAACTTCAACGCAAA	1179	9488212
F	TGCCAGCGGACCTTAAAA	1105	9488138
R	GCTGGTTGCATCTGTGTGG	1239	9488272
Hsp70			
F	GCAATAAAGTGCAAGTTAAAGTGA	87	7784344
R	CTTCTTGGTTGATTTCAGTAGTTGC	179	7784436
F	AAAGTAACCAACAACCAAGTAA	119	7784376
R	TCAGAGTTCTCTTCTTGTCTTC	209	7784466
F	ACTGCAACTACTGAAATCAACCAAG	152	7784409
R	TGTGTGTGAGTTCTTCTTCCTCGG	253	7784510
F	TGAAGACAAGAAGAGAACTCTGAA	187	7784444
R	CAGATCGATTCCAATAGCAGGC	277	7784534
F	CTTTCAACAAGTCGTTACCGAGG	213	7784470
R	ATGTTGGTAGACACCCACGCA	313	7784570
F	AGAACTCACACACAATGCCTGC	240	7784497
R	GCGATAATCTCCACCTTGCCAT	333	7784590
F	ATTGGAATCGATCTGGGCAC	263	7784520
R	AAAGCCACGTAGGACGGC	375	7784632
F	TGGGTGTCTACCAACATGGCAA	297	7784554
R	ATGAGGCGTTCCGAATCTGTGA	396	7784653
F	ATTATCGCCAACGACCAGGGCAA	326	7784583
R	TTCATGGCCACCTGGTTCTT	429	7784686
F	CGTCCTACGTGGCTTTCACAGATT	360	7784617
R	TCGCTTGGCGTCAAACACT	460	7784717
F	TCATCGGCGATCCGGCTAAGAA	393	7784650
R	TCTTGGGGTCGTCGTATTTT	491	7784748
F	TAAGAACCAGGTGGCCATGA	409	7784666
R	AGTGCTTCATGTCCTCTGCGAT	512	7784769
F	TGTTTGACGCCAAGCGACTGAT	444	7784701
R	TCGCTTACAACCTTGAAAGGCCAG	534	7784791
F	CCAAGATCGCAGAGGACATGAA	486	7784743
R	TGGACTCACCCTTATACTCCAC	578	7784835
F	ACGGCGGAAAGCCCAAGAT	534	7784791

R	CCGTCTCCTTCATCTTGGTCAGTA	635	7784892

Location of lacO 96C / P11.3 insertion cite
GTTCGGGCGGCAAAAAGCCGAAGACGAGGACGAAAGCTGCTCTCTCACTGGCTC TCTCCCTCTCTCTCTCTCTCTCTCTTAAGGAAGAGGATGTTCGGTTCTCATTTGCC TCAGCTCTTAGCGALACGGTCGCGAAAGAGAGGCGAGCCCACGTAATCTGCGAT GAAGGCATGTATCAAAACAAAGCGAGGAAAACTGGCCGCAATCACAACAGCAACA ACTGCAGCACATGACAGCGGGAAAACTAGCAGAATTATCAGTGACGATAAAAGGC GCACCCCCTACTGCGAAAATTAGACAGGGATTTCGGCTAGGTTTTTCACGTTCTT CTCGCAGATCCGTTGCTCGTTTGATAGTTGTTGCCCAGCGTTTAAAGGAGCAGAA AATGGCTTAGCTAAACGCAAGCAAATGCCTCCTGAGGTTGCACACAGTCTTACAC TGGAAAAAATCTAGATTTTACCTAAAACTAATACAGAATACAAGGAAATATAAGCTT GGCAGAAAAGTAATATGTACTTTCCATCACAAGCGATCGTATCATATATTCAATAA TTTGTATGAAATTTCATTTTCATAGTTATAATCATGGAATATATGTACATAACTAAGA GATACAAAATTGCTAAATTATTACACTAAATATCGAATTCTTACCAAATTTAATCAAA TTATCTTTTCTAAGGTGTCACCATTTTTCTCTCTGTGCTCACACATACACGTGAGC CGCAAGAAAGGAGGCCGAAAAGGATGTGCGTCTCTATCTCAAAAGCCTAGCACG AGTTTTGCGTCGTTTCGTTGCACACACTTGTGTGTCCCACGTGTGTGTGTGTGTG TTTTTGGGAGTGCTG Location in *Drosophila* genome dm3 begins at location 21009380 ~1353bp upstream of gene dan, variants A and B, 725 bp upstream of dan C, in the middle of intron 2 of gene lobo **Unpublished data sent to us from Lori Wallrath PhD**

Bibliography

Alfert, A., N. Moreno, and K. Kerl. 2019. The BAF complex in development and disease. *Epigenetics Chromatin*. 12:19. doi:10.1186/s13072-019-0264-y.

Armstrong, J.A., O. Papoulas, G. Daubresse, A.S. Sperling, J.T. Lis, M.P. Scott, and J.W. Tamkun. 2002. The Drosophila BRM complex facilitates global transcription by RNA polymerase II. *EMBO J.* 21:5245–5254. doi:10.1093/emboj/cdf517.

Aze, A., M. Fragkos, S. Bocquet, J. Cau, and M. Méchali. 2017. RNAs coordinate nuclear envelope assembly and DNA replication through ELYS recruitment to chromatin. *Nat. Commun.* 8. doi:10.1038/s41467-017-02180-1.

Baldi, S. 2019. Nucleosome positioning and spacing: from genome-wide maps to single arrays. *Essays Biochem.* 63:5–14. doi:10.1042/EBC20180058.

Bernstein, B.E., M. Kamal, K. Lindblad-Toh, S. Bekiranov, D.K. Bailey, D.J. Huebert, S. McMahon, E.K. Karlsson, E.J. Kulbokas, T.R. Gingeras, S.L. Schreiber, and E.S. Lander. 2005. Genomic Maps and Comparative Analysis of Histone Modifications in Human and Mouse. *Cell*. 120:169–181. doi:10.1016/j.cell.2005.01.001.

Blobel, G. 1985. Gene gating: A hypothesis. *Proc. Natl. Acad. Sci. U. S. A.* 82:8527–8529. doi:10.1073/pnas.82.24.8527.

Boeger, H., J. Griesenbeck, J.S. Strattan, and R.D. Kornberg. 2004. Removal of promoter nucleosomes by disassembly rather than sliding in vivo. *Mol. Cell*. 14:667–673. doi:10.1016/j.molcel.2004.05.013.

Bouazoune, K., and A. Brehm. 2006. ATP-dependent chromatin remodeling complexes in Drosophila. *Chromosom. Res.* 14:433–449. doi:10.1007/s10577-006-1067-0.

Brickner, D.G., I. Cajigas, Y. Fondufe-Mittendorf, S. Ahmed, P.-C. Lee, J. Widom, and J.H. Brickner. 2007. H2A.Z-Mediated Localization of Genes at the Nuclear Periphery Confers Epigenetic Memory of Previous Transcriptional State. *PLoS Biol.* 5:e81. doi:10.1371/journal.pbio.0050081.

Brickner, D.G., C. Randise-Hinchliff, M.L. Corbin, J.M. Liang, S. Kim, B. Sump, A. D'Urso, S.H. Kim, A. Satomura, H. Schmit, R. Coukos, S. Hwang, R. Watson, and J.H. Brickner. 2019. The Role of Transcription Factors and Nuclear Pore Proteins in Controlling the Spatial Organization of the Yeast Genome. *Dev. Cell*. 49:936-947.e4. doi:10.1016/j.devcel.2019.05.023.

Brown, C.R., C.J. Kennedy, V.A. Delmar, D.J. Forbes, and P.A. Silver. 2008. Global histone acetylation induces functional genomic reorganization at mammalian nuclear pore complexes. *Genes Dev.* 22:627–39. doi:10.1101/gad.1632708.

Brown, C.R., C. Mao, E. Falkovskaia, J.K. Law, and H. Boeger. 2011. In vivo role for the chromatin-remodeling enzyme SWI/SNF in the removal of promoter nucleosomes

by disassembly rather than sliding. *J. Biol. Chem.* 286:40556–65. doi:10.1074/jbc.M111.289918.

Cabal, G.G., A. Genovesio, S. Rodriguez-Navarro, C. Zimmer, O. Gadal, A. Lesne, H. Buc, F. Feuerbach-Fournier, J.-C. Olivo-Marin, E.C. Hurt, and U. Nehrbass. 2006. SAGA interacting factors confine sub-diffusion of transcribed genes to the nuclear envelope. *Nature*. 441:770–773. doi:10.1038/nature04752.

Capelson, M., and M.W. Hetzer. 2009. The role of nuclear pores in gene regulation, development and disease. *EMBO Rep.* 10:697–705. doi:10.1038/embor.2009.147.

Capelson, M., Y. Liang, R. Schulte, W. Mair, U. Wagner, and M.W. Hetzer. 2010. Chromatin-Bound Nuclear Pore Components Regulate Gene Expression in Higher Eukaryotes. *Cell*. 140:372–383. doi:10.1016/j.cell.2009.12.054.

Casolari, J.M., C.R. Brown, S. Komili, J. West, H. Hieronymus, and P.A. Silver. 2004. Genome-Wide Localization of the Nuclear Transport Machinery Couples Transcriptional Status and Nuclear Organization. 117. 427–439 pp.

Cenci, G., G. Siriaco, G.D. Raffa, R. Kellum, and M. Gatti. 2003. The Drosophila HOAP protein is required for telomere capping. *Nat. Cell Biol.* 5:82–84. doi:10.1038/ncb902.

D'Angelo, M.A., and M.W. Hetzer. 2008. Structure, dynamics and function of nuclear pore complexes. *Trends Cell Biol.* 18:456–466. doi:10.1016/j.tcb.2008.07.009.

D'Urso, A., and J.H. Brickner. 2014. Mechanisms of epigenetic memory. *Trends Genet.* 30:230–236. doi:10.1016/j.tig.2014.04.004.

D'Urso, A., and J.H. Brickner. 2017. Epigenetic transcriptional memory. *Curr. Genet.* 63:435–439. doi:10.1007/s00294-016-0661-8.

D'Urso, A., Y. Takahashi, B. Xiong, J. Marone, R. Coukos, C. Randise-Hinchliff, J.-P. Wang, A. Shilatifard, and J.H. Brickner. 2016. Set1/COMPASS and Mediator are repurposed to promote epigenetic transcriptional memory. *Elife*. 5:1–29. doi:10.7554/elife.16691.

Danzer, J.R., and L.L. Wallrath. 2004. Mechanisms of HP1-mediated gene silencing in Drosophila. *Development*. 131:3571–3580. doi:10.1242/dev.01223.

Deng, H., X. Bao, W. Cai, M.J. Blacketer, A.S. Belmont, J. Girton, J. Johansen, and K.M. Johansen. 2008. Ectopic histone H3S10 phosphorylation causes chromatin structure remodeling in Drosophila. *Development*. 135:699–705. doi:10.1242/dev.015362.

Dixon, J.R., D.U. Gorkin, and B. Ren. 2016. Chromatin Domains: The Unit of Chromosome Organization. *Mol. Cell*. 62:668–680. doi:10.1016/j.molcel.2016.05.018.

Erdel, F., and K. Rippe. 2018. Formation of Chromatin Subcompartments by Phase Separation. *Biophys. J.* 114:2262–2270. doi:10.1016/j.bpj.2018.03.011.

Ertl, I., M. Porta-De-La-Riva, E. Gómez-Orte, K. Rubio-Peña, D. Aristizábal-Corrales, E. Cornes, L. Fontrodona, X. Osteikoetxea, C. Ayuso, P. Askjaer, J. Cabello, and J. Cerón. 2016. Functional Interplay of Two Paralogs Encoding SWI/SNF Chromatin-Remodeling Accessory Subunits During Caenorhabditis elegans Development. *Genetics*. 202:961–975.

Fasci, D., H. Van Ingen, R.A. Scheltema, and A.J.R. Heck. 2018. Histone Interaction Landscapes Visualized by Crosslinking Mass Spectrometry in Intact Cell Nuclei □ S. *Mol. Cell. Proteomics*. 17. doi:10.1074/mcp.RA118.000924.

Fernandez, A.G., E.K. Mis, A. Lai, M. Mauro, A. Quental, C. Bock, and F. Piano. 2014. Uncovering buffered pleiotropy: A genome-scale screen for mel-28 genetic interactors in caenorhabditis elegans. *G3 Genes, Genomes, Genet.* 4:185–196. doi:10.1534/g3.113.008532.

Fišerová, J., M. Efenberková, T. Sieger, M. Maninová, J. Uhlířová, and P. Hozák. 2017. Chromatin organization at the nuclear periphery as revealed by image analysis of structured illumination microscopy data. *J. Cell Sci.* 130:2066–2077. doi:10.1242/jcs.198424.

Franks, T.M., A. McCloskey, M.N. Shokirev, C. Benner, A. Rathore, and M.W. Hetzer. 2017. Nup98 recruits the Wdr82-Set1A/COMPASS complex to promoters to regulate H3K4 trimethylation in hematopoietic progenitor cells. *Genes Dev.* 31:2222–2234. doi:10.1101/gad.306753.117.

Franz, C., R. Walczak, S. Yavuz, R. Santarella, M. Gentzel, P. Askjaer, V. Galy, M. Hetzer, I.W. Mattaj, and W. Antonin. 2007. MEL-28/ELYS is required for the recruitment of nucleoporins to chromatin and postmitotic nuclear pore complex assembly. *EMBO Rep.* 8:165–172. doi:10.1038/sj.embor.7400889.

Fuda, N.J., M.J. Guertin, S. Sharma, C.G. Danko, A.L. Martins, A. Siepel, and J.T. Lis. 2015. GAGA Factor Maintains Nucleosome-Free Regions and Has a Role in RNA Polymerase II Recruitment to Promoters. *PLOS Genet.* 11:e1005108. doi:10.1371/journal.pgen.1005108.

Gdula, D.A., R. Sandaltzopoulos, T. Tsukiyama, V. Ossipow, and C. Wu. 1998. Inorganic pyrophosphatase is a component of the Drosophila nucleosome remodeling factor complex. *Genes Dev.* 12:3206–3216. doi:10.1101/gad.12.20.3206.

Géli, V., and M. Lisby. 2015. Recombinational DNA repair is regulated by compartmentalization of DNA lesions at the nuclear pore complex. *BioEssays*. 37:1287–1292. doi:10.1002/bies.201500084.

Gómez-Saldivar, G., A. Fernandez, Y. Hirano, M. Mauro, A. Lai, C. Ayuso, T. Haraguchi, Y. Hiraoka, F. Piano, and P. Askjaer. 2016. Identification of Conserved MEL-

28/ELYS Domains with Essential Roles in Nuclear Assembly and Chromosome Segregation. *PLoS Genet.* 12. doi:10.1371/journal.pgen.1006131.

Gottesfeld, J.M., X. Michael, and F. Carey. 2018. Chromatin and transcription. *J. Biol. Chem*. 13775. doi:10.1074/jbc.TM118.004544.

Grimaud, C., and P.B. Becker. 2009. The dosage compensation complex shapes the conformation of the X chromosome in Drosophila. *Genes Dev.* 23:2490–5. doi:10.1101/gad.539509.

Handler, D., K. Meixner, M. Pizka, K. Lauss, C. Schmied, F.S. Gruber, and J. Brennecke. 2013. The genetic makeup of the Drosophila piRNA pathway. *Mol. Cell*. 50:762–77. doi:10.1016/j.molcel.2013.04.031.

Hargreaves, D.C., and G.R. Crabtree. 2011. ATP-dependent chromatin remodeling: genetics, genomics and mechanisms. *Cell Res.* 21:396–420. doi:10.1038/cr.2011.32.

Hochstrasser, M., and J.W. Sedat. 1987. Three-dimensional organization of Drosophila melanogaster interphase nuclei. I. Tissue-specific aspects of polytene nuclear architecture. *J. Cell Biol.* 104:1455–1470. doi:10.1083/jcb.104.6.1455.

Hutchison, N., and H. Weintraub. 1985. Localization of DNAase I-sensitive sequences to specific regions of interphase nuclei. *Cell*. 43:471–482. doi:10.1016/0092-8674(85)90177-1.

Ibarra, A., C. Benner, S. Tyagi, J. Cool, and M.W. Hetzer. 2016. Nucleoporin-mediated regulation of cell identity genes. *Genes Dev.* 30:2253–2258. doi:10.1101/gad.287417.116.

Ibarra, A., and M.W. Hetzer. 2015. Nuclear pore proteins and the control of genome functions. *Genes Dev.* 29:337–349. doi:10.1101/gad.256495.114.

Ilyin, A.A., S.S. Ryazansky, S.A. Doronin, O.M. Olenkina, E.A. Mikhaleva, E.Y. Yakushev, Y.A. Abramov, S.N. Belyakin, A. V Ivankin, A. V Pindyurin, V.A. Gvozdev, M.S. Klenov, and Y.Y. Shevelyov. 2017. Piwi interacts with chromatin at nuclear pores and promiscuously binds nuclear transcripts in Drosophila ovarian somatic cells. *Nucleic Acids Res.* 45:7666–7680. doi:10.1093/nar/gkx355.

Infante, J.J., G.L. Law, and E.T. Young. 2012. Analysis of nucleosome positioning using a nucleosome-scanning assay. 833. 63–87 pp.

Inoue, A., and Y. Zhang. 2014. Nucleosome assembly is required for nuclear pore complex assembly in mouse zygotes. *Nat. Struct. Mol. Biol.* 21:609–616. doi:10.1038/nsmb.2839.

Jacinto, F. V, C. Benner, and M.W. Hetzer. 2015. The nucleoporin Nup153 regulates embryonic stem cell pluripotency through gene silencing. *Genes Dev.* 29:1224–38. doi:10.1101/gad.260919.115.

Janicki, S.M., T. Tsukamoto, S.E. Salghetti, W.P. Tansey, R. Sachidanandam, K. V. Prasanth, T. Ried, Y. Shav-Tal, E. Bertrand, R.H. Singer, and D.L. Spector. 2004. From silencing to gene expression: Real-time analysis in single cells. *Cell*. 116:683–698. doi:10.1016/S0092-8674(04)00171-0.

Jin, Q., L.-R. Yu, L. Wang, Z. Zhang, L.H. Kasper, J.-E. Lee, C. Wang, P.K. Brindle, S.Y.R. Dent, and K. Ge. 2011. Distinct roles of GCN5/PCAF-mediated H3K9ac and CBP/p300-mediated H3K18/27ac in nuclear receptor transactivation. *EMBO J.* 30:249–62. doi:10.1038/emboj.2010.318.

Jühlen, R., and B. Fahrenkrog. 2018. Moonlighting nuclear pore proteins: tissue-specific nucleoporin function in health and disease. *Histochem. Cell Biol.* 150:593–605. doi:10.1007/s00418-018-1748-8.

Kalverda, B., H. Pickersgill, V. V. Shloma, and M. Fornerod. 2010. Nucleoporins Directly Stimulate Expression of Developmental and Cell-Cycle Genes Inside the Nucleoplasm. *Cell*. 140:360–371. doi:10.1016/J.CELL.2010.01.011.

Kasper, L.H., P.K. Brindle, C.A. Schnabel, C.E. Pritchard, M.L. Cleary, and J.M. van Deursen. 1998. CREB binding protein interacts with nucleoporin-specific FG repeats that activate transcription and mediate NUP98-HOXA9 oncogenicity. 19:764–776.

Kasper, L.H., P.K. Brindle, C.A. Schnabel, C.E.J. Pritchard, M.L. Cleary, and J.M.A. Van Deursen. 1999. CREB Binding Protein Interacts with Nucleoporin-Specific FG Repeats That Activate Transcription and Mediate NUP98-HOXA9 Oncogenicity. 19. 764–776 pp.

Kehat, I., F. Accornero, B.J. Aronow, and J.D. Molkentin. 2011. Modulation of chromatin position and gene expression by HDAC4 interaction with nucleoporins. *J. Cell Biol.* 193:21–9. doi:10.1083/jcb.201101046.

Kimura, N., M. Takizawa, K. Okita, O. Natori, K. Igarashi, M. Ueno, K. Nakashima, I. Nobuhisa, and T. Taga. 2002. Identification of a novel transcription factor, ELYS, expressed predominantly in mouse foetal haematopoietic tissues. *Genes to Cells*. 7:435–446. doi:10.1046/j.1365-2443.2002.00529.x.

Knockenhauer, K.E., and T.U. Schwartz. 2016. The Nuclear Pore Complex as a Flexible and Dynamic Gate. *Cell*. 164:1162–1171. doi:10.1016/j.cell.2016.01.034.

Koch, C.M., R.M. Andrews, P. Flicek, S.C. Dillon, U. Karaoz, G.K. Clelland, S. Wilcox, D.M. Beare, J.C. Fowler, P. Couttet, K.D. James, G.C. Lefebvre, A.W. Bruce, O.M. Dovey, P.D. Ellis, P. Dhami, C.F. Langford, Z. Weng, E. Birney, N.P. Carter, D. Vetrie, and I. Dunham. 2007. The landscape of histone modifications across 1% of the human genome in five human cell lines. *Genome Res.* 17:691–707. doi:10.1101/gr.5704207.

Krull, S., J. Dö rries, B. rn Boysen, S. Reidenbach, L. Magnius, H. Norder, J. Thyberg, and V.C. Cordes. 2010. Protein Tpr is required for establishing nuclear pore-

associated zones of heterochromatin exclusion. *EMBO J.* 29:1659–1673. doi:10.1038/emboj.2010.54.

Labade, A.S., K. Karmodiya, and K. Sengupta. 2016. HOXA repression is mediated by nucleoporin Nup93 assisted by its interactors Nup188 and Nup205. *Epigenetics Chromatin*. doi:10.1186/s13072-016-0106-0.

Lapetina, D.L., C. Ptak, U.K. Roesner, and R.W. Wozniak. 2017. Yeast silencing factor Sir4 and a subset of nucleoporins form a complex distinct from nuclear pore complexes. *J. Cell Biol.* 216:3145–3159. doi:10.1083/jcb.201609049.

Lee, S.H., H. Sterling, A. Burlingame, and F. McCormick. 2008. Tpr directly binds to Mad1 and Mad2 and is important for the Mad1-Mad2-mediated mitotic spindle checkpoint. *Genes Dev.* 22:2926–31. doi:10.1101/gad.1677208.

Lelek, M., N. Casartelli, D. Pellin, E. Rizzi, P. Souque, M. Severgnini, C. Di Serio, T. Fricke, F. Diaz-Griffero, C. Zimmer, P. Charneau, and F. Di Nunzio. 2015. Chromatin organization at the nuclear pore favours HIV replication. *Nat. Commun.* 6:6483. doi:10.1038/ncomms7483.

Li, Y., J.R. Danzer, P. Alvarez, A.S. Belmont, and L.L. Wallrath. 2003. Effects of tethering HP1 to euchromatic regions of the Drosophila genome. *Development*. 130:1817–1824. doi:10.1242/dev.00405.

Liang, Y., T.M. Franks, M.C. Marchetto, F.H. Gage, and M.W. Hetzer. 2013. Dynamic Association of NUP98 with the Human Genome. *PLoS Genet.* 9:e1003308. doi:10.1371/journal.pgen.1003308.

Light, W.H., D.G. Brickner, V.R. Brand, and J.H. Brickner. 2010. Interaction of a DNA Zip Code with the Nuclear Pore Complex Promotes H2A.Z Incorporation and INO1 Transcriptional Memory. *Mol. Cell*. 40:112–125. doi:10.1016/j.molcel.2010.09.007.

Light, W.H., J. Freaney, V. Sood, A. Thompson, A. D'Urso, C.M. Horvath, and J.H. Brickner. 2013. A Conserved Role for Human Nup98 in Altering Chromatin Structure and Promoting Epigenetic Transcriptional Memory. *PLoS Biol.* 11:e1001524. doi:10.1371/journal.pbio.1001524.

Lince-Faria, M., S. Maffini, B. Orr, Y. Ding, C. Cláudia Florindo, C.E. Sunkel, A. Tavares, J. Johansen, K.M. Johansen, and H. Maiato. 2009. Spatiotemporal control of mitosis by the conserved spindle matrix protein Megator. *J. Cell Biol.* 184:647–57. doi:10.1083/jcb.200811012.

Liu, Z., M. Yan, Y. Liang, W. Mo, B.M. Fontoura, L. Zhang Correspondence, Z. Liu, M. Liu, K. Zhang, D. Shao, R. Jiang, L. Li, C. Wang, D.R. Nussenzveig, K. Zhang, S. Chen, C. Zhong, and L. Zhang. 2019. Nucleoporin Seh1 Interacts with Olig2/Brd7 to Promote Oligodendrocyte Differentiation and Myelination. *Neuron*. 102:1–15. doi:10.1016/j.neuron.2019.02.018.

Liyanage, V.R.B., R.M. Zachariah, G.P. Delcuve, J.R. Davie, and M. Rastegar. 2012.

Chromatin structure and epigenetics. *New Dev. Chromatin Res.* 72:29–60. doi:10.1016/j.bcp.2006.06.016.

Lucchesi, J.C. 2018. Transcriptional modulation of entire chromosomes: dosage compensation. *J. Genet.* 97:357–364.

Luthra, R., S.C. Kerr, M.T. Harreman, L.H. Apponi, M.B. Fasken, S. Ramineni, S. Chaurasia, S.R. Valentini, and A.H. Corbett. 2007. Actively transcribed GAL genes can be physically linked to the nuclear pore by the SAGA chromatin modifying complex. *J. Biol. Chem.* 282:3042–3049. doi:10.1074/jbc.M608741200.

Maeshima, K., S. Ide, and M. Babokhov. 2019. Dynamic chromatin organization without the 30-nm fiber. *Curr. Opin. Cell Biol.* 58:95–104. doi:10.1016/j.ceb.2019.02.003.

Manhas, S., L. Ma, and V. Measday. 2018. The yeast Ty1 retrotransposon requires components of the nuclear pore complex for transcription and genomic integration. *Nucleic Acids Res.* 46:3552–3578. doi:10.1093/nar/gky109.

Marini, B., A. Kertesz-Farkas, H. Ali, B. Lucic, K. Lisek, L. Manganaro, S. Pongor, R. Luzzati, A. Recchia, F. Mavilio, M. Giacca, and M. Lusic. 2015. Nuclear architecture dictates HIV-1 integration site selection. *Nature*. 521:227–231. doi:10.1038/nature14226.

Mendjan, S., M. Taipale, J. Kind, H. Holz, P. Gebhardt, M. Schelder, M. Vermeulen, A. Buscaino, K. Duncan, J. Mueller, M. Wilm, H.G. Stunnenberg, H. Saumweber, and A. Akhtar. 2006. Nuclear Pore Components Are Involved in the Transcriptional Regulation of Dosage Compensation in Drosophila. *Mol. Cell*. 21:811–823. doi:10.1016/j.molcel.2006.02.007.

Mizuguchi, G., and C. Wu. 1999. Nucleosome Remodeling Factor NURF and In Vitro Transcription of Chromatin. *In* Chromatin Protocols. Humana Press, New Jersey. 333–342.

Mohrmann, L., K. Langenberg, J. Krijgsveld, A.J. Kal, A.J.R. Heck, and C.P. Verrijzer. 2004. Differential targeting of two distinct SWI/SNF-related Drosophila chromatin-remodeling complexes. *Mol. Cell. Biol.* 24:3077–88. doi:10.1128/mcb.24.8.3077-3088.2004.

Mohrmann, L., and C.P. Verrijzer. 2005. Composition and functional specificity of SWI2/SNF2 class chromatin remodeling complexes. *Biochim. Biophys. Acta - Gene Struct. Expr.* 1681:59–73. doi:10.1016/j.bbaexp.2004.10.005.

Mossaid, I., and B. Fahrenkrog. 2015. Complex Commingling: Nucleoporins and the Spindle Assembly Checkpoint. *Cells*. 4:706–725. doi:10.3390/cells4040706.

Muerdter, F., P.M. Guzzardo, J. Gillis, Y. Luo, Y. Yu, C. Chen, R. Fekete, and G.J. Hannon. 2013. A genome-wide RNAi screen draws a genetic framework for transposon control and primary piRNA biogenesis in Drosophila. *Mol. Cell*. 50:736–48. doi:10.1016/j.molcel.2013.04.006.

Muller, W.G., D. Rieder, G. Kreth, C. Cremer, Z. Trajanoski, and J.G. McNally. 2004. Generic Features of Tertiary Chromatin Structure as Detected in Natural Chromosomes. *Mol. Cell. Biol.* 24:9359–9370. doi:10.1128/mcb.24.21.9359-9370.2004.

Müller, W.G., D. Walker, G.L. Hager, and J.G. McNally. 2001. Large-scale chromatin decondensation and recondensation regulated by transcription from a natural promoter. *J. Cell Biol.* 154:33–48. doi:10.1083/jcb.200011069.

Nagai, S., N. Davoodi, and S.M. Gasser. 2011. Nuclear organization in genome stability: SUMO connections. *Cell Res.* 21:474–485. doi:10.1038/cr.2011.31.

Nakayama, T., T. Shimojima, and S. Hirose. 2012. The PBAP remodeling complex is required for histone H3.3 replacement at chromatin boundaries and for boundary functions. *Dev.* 139:4582–4590. doi:10.1242/dev.083246.

Nanni, S., A. Re, C. Ripoli, A. Gowran, P. Nigro, D. D'Amario, A. Amodeo, F. Crea, C. Grassi, A. Pontecorvi, A. Farsetti, and C. Colussi. 2016. The nuclear pore protein Nup153 associates with chromatin and regulates cardiac gene expression in dystrophic mdx hearts. *Cardiovasc. Res.* 112:555–567. doi:10.1093/cvr/cvw204.

Ohtsuki, S., and M. Levine. 1998. GAGA mediates the enhancer blocking activity of the eve promoter in the Drosophila embryo. *Genes Dev.* 12:3325–3330. doi:10.1101/gad.12.21.3325.

Oka, M., S. Mura, K. Yamada, P. Sangel, S. Hirata, K. Maehara, K. Kawakami, T. Tachibana, Y. Ohkawa, H. Kimura, and Y. Yoneda. 2016. Chromatin-prebound Crm1 recruits Nup98-HoxA9 fusion to induce aberrant expression of Hox cluster genes. *Elife*. 5:1–21. doi:10.7554/eLife.09540.

Ollion, J., J. Cochennec, F. Loll, C. Escudé, and T. Boudier. 2013. TANGO: A generic tool for high-throughput 3D image analysis for studying nuclear organization. *Bioinformatics*. 29:1840–1841. doi:10.1093/bioinformatics/btt276.

Panda, D., P. Pascual-Garcia, M. Dunagin, M. Tudor, K.C. Hopkins, J. Xu, B. Gold, A. Raj, M. Capelson, and S. Cherry. 2014. Nup98 promotes antiviral gene expression to restrict RNA viral infection in Drosophila. *Proc. Natl. Acad. Sci. U. S. A.* 111:E3890–E3899. doi:10.1073/pnas.1410087111.

Parikh, R.Y., H. Lin, and V.K. Gangaraju. 2018. A critical role for nucleoporin 358 (Nup358) in transposon silencing and piRNA biogenesis in Drosophila. *J. Biol. Chem.* 293:9140–9147. doi:10.1074/jbc.AC118.003264.

Pascual-Garcia, P., B. Debo, J.R. Aleman, N.H. Nguyen, K.J. Won, and M. Capelson Correspondence. 2017. Metazoan Nuclear Pores Provide a Scaffold for Poised Genes and Mediate Induced Enhancer-Promoter Contacts. *Mol. Cell*. 66:63-76.e6. doi:10.1016/j.molcel.2017.02.020.

Pascual-Garcia, P., J. Jeong, and M. Capelson. 2014. Nucleoporin Nup98 Associates

with Trx/MLL and NSL Histone-Modifying Complexes and Regulates Hox Gene Expression. *Cell Rep.* 9:433–442. doi:10.1016/j.celrep.2014.09.002.

Peterson, C.L., and I. Herskowitz. 1992. Characterization of the yeast SWI1, SWI2, and SWI3 genes, which encode a global activator of transcription. *Cell*. 68:573–583. doi:10.1016/0092-8674(92)90192-F.

Petesch, S.J., and J.T. Lis. 2008. Rapid, Transcription-Independent Loss of Nucleosomes over a Large Chromatin Domain at Hsp70 Loci. *Cell*. 134:74–84. doi:10.1016/j.cell.2008.05.029.

Phatnani, H.P., and A.L. Greenleaf. 2006. Phosphorylation and functions of the RNA polymerase II CTD. *Genes Dev.* 20:2922–36. doi:10.1101/gad.1477006.

Platani, M., I. Samejima, K. Samejima, M.T. Kanemaki, and W.C. Earnshaw. 2018. Seh1 targets GATOR2 and Nup153 to mitotic chromosomes. *J. Cell Sci.* 131:jcs213140. doi:10.1242/jcs.213140.

Ptak, C., and R.W. Wozniak. 2016. Nucleoporins and chromatin metabolism. *Curr. Opin. Cell Biol.* 40:153–160. doi:10.1016/j.ceb.2016.03.024.

Rabut, G., V. Doye, and J. Ellenberg. 2004. Mapping the dynamic organization of the nuclear pore complex inside single living cells. *Nat. Cell Biol.* 6:1114–1121. doi:10.1038/ncb1184.

Raices, M., L. Bukata, S. Sakuma, J. Borlido, L.S. Hernandez, D.O. Hart, and M.A. D'angelo. 2017. Nuclear Pores Regulate Muscle Development and Maintenance by Assembling a Localized Mef2C Complex Article Nuclear Pores Regulate Muscle Development and Maintenance by Assembling a Localized Mef2C Complex. *Dev. Cell*. 41:540–554. doi:10.1016/j.devcel.2017.05.007.

Raices, M., and M.A. D'Angelo. 2012. Nuclear pore complex composition: A new regulator of tissue-specific and developmental functions. *Nat. Rev. Mol. Cell Biol.* 13:687–699. doi:10.1038/nrm3461.

Raices, M., and M.A. D'Angelo. 2017. Nuclear pore complexes and regulation of gene expression. *Curr. Opin. Cell Biol.* 46:26–32. doi:10.1016/j.ceb.2016.12.006.

Raich, N., S. Mahmoudi, D. Emre, and R.E. Karess. 2018. Mad1 influences interphase nucleoplasm organization and chromatin regulation in Drosophila. *Open Biol.* 8. doi:10.1098/rsob.180166.

Rasala, B.A., A. V. Orjalo, Z. Shen, S. Briggs, and D.J. Forbes. 2006. ELYS is a dual nucleoporin/kinetochore protein required for nuclear pore assembly and proper cell division. *Proc. Natl. Acad. Sci. U. S. A.* 103:17801–17806. doi:10.1073/pnas.0608484103.

Rasala, B.A., C. Ramos, A. Harel, and D.J. Forbes. 2008. Capture of AT-rich Chromatin by ELYS Recruits POM121 and NDC1 to Initiate Nuclear Pore Assembly. *Mol. Biol.*

Cell. 19:3982–3996. doi:10.1091/mbc.e08-01-0012.

Ricci, M.A., C. Manzo, M.F. García-Parajo, M. Lakadamyali, and M.P. Cosma. 2015. Chromatin fibers are formed by heterogeneous groups of nucleosomes in vivo. *Cell*. 160:1145–1158. doi:10.1016/j.cell.2015.01.054.

Rochman, M., Y. Postnikov, S. Correll, C. Malicet, S. Wincovitch, T.S. Karpova, J.G. McNally, X. Wu, N.A. Bubunenko, S. Grigoryev, and M. Bustin. 2009. The Interaction of NSBP1/HMGN5 with Nucleosomes in Euchromatin Counteracts Linker Histone-Mediated Chromatin Compaction and Modulates Transcription. *Mol. Cell*. 35:642–656. doi:10.1016/j.molcel.2009.07.002.

Rosin, L.F., S.C. Nguyen, and E.F. Joyce. 2018. Condensin II drives large-scale folding and spatial partitioning of interphase chromosomes in Drosophila nuclei. *PLoS Genet.* 14:e1007393. doi:10.1371/journal.pgen.1007393.

Sachani, S.S., L.S. Landschoot, L. Zhang, C.R. White, W.A. MacDonald, M.C. Golding, and M.R.W. Mann. 2018. Nucleoporin 107, 62 and 153 mediate Kcnq1ot1 imprinted domain regulation in extraembryonic endoderm stem cells. *Nat. Commun.* 9:2795. doi:10.1038/s41467-018-05208-2.

Schindelin, J., I. Arganda-Carreras, E. Frise, V. Kaynig, M. Longair, T. Pietzsch, S. Preibisch, C. Rueden, S. Saalfeld, B. Schmid, J.Y. Tinevez, D.J. White, V. Hartenstein, K. Eliceiri, P. Tomancak, and A. Cardona. 2012. Fiji: An open-source platform for biological-image analysis. *Nat. Methods*. 9:676–682. doi:10.1038/nmeth.2019.

Schmid, M., G. Arib, C. Laemmli, J. Nishikawa, T. Durussel, and U.K. Laemmli. 2006. Nup-PI: The nucleopore-promoter interaction of genes in yeast. *Mol. Cell*. 21:379–391. doi:10.1016/j.molcel.2005.12.012.

Schneider, M., D. Hellerschmied, T. Schubert, B.F. Pugh, T. Clausen, and A. Kö Hler Correspondence. 2015. The Nuclear Pore-Associated TREX-2 Complex Employs Mediator to Regulate Gene Expression Graphical Abstract Highlights d The nuclear pore-associated TREX-2 complex directly interacts with Mediator d TREX-2 regulates Mediator association with Cdk8 and RNA Pol II Ser5 phosphorylation d TREX-2 and the Med31 submodule co-regulate specific inducible and constitutive genes d A similar TREX-2 surface promotes both transcription and mRNA export In Brief Accession Numbers 4trq Schneider et al. *Cell*. 162:1016–1028. doi:10.1016/j.cell.2015.07.059.

Sharma, R., D. Jost, J. Kind, G. Gómez-Saldivar, B. van Steensel, P. Askjaer, C. Vaillant, and P. Meister. 2014. Differential spatial and structural organization of the X chromosome underlies dosage compensation in C. elegans. *Genes Dev.* 28:2591–2596. doi:10.1101/GAD.248864.114.

Shilatifard, A. 2012. The COMPASS family of histone H3K4 methylases: mechanisms of regulation in development and disease pathogenesis. *Annu. Rev. Biochem.* 81:65–95. doi:10.1146/annurev-biochem-051710-134100.

Sonneville, R., G. Craig, K. Labib, A. Gartner, and J.J. Blow. 2015. Both Chromosome Decondensation and Condensation Are Dependent on DNA Replication in C. elegans Embryos. *Cell Rep.* 12:405–17. doi:10.1016/j.celrep.2015.06.046.

Sood, V., and J.H. Brickner. 2014. Nuclear pore interactions with the genome. *Curr. Opin. Genet. Dev.* 25:43–49. doi:10.1016/j.gde.2013.11.018.

Szabo, Q., F. Bantignies, and G. Cavalli. 2019. Principles of genome folding into topologically associating domains. *Sci. Adv.* 5. doi:10.1126/SCIADV.AAW1668.

Taddei, A., G. Van Houwe, F. Hediger, V. Kalck, F. Cubizolles, H. Schober, and S.M. Gasser. 2006. Nuclear pore association confers optimal expression levels for an inducible yeast gene. *Nature*. 441:774–778. doi:10.1038/nature04845.

Talamas, J.A., and M. Capelson. 2015. Nuclear envelope and genome interactions in cell fate. *Front. Genet.* 5:95. doi:10.3389/fgene.2015.00095.

Tamkun, J.W., R. Deuring, M.P. Scott, M. Kissinger, A.M. Pattatucci, T.C. Kaufman, and J.A. Kennison. 1992. brahma: A regulator of Drosophila homeotic genes structurally related to the yeast transcriptional activator SNF2 SWI2. *Cell*. 68:561–572. doi:10.1016/0092-8674(92)90191-E.

Tan-Wong, S.M., H.D. Wijayatilake, and N.J. Proudfoot. 2009. Gene loops function to maintain transcriptional memory through interaction with the nuclear pore complex. *Genes Dev.* 23:2610–2624. doi:10.1101/gad.1823209.

Tie, F., R. Banerjee, P.A. Conrad, P.C. Scacheri, and P.J. Harte. 2012. Histone Demethylase UTX and Chromatin Remodeler BRM Bind Directly to CBP and Modulate Acetylation of Histone H3 Lysine 27. *Mol. Cell. Biol.* 32:2323–2334. doi:10.1128/mcb.06392-11.

Titus, L.C., T.R. Dawson, D.J. Rexer, K.J. Ryan, and S.R. Wente. 2010. Members of the RSC Chromatin-Remodeling Complex Are Required for Maintaining Proper Nuclear Envelope Structure and Pore Complex Localization. *Mol. Biol. Cell*. 21:1072–1087. doi:10.1091/mbc.e09-07-0615.

Toda, T., J.Y. Hsu, S.B. Linker, F. V Jacinto, M.W. Hetzer, and F.H. Gage Correspondence. 2017. Nup153 Interacts with Sox2 to Enable Bimodal Gene Regulation and Maintenance of Neural Progenitor Cells Data Resources GSE99783 Toda et al. *Cell Stem Cell*. 21:618–634. doi:10.1016/j.stem.2017.08.012.

Tolsma, T.O., and J.C. Hansen. 2019. Post-translational modifications and chromatin dynamics. *Essays Biochem.* 63:89–96. doi:10.1042/EBC20180067.

Tumbar, T., G. Sudlow, and A.S. Belmont. 1999. Large-scale chromatin unfolding and remodeling induced by VP16 acidic activation domain. *J. Cell Biol.* 145:1341–1354. doi:10.1083/jcb.145.7.1341.

Tyagi, M., N. Imam, K. Verma, and A.K. Patel. 2016. Chromatin remodelers: We are the

drivers!! *Nucleus*. 7:388–404. doi:10.1080/19491034.2016.1211217.

Ulianov, S. V., E.E. Khrameeva, A.A. Gavrilov, I.M. Flyamer, P. Kos, E.A. Mikhaleva, A.A. Penin, M.D. Logacheva, M. V. Imakaev, A. Chertovich, M.S. Gelfand, Y.Y. Shevelyov, and S. V. Razin. 2016. Active chromatin and transcription play a key role in chromosome partitioning into topologically associating domains. *Genome Res.* 26:70–84. doi:10.1101/gr.196006.115.

Van de Vosse, D.W., Y. Wan, D.L. Lapetina, W.-M. Chen, J.-H. Chiang, J.D. Aitchison, and R.W. Wozniak. 2013. A Role for the Nucleoporin Nup170p in Chromatin Structure and Gene Silencing. *Cell*. 152:969–983. doi:10.1016/J.CELL.2013.01.049.

Vaquerizas, J.M., R. Suyama, J. Kind, K. Miura, and N.M. Luscombe. 2010. Nuclear Pore Proteins Nup153 and Megator Define Transcriptionally Active Regions in the Drosophila Genome. *PLoS Genet*. 6:1000846. doi:10.1371/journal.pgen.1000846.

Walther, T.C., A. Alves, H. Pickersgill, I. Loïodice, M. Hetzer, V. Galy, B.B. Hülsmann, T. Köcher, M. Wilm, T. Allen, I.W. Mattaj, and V. Doye. 2003. The conserved Nup107-160 complex is critical for nuclear pore complex assembly. *Cell*. 113:195–206. doi:10.1016/S0092-8674(03)00235-6.

Watson, M.L. 1959. Further Observations on the Nuclear Envelope of the Animal Cell. *J. Cell Biol.* 6:147–156. doi:10.1083/jcb.6.2.147.

Weintraub, H., and M. Groudine. 1976. Chromosomal subunits in active genes have an altered conformation. *Science*. 193:848–56. doi:10.1126/SCIENCE.948749.

Wolffe, A.P., and J.J. Hayes. 1999. Chromatin disruption and modification. *Nucleic Acids Res.* 27:711–720. doi:10.1093/nar/27.3.711.

Xu, F., Q. Zhang, K. Zhang, W. Xie, and M. Grunstein. 2007. Sir2 deacetylates histone H3 lysine 56 to regulate telomeric heterochromatin structure in yeast. *Mol. Cell*. 27:890–900. doi:10.1016/j.molcel.2007.07.021.

Zierhut, C., C. Jenness, H. Kimura, and H. Funabiki. 2014. Nucleosomal regulation of chromatin composition and nuclear assembly revealed by histone depletion. *Nat. Struct. Mol. Biol.* 21:617–625. doi:10.1038/nsmb.2845.

Zullo, J.M., I.A. Demarco, R. Piqué-Regi, D.J. Gaffney, C.B. Epstein, C.J. Spooner, T.R. Luperchio, B.E. Bernstein, J.K. Pritchard, K.L. Reddy, and H. Singh. 2012. DNA sequence-dependent compartmentalization and silencing of chromatin at the nuclear lamina. *Cell*. 149:1474–1487. doi:10.1016/j.cell.2012.04.035.